Dosimetric Investigation of Image-guided Radiotherapy for Prostate Cancer using Cone-Beam Computed Tomography

Hemal Ariyaratne

UCL

A thesis submitted to UCL for the degree of

MD (Res)

Declaration

I, Hemal Ariyaratne, confirm that the work presented in this thesis is my own. Where information has been derived from other sources, I confirm that this has been indicated in the thesis.

Dedication

This work is dedicated to my wife Tracy and son Daniel, who make it all worthwhile

Acknowledgement

I would like to acknowledge the support of my supervisors Dr. Roberto Alonzi and Prof. Peter Hoskin. Roberto was instrumental in arranging my research fellowship and providing guidance. Despite his busy schedule, he found time to give constructive feedback throughout the process. Most importantly, it has been an absolute pleasure to work with him.

Prof. Hoskin has provided excellent leadership to the Marie Curie Research Centre at Mount Vernon Cancer Centre where I was based, and been an inspirational figure throughout my radiotherapy training.

My thanks also go out to Hayley Chesham, radiotherapy dosimetrist at the Elstree Radiotherapy Centre. She worked efficiently to provide dosimetry support for the project, and collaborated in conference presentations and publications.

I would like to acknowledge funding from Cancer Partners UK for my two-year clinical research fellowship. The Mount Vernon Marie Curie Research Wing Trust generously funded my academic fees, and provided an excellent base for research.

Abstract

Objectives

1. To survey the current practice of image-guided radiotherapy (IGRT) for prostate cancer in the United Kingdom.
2. To validate a practical dose calculation strategy on cone-beam computed tomography (CBCT)
3. To assess the effect of CBCT verification imaging frequency on actual dose delivered to target volume and organs at risk during a course of image-guided radiotherapy for prostate cancer.
4. To compare the dosimetric effects of reduction of CTV-PTV margin with daily imaging.

Material and Methods

59 radiotherapy centres in the United Kingdom were included in an online survey of IGRT practice. The survey covered details of verification strategy during prostate radiotherapy, with specific questions on imaging frequency.

A validation study of the CBCT dose calculation strategy was evaluated on 37 fractions using Bland-Altman plots. The study technique was compared to the density-override technique. A pilot comparison of CTV coverage with bone matching to soft tissue matching was performed.

For the principal dosimetric analysis, 844 cone-beam CT (CBCT) images from 20 patients undergoing radical prostate radiotherapy were included. Patients received a dose of 74 Gy in 37 fractions using 7-field intensity-modulated radiotherapy. Target volume and organs at risk were contoured manually on each CBCT image.

A daily online CBCT verification schedule was compared with a protocol of day 1-3 followed by weekly imaging. 3 mm, 5 mm, and 7 mm CTV-PTV margins were compared for daily imaging.

Results

CBCT is the principal verification imaging modality in the UK for prostate cancer, used by 66% of centres. There is no consensus on optimal imaging schedule, with 2 main strategies used. These are the daily online schedule and the day 1-3 followed by weekly schedule.

Use of CBCT contours on planning CT showed good agreement with the density-override technique, provided multifield IMRT was used. There were clear drops in target coverage if a bone match strategy was used in comparison to soft tissue matching.

90% of patients had improved target coverage with daily online in comparison to weekly online soft tissue match. A median of 37 fractions achieved CTV coverage with daily imaging compared with 34 fractions with a weekly online protocol. 80% of patients had a reduction in rectal dose with the daily protocol. Margin reduction to 5 mm with adequate target coverage was feasible with daily imaging.

Conclusions

Daily online CBCT verification improves CTV coverage and reduces rectal dose during IGRT for prostate cancer. Daily CBCT imaging allows reduction of CTV-PTV margin for radiotherapy.

Table of Contents

List of Tables

List of Figures

Chapter 1. Introduction

Image Guided Radiotherapy (IGRT) is the use of imaging in the treatment room either immediately before or during treatment to evaluate and correct setup errors (Royal College of Radiologists et al., 2008).

1.1 History of IGRT technology

Strategies to improve radiotherapy accuracy during the early years of radiotherapy focussed on patient immobilization, with large margins to allow for error. A few institutions introduced imaging devices in the late 20th century. Holloway reported the use of a x-ray camera mounted on the gantry of a cobalt machine in 1958 (Holloway, 1958). A similar device for cobalt-60 radiotherapy was also reported in 1959 (Johns and Cunningham, 1959). However, the use of these imaging devices was limited to a few research-oriented institutions.

When linear accelerators were introduced in the 1950s, first at the Hammersmith Hospital in London (Miller, 1954), and subsequently in Stanford University, image-guidance was not available on the treatment machine. It was only after 1985 that x-ray imaging devices were

incorporated into linear accelerators (Biggs et al., 1985), but even this was not adopted immediately due to restriction of collimator by the device. Electronic portal imaging technology for 2-D planar imaging was developed in Harvard (Leong, 1986) and reported in the Netherlands in 1985 (van Herk and Meertens).

3-D imaging using cone beam CT was subsequently developed. The algorithms for cone beam CT reconstruction after arc acquisition were developed in the late 1990s (Wang and Ning, 1999). Flat panel detectors were then optimized for radiotherapy use (Jaffray and Siewerdsen, 2000). The first implementation of cone beam CT using a kilovoltage (kV) source and flat-panel detectors in a medical linear accelerator was described in 2002 (Jaffray et al., 2002). The technology will be discussed in detail further in this manuscript.

There is continuing progress in image-guided radiotherapy, with the development of prototype hybrid MRI-linear accelerators (Lagendijk et al., 2008, Keall et al., 2014, Stanescu et al., 2013).

1.2 External beam radiotherapy for prostate cancer

Radical external beam radiotherapy is a very effective treatment modality for localized prostate cancer, with outcomes at least as good as prostate surgery (D'Amico et al., 1998). Brachytherapy using direct radiotherapy sources for localized prostate cancer is another effective treatment modality which is outside the scope of this work. The curative efficacy of radiation treatment should be balanced against toxicity to surrounding organs. These organs at risk include the bladder and rectum, and potential side effects may have long-term consequences on quality of life.

Dose escalation has been attempted to improve cure rates further. Attempts at escalation of dose using older conformal radiotherapy led to improved progression-free survival, but higher rates of toxicity (Dearnaley et al., 2007, Zelefsky et al., 1998). The use of intensity-modulated radiotherapy (IMRT) has led to reduced toxicity (Zelefsky et al., 2002), due to improved dosimetric characteristics (Vanasek et al., 2013). However, further improvement of outcomes in prostate radiotherapy requires intensive management of sources of error during treatment. This is the basis for the use of advanced image guidance in image-guided radiotherapy (IGRT).

1.3 Sources of error in prostate radiotherapy

The causes of local failure of prostate radiotherapy could be classified in several ways. It may be classified as treatment-related factors or tumour-related factors. Tumour factors such as intrinsic radio-resistance are outside the scope of this work. Treatment factors include the multiple sources of error during radiotherapy, which occur throughout the process of treatment (Fig. 1).

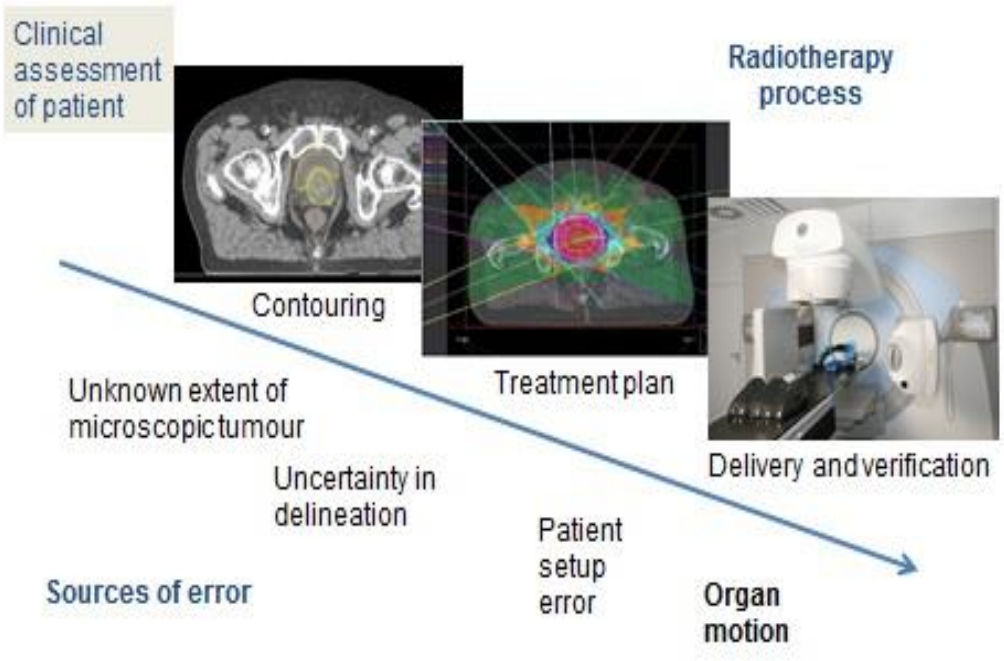

Fig. 1. Sources of error during radiotherapy

In the case of prostate radiotherapy, a key source of error is geometric uncertainty due to pelvic organ movement. In particular, rectal and bladder changes lead to prostate target movement and could lead to ‘geographic miss’. Rectal movement assessed using cine MRI has been shown to be associated with prostate movement, particularly if the rectum is distended (Padhani et al., 1999, Ghilezan et al., 2005). Highly conformal modern intensity-modulated radiotherapy utilizes steep dose gradients, and the effect of organ movement can lead to even greater errors.

Discrepancies between intended and actual treatment positions during radiotherapy are referred to as setup errors. They have a systematic component and random component. A systematic error is a deviation that occurs in the same direction and is of similar magnitude throughout the course of radiotherapy (Royal College of Radiologists et al., 2008). It can occur due to errors in treatment preparation for example, organ motion between the planning scan and start of treatment. A random error is an error that can vary in deviation and magnitude during each fraction. For example, organ motion in between treatment fractions during treatment.

Imaging prior to treatment has the potential to correct for inter-fraction variation due to organ motion. However, there can be other sources of residual errors such as rotational errors (Graf et al., 2012, Shang et al., 2013), intrafraction motion (Kron et al., 2010, Thomas et al., 2013) and

registration errors (Morrow et al., 2012). Image guidance should therefore be used in conjunction with appropriate immobilization of the patient and with suitable margins to account for residual errors.

1.4 Clinical benefits of image-guided radiotherapy for prostate cancer

Image-guided radiotherapy (IGRT) is becoming the standard of care for delivery of external beam radiation treatment for prostate cancer. The benefits of image-guided radiotherapy have been shown in retrospective patient series of fiducial-based IGRT. There have not been any randomized controlled trials directly comparing IGRT and non-IGRT approaches, due to ethical considerations.

A reduction in urinary toxicity has been clearly demonstrated in several studies (Zelefsky et al., 2012, Gill et al., 2011). In the Gill series, acute toxicity measured as urinary frequency more than grade 2 was 7% in the IGRT group compared with 23% in the non-IGRT group. Late urinary toxicity rates were 10.4% in the IGRT group in comparison to 20.0% in the non-IGRT group in the Zelefsky series.

Other retrospective studies have shown reductions GI toxicity. Acute GI toxicity is lower, with one study showing a rate of 3% for GI toxicity (CTC grade 2 and higher) in the IGRT group in comparison with 15% in the non-IGRT group (Gill et al., 2011). Late GI toxicity showed an even more prominent difference in another series. There was a rate of 6% GI toxicity

(greater than CTC grade 2) at 2 years in the IGRT group compared with 57% in the non-IGRT group (Sveistrup et al., 2014).

Zelefsky et al. also demonstrated improvements in biochemical control at three years for high-risk patients (Zelefsky et al., 2012). The prostate specific antigen (PSA) relapse-free survival rate was 97% in the IGRT group in comparison to 78% in the non-IGRT group. Cox regression analysis in the study confirmed IGRT as a positive predictive factor for biochemical control after radiotherapy for prostate cancer.

1.5 Strategies for image-guidance in prostate radiotherapy

There are different strategies of image-guided radiotherapy and verification used in prostate treatment centres around the world. Imaging modalities for on-treatment verification have evolved from planar or 2-D imaging (such as MV portal imaging) to 3-D imaging (e.g. cone beam CT). 4-D imaging where the tumour is imaged during the additional dimension of time has been less widely adapted in prostate cancer, although its use is common in lung cancer. Volumetric or 3-D imaging has emerged as the main verification modality in the US (Simpson et al., 2010), but there is no published survey data on prostate IGRT techniques used in the UK.

A fiducial-based approach relies on matching implanted markers in the prostate to imaging obtained at treatment planning. The most commonly technique is the use of three small gold seeds implanted with the aid of a transrectal ultrasound probe. The fiducial markers are used as a proxy for the position of the prostate. However, in-migration can occur at a rate of approximately 0.05 mm per fraction (Nichol et al., 2007, Shirato et al., 2003). Also, prostate deformation can be significant in some patients, particularly those who have previously had a transurethral resection of the prostate (TURP) (Nichol et al., 2007).

Another disadvantage of all fiducial-based systems is that an invasive procedure is required to implant markers prior to treatment. Serious complications such as sepsis are uncommon, but self-limiting low-grade side-effects are common. In the most cited series from the United Kingdom, 32% of patients developed at least one new symptom after the procedure (Gill et al., 2012). In another series from Australia, the rate of symptomatic infection was 7.7% with a third of those patients requiring hospital admission (Loh et al., 2015).

Ultrasound-based pre-treatment and intra-treatment monitoring has been evaluated by some centres with promising results (Fargier-Voiron et al., 2015). The use of magnetic electro-transponders such as the Calypso® system allows to real-time tracking of the fiducial markers during treatment (Willoughby et al., 2006, Kupelian et al., 2007). The Calypso® system has been found to be superior to standard transabdominal ultrasound verification (Foster et al., 2010). In the United Kingdom, use of transperineal ultrasound using the Elekta Clarity® system has been reported by one centre (Hilman et al.). Although good agreement has been obtained by the use of transperineal ultrasound, they have reported that radiographer training for optimal imaging has been challenging.

Stereotactic radiotherapy using the Cyberknife® (Accuray Technologies) system uses repeated stereoscopic x-ray monitoring of fiducial markers

during hypofractionated prostate radiotherapy. Although the precision of the system is very good, an adequate sampling rate of at least an x-ray every 40 seconds is required to ensure submillimetre tracking (Xie et al., 2008).

There is continuing progress in image-guided radiotherapy, with the development of prototype hybrid MRI-linear accelerators (Lagendijk et al., 2008, Keall et al., 2014, Stanescu et al., 2013). These could provide much better soft-tissue contrast, overcoming the image quality drawbacks with cone beam CT. There are also no concomitant radiation dose issues, and there is greater scope for real-time adaptive radiotherapy.

The challenges of MRI integration are due to two factors. The first is the radio-frequency (RF) signal used in the MRI system interfering with the RF pulses used to accelerate electrons in the linear accelerator. The other is the strong magnetic field of the MRI potentially affecting secondary electron distribution in the patient during treatment. These challenges are being circumvented and working prototypes have been developed.

However, MRI linear accelerators are still a research technology limited to a few centres in the UK. In view of the costs involved, it is likely to be

many years before MRI-integrated linear accelerators come into widespread use in the UK National Health Service.

1.6 Comparison of fiducial-based and CBCT image-guidance during prostate radiotherapy

There have not been any head-to-head dosimetric comparisons between patients treated with fiducial-based and CBCT-based IGRT. However, the correlation of shifts has been assessed in previous studies. In general, there is poor correlation particularly in the supero-inferior and antero-posterior directions.

On assessment of shifts, automatic grey-value matching on CBCT has been found to be different to fiducial matching (Shi et al., 2011). There was minimal difference along the lateral direction, with a mean of -0.02 cm (SD 0.13 cm). However, there were large discrepancies along the superior-inferior and anterior-posterior direction alignments. On the supero-inferior direction there was a mean difference of 0.55 cm (SD 0.48 cm). In the anterior-posterior direction the mean difference was 0.31 cm (SD 0.43 cm).

There is also some published work on the correlation of the shifts obtained by manual CBCT soft tissue matching and fiducial matching. Barney et al. found that there were clinically relevant differences between the shifts

using the different IGRT techniques. There was a mean difference in shifts of more than 3 mm in two out of three dimensions (Barney et al., 2011).

Moseley et al. found that the shifts with manual soft tissue matching using CBCT was comparable to standard fiducial matching with portal imaging, in terms of the correlation of left-right shifts, but there was weaker correlation in the other dimensions (Moseley et al., 2007). The Pearson correlation coefficient was 0.90, 0.49 and 0.51 in the left-right, antero-posterior and supero-inferior directions. One postulated reason was poorer observer demarcation of the apex of the prostate and the bladder-prostate interface on CT. There was no delineation of target organs undertaken in the study so this hypothesis could not be tested any further.

1.7 Overview of CBCT technology

Cone beam CT uses a cone-shaped beam emitted from the x-ray source (Fig. 2) compared to a fan-shaped beam emitted from a diagnostic CT machine. The volume is reconstructed from the volume projections received by a 2-D detector using a circular motion around the target. This is in contrast to the slice-by-slice acquisition and 1-D detector used in conventional CT. The x-rays are received onto a flat-panel detector for reconstruction.

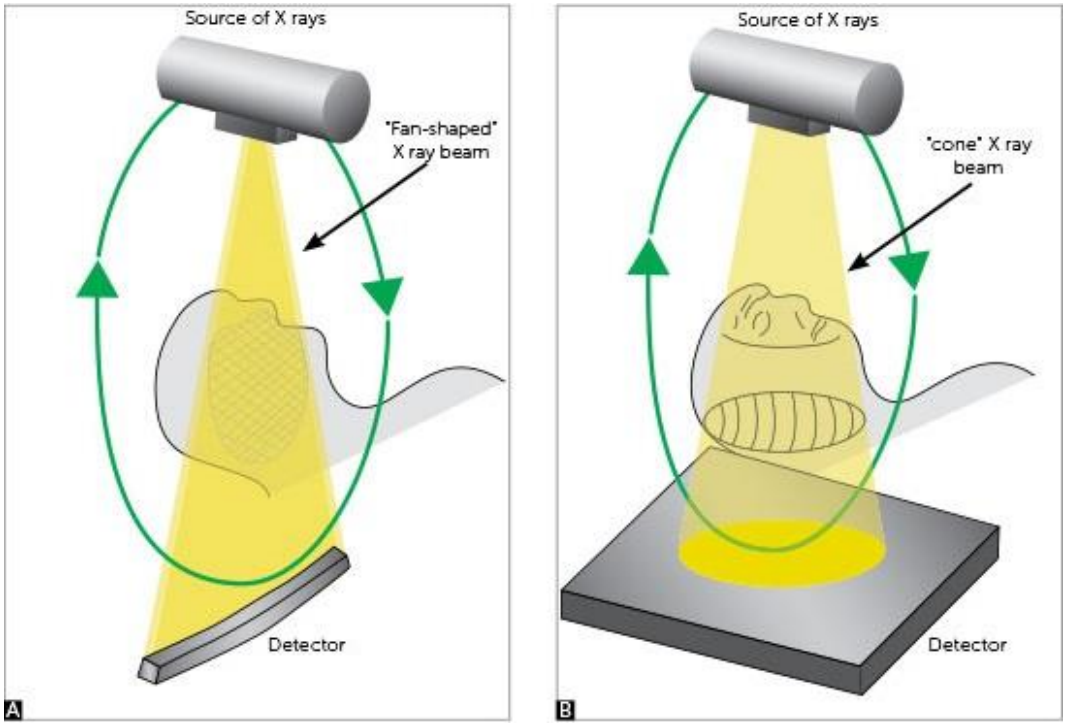

Fig. 2. Comparison of fan beam and cone-beam CT imaging technique

(Sukovic, 2003)

Cone beam technology utilizes x-rays more efficiently, so lower heat capacity x-ray tubes can be used. It allows for the use of smaller and less expensive x-ray components than fan-beam CT. Therefore, the technology lends itself to miniaturization for use in conjunction with a linear accelerator. The cone beam CT data can be referenced directly to the treatment coordinates as a result of such incorporation.

It has been adopted by a number of manufacturers in image-guidance packages such as the Varian Trilogy®, Elekta Synergy® (Fig. 3) and Siemens Artiste® systems. Comparison of the main CBCT systems from the different manufacturers has shown that they have comparable image quality (Chan et al., 2011).

Megavoltage (MV) CBCT is less widely available. MV CBCT is predominantly used in conjunction with helical tomotherapy (Ruchala et al., 1999), although it has been investigated with standard linear accelerators (Pouliot et al., 2005). Due to the physical characteristics of MV x-ray beams, the achievable image quality is limited.

Fig. 3. Elekta© CBCT on-board imager used in study

The length and width of the x-ray field scanned during the cone beam CT imaging can be varied. The field of view refers to the width of the x-ray field to be scanned. In the smallest setting, the field is centred on the patient. In the larger settings, the beam is offset as shown in Fig. 4, to allow larger patient diameters to be scanned (Lehmann et al., 2007). There are also limited settings to adjust the length of field. The settings are chosen to achieve the imaging objective while minimizing dose to the patient.

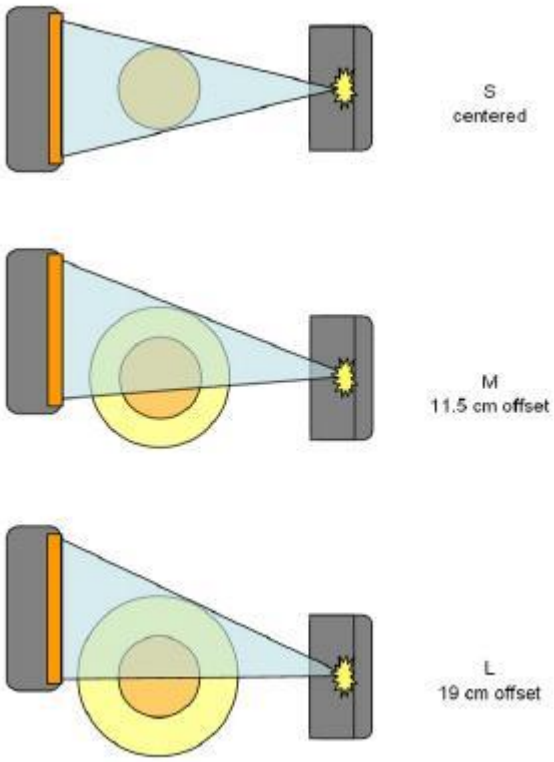

Fig. 4. Field of view settings in kV CBCT imager

A bow-tie filter (Fig. 5) is often used between the CBCT x-ray source and the patient. This functions as a compensator to modulate fluence and reduce scatter. It results in reduced skin dose and improved image quality, in particular image uniformity and low-contrast detectability (Mail et al., 2009).

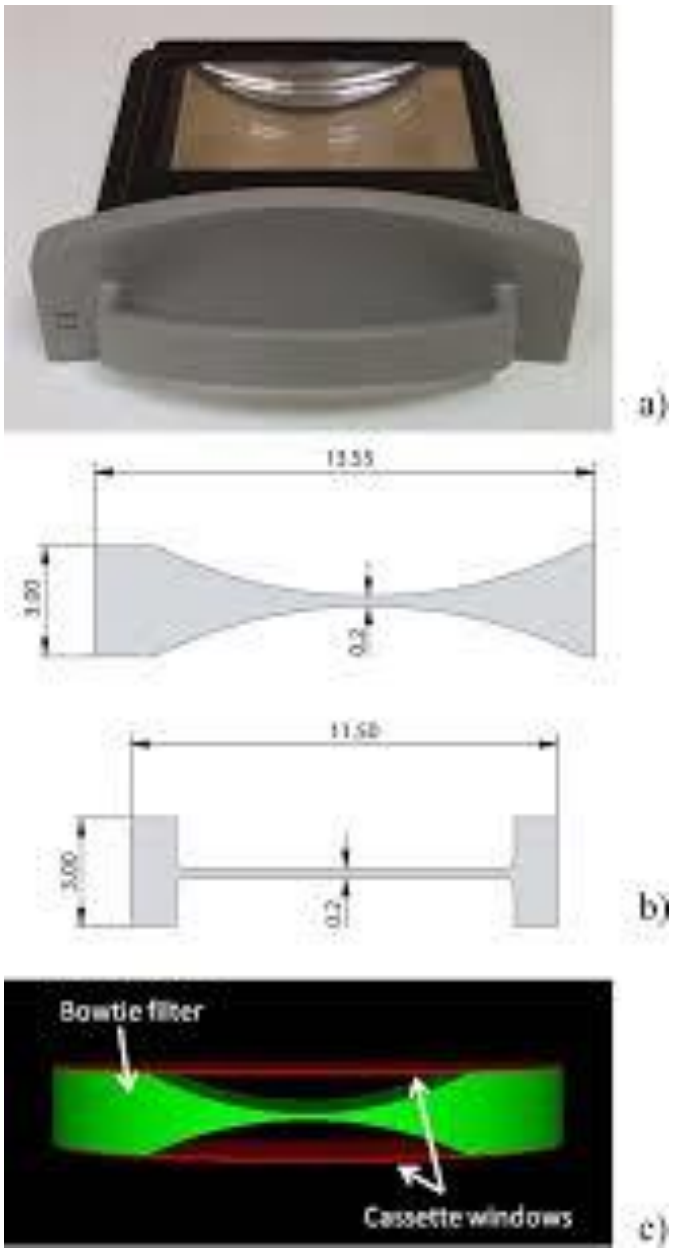

Fig. 5. CBCT bowtie filter

a) External view of filter cassette b) Profile view in both dimensions c) 3-D representation. (Downes et al., 2009)

1.8 Quality of CBCT imaging

CBCT machines operate with lower energy than diagnostic machines to reduce exposure dose. This results in a lower signal to noise ratio. Scatter is a result of the larger detector area, and can result in streaking and lower soft-tissue tissue contrast. Other types of artefact include extinction artefacts, beam hardening artefacts, aliasing artefact, ring artefact and motion artefact (Schulze et al., 2011).

Due to the above reasons, imaging on CBCT is of poorer quality than diagnostic CT. Phantom studies have shown that key imaging characteristics such as low-contrast visibility, spatial resolution, uniformity and image noise are all inferior for CBCT compared to diagnostic CT (Stock et al., 2009).

The difference in image quality between CBCT and planning CT is demonstrated in Figs. 6 and 7 below. These show axial slices of a patient due to have prostate radiotherapy, and are taken at comparable levels. The soft tissue contrast is clearly lower in the CBCT compared to the planning CT. Nevertheless, the image quality is sufficient for organ contouring on a suitable high-resolution display.

However, kV CBCT imaging has better image quality than MVCT images (Varadhan et al., 2009). They quantified soft tissue contrast between kV CBCT and MVCT using three parameters – 3D low-contrast visibility, 3D image uniformity and 3D spatial resolution. On each of those image quality parameters kV CBCT performed better than MVCT. In their study, in terms of 3D spatial resolution, kV CBCT was even equivalent to standard kV CT.

Fig. 6. Axial image from pelvic planning CT

Bladder (orange), Prostate (yellow), Rectum (red)

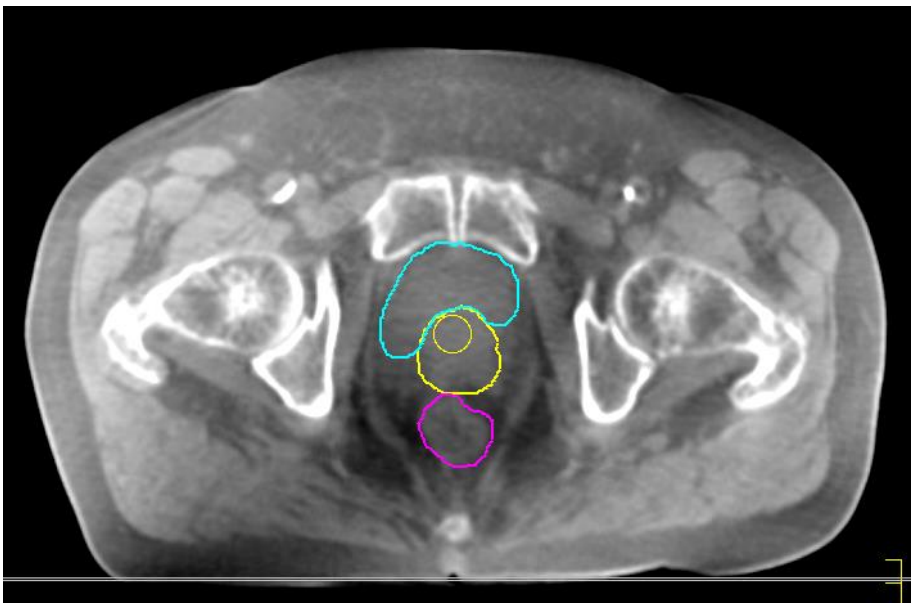

Fig. 7. Axial image from CBCT scan

Bladder (blue), Prostate (yellow), Rectum (magenta)

1.9 Dose calculation challenges

Dose calculation on CBCT is limited mainly by non-comparability of CT density units (Yang et al., 2007). There are wide variations in CT density units in comparison to the planning CT scan, with the range of density being less in the cone beam CT. Radiotherapy treatment planning system algorithms depend on the electron density variations in the CT scan which can be calibrated from Hounsfield units in a standard planning CT scan.

The differences in CT density units in cone beam CT lead to inaccuracies in dose calculation, unless corrective strategies are used. Some investigators have attempted to develop algorithms to enhance CBCT quality (Lou et al., 2013, Marchant et al., 2008), but dose calculation on these models have not been validated.

There are two main approaches to calculate dose on CBCT. The first approach is the use of CBCT calibration tables. However, this is dependent on CBCT scanner, image acquisition parameters, body site and phantom used. Errors have been reported to be in the range of 1-3% with phantoms (Fotina et al., 2012). However, other investigators have reported errors of up to 10% with phantom-based calibration for the pelvic

site (Richter et al., 2008), and have recommended patient group-specific calibration tables.

The other problem is that pixel values in CBCT systems can vary with the current-time product (mAs) setting for the x-ray tube. This is particularly seen with the Elekta XVI system (Kamath et al., 2011). This means that a single constant calibration factor cannot be applied for each site and patient.

The second dose calculation approach is through the use of density-override on CBCT. This could be done in two ways. The first method is the replacement of CBCT densities by standard densities for air, water and bone (Fotina et al., 2012). Alternatively, a region of interest (ROI) mapping method could be used where the tissue densities for each of the surrounding areas are mapped from the planning CT on to the CBCT (Hu et al., 2010, Fotina et al., 2012). However, this is particularly time-intensive as all surrounding organs have to be contoured and tissue densities replaced by those from the planning CT scan.

My hypothesis for the initial phase was that density-override may not be required when calculating treatment dose in multi-field intensity-modulated radiotherapy (IMRT) to the prostate, particularly when 7 fields are used. In

such an instance, the main influence on dose change will be organ movement in relation to the high-dose field, rather than minor variations in tissue density of surrounding organs.

The hypothesis is supported by previous prostate dosimetric studies (Orton and Tomé, 2004, Schulze et al., 2009). I therefore evaluated a method using kV CBCT contours on the planning CT, and compared this to the density-override method.

1.10 Previous CBCT dosimetric studies

One of the initial dosimetric studies in prostate IGRT was done by Kupelian et al (Kupelian et al., 2006). They investigated the effects of organ motion during prostate radiotherapy. They had a relatively small cohort of 10 patients who underwent helical tomotherapy using implanted fiducials for image guidance. Patients were treated with a dose of 78 Gy in 39 fractions, and a total of 390 megavoltage CT (MVCT) scans were available.

Manual contouring was stated to have been performed on each MVCT scan, although the authors have not commented on the image quality of the megavoltage scans. Dose calculation was performed directly on the MVCT scan and dosimetric parameters reported were the D95 for the prostate and D2cc for the rectum. They found that there was insignificant variation in delivered dose to the prostate. The dose delivered to the prostate per fraction was 2.02 +/- 0.04 Gy. There were however large fluctuations in dose to rectum due to volume changes.

The strength of this study was the availability of a complete set of CT images for the whole course of radiotherapy. Limitations of this study include the use of MVCT scans which have poorer image quality due to

the intrinsic characteristics of megavoltage energy. The MVCT scans did not fully encompass the bladder in some cases, leading to unreliability of the dose-volume parameters for the rectum and bladder in those instances. The small sample size meant that assessing predictive factors was difficult. The MVCT scans were not used for image guidance, so the study reflects on the use of fiducials for image guidance. The technique of tomotherapy that was used for radiotherapy delivery is also not widely used.

Hammoud et al. (Hammoud et al., 2008) evaluated PTV margins using 141 kV CBCT scans from 5 patients having prostate radiotherapy. They evaluated a 10/6 mm and 5/3 mm anisotropic margin, with a smaller margin posteriorly. They found that both margins allowed doses within 2% of the planned dose. The smaller margin allowed 30-50% sparing of high-dose region in the rectum and bladder, although seminal vesicle coverage was reduced with a 5/3 mm margin.

A major weakness of the Hammoud study was the small number of patients. In addition, only 72% of CBCTs could be used due to poor image quality in the rest. Although the patients had daily CBCT scans for research purposes, actual treatment verification and shifts were done using kV portal images. Therefore, the study could not assess the utility of the CBCT technique for imaging practice or assess the optimal frequency

of imaging. The dose calculation technique on CBCT was not described in detail. It appeared to be directly calculated on the CBCT using the treatment planning system, with no mention of a calibration table.

A more recent study evaluated both dose distributions and margin reduction in 18 patients with who were treated with daily CBCT verification (Maund et al., 2014). Manual contouring of the prostate CTV and rectum was done by a single oncologist. Dose distributions were calculated using the cone beam contours transposed on the planned dose distribution, although the method used has not been described in any more detail. The investigators went on to evaluate biological parameters such as tumour control probability (TCP) and normal tissue complication probability (NTCP).

Maund et al. found that there was no loss of TCP when plans with a 5-mm margin were re-optimized using 4 mm and 3 mm margins. Margin reduction was associated with a statistically significant reduction in rectal NTCP. The NTCP reduction was only 5% with a reduction in margin of 1 mm. However, if a 2-mm margin reduction was used, there was a 36% reduction in NTCP.

The strengths of the study include the high quality of the imaging, allowing contouring of structures on all the included images. NTCP was calculated based on the validated Lyman-Kutcher-Burman model.

The study cohort was small as only one CBCT per week was actually included in the analysis. As a result, the study could not be representative of the actual dose received throughout the course of radiotherapy. In particular, random variation in organ position cannot be assessed if only weekly CBCTs are analysed. The dose calculation technique was not specified in detail and no validation results were reported. Cumulative dose-volume histogram (DVH) curves were calculated by simple summation of the curves for seven fractions for each patient. TCP for the prostate and NTCP for the rectum were therefore not based on a voxel-based cumulative distribution.

A more recent study by Gill et al. evaluated PTV margins using daily CBCTs (Gill et al., 2015). They did not evaluate CBCT protocols. It was a retrospective study of five patients treated with hypofractionated radiotherapy 70 Gy in 28 fractions. Patients were treated with daily CBCT verification so a total sample size of 140 CBCT were available. Margins of 1, 3, 5, and 7 mm were used to created separate plans and dosimetric analysis carried out.

Gill et al. used a CBCT calibration chart methodology for dose calculation. They found that the actual cumulative CTVs V100% were 96.55% ± 2.94%, 99.49% ± 1.36%, 99.98% ± 0.26%, and 99.99% ± 0.05% for 1, 3, 5, and 7 mm uniform PTV margins, respectively. Delivered bladder and rectum doses were different to the planned doses, with the magnitude of differences increasing with PTV margin. Their conclusion was that when daily CBCT was used for soft-tissue alignment of the prostate, a 3 mm PTV margin allowed for CTV to be covered for 99% of cases. The main limitation of the study was the small sample size of five patients.

In summary, there are some dosimetric studies which have looked at the use of cone beam CT in prostate IGRT. However, there are significant weaknesses in these studies. Most studies did not evaluate daily CBCTs. Even in the single margin comparison study by Gill et al. which looked at daily CBCT, the number of patients was small. There remains no consensus on the optimum protocol for CBCT use in prostate radiotherapy. There is also no robust dosimetric validation of margin reduction with daily CBCT.

1.11 Study Objectives

The overall objectives of this MD(Res) project were:

1. To survey the current practice of image-guided radiotherapy for prostate cancer in the United Kingdom.
2. To validate a practical dose calculation strategy on cone beam CT
3. To assess the effects of CBCT verification imaging frequency on the actual dose delivered to the target volume and organs at risk during a course of image-guided radiotherapy (IGRT) for prostate cancer.
4. To compare the dosimetric effects of reduction of CTV-PTV margin with daily imaging.

Chapter 2. Survey of current IGRT practice in the UK

2.1 Background for IGRT survey

Image-guided radiotherapy (IGRT) has become the standard of care for delivery of radiation treatment for prostate cancer. In its broadest definition, it encompasses a wide range of techniques ranging from simple visual checks to advanced techniques incorporating specialist imaging. The clinical benefit of using advanced IGRT in prostate cancer has been demonstrated in retrospective studies (Zelefsky et al., 2012, Gill et al., 2011) which used fiducial marker techniques.

In the United Kingdom (UK), the need for advanced verification techniques was recognized by the National Radiotherapy Action Group in 2007 (Department of Health, 2007). They recommended that all new and replacement radiotherapy machines should have image-guided adaptive radiotherapy capability. The 2008 RCR report ‘On target: ensuring geometric accuracy in radiotherapy’ provided guidelines on verification for tumour sites including prostate (Royal College of Radiologists et al., 2008). Further guidance on the use of IGRT was provided by the National Radiotherapy Implementation Group (NRIG) in 2012 (National

Radiotherapy Implementation Group, 2012). A national program has also been in place to provide dedicated clinical support for IGRT implementation (Society of Radiographers, 2013).

A survey on the use of advanced radiotherapy technology in the UK was done in 2008 (Mayles and Radiotherapy Development, 2010). It demonstrated that there was limited availability of IGRT facilities, with only 26 of 50 centres even having kilovoltage imaging capability. Lack of equipment was also the main reason cited by centres not carrying out IGRT. Online MV imaging was the main mode of prostate IGRT, with 50% of centres using this verification technique. Since the 2008 survey, there have been improvements in radiotherapy equipment in the UK. 87% of current linear accelerators are less than 10 years old, according to the National Radiotherapy Equipment Survey (National Clinical Analysis and Specialized Applications Team, 2011). The data from this 2010 survey also shows that 23% of installed machines have 3D imaging capability.

The purpose of this survey was to evaluate the current status of prostate IGRT practice in the UK. In particular, it sought to identify the main verification strategies to be compared in the dosimetric analysis.

2.2 Survey methodology

59 NHS radiotherapy centres were identified from the 2012 RCR Clinical Oncology UK Workforce Report (The Royal College of Radiologists, 2013). Five private radiotherapy provider networks were also contacted. Centres were invited to the survey individually by phone, and respondents were identified by discussion with radiotherapy service managers. The survey was published using Opinio software, with online input of data. The survey was carried out from March 1, 2014 – April 30, 2014. An amendment to clarify one survey question was sent to all centres. Two reminders were sent to all centres which had not completed the survey.

The pre-tested semi-structured survey questionnaire tool had 23 questions on radical prostate radiotherapy (Appendix 1). Post-prostatectomy radiotherapy was not evaluated in this survey. Survey questions covered details of patient preparation, use of fiducial markers, treatment planning system, radiotherapy dose/fractionation, type of verification imaging and correction strategies. Free text fields were also provided to capture additional data on variations in protocols.

2.3 Survey results

50 NHS centres and three private radiotherapy providers responded giving an overall response rate was 83%. The survey was completed by physicists, radiotherapy dosimetrists, radiotherapy superintendents and specialist radiographers.

Patient preparation

There was a wide variation in bowel preparation protocols for prostate radiotherapy between centres. Daily micro-enemas (44%) and dietary information (35%) were the most common strategies used. Some centres reported using micro-enemas daily for the first 9-15 fractions followed by laxatives only if required. Five centres (9%) reported no fixed bowel preparation protocol.

The majority of centres had a bladder preparation protocol with the patient drinking a specified volume of water prior to treatment. The volume given ranged from 300 – 500 ml, followed by a 20-60 minutes' interval before radiotherapy treatment. Two centres used an empty bladder protocol, with one of these treating patients in the prone position.

Fiducial markers

30 centres (55%) did not use fiducial markers for any patients. 12 centres (22%) used fiducial markers for all prostate radiotherapy patients and nine centres (16%) used markers for selected patients. The availability of marker insertion slots was cited as a limiting factor.

In centres which used fiducial markers, the procedure was usually performed by a consultant urologist (43%). In 17% of centres an oncologist inserted the markers, while radiologists performed the procedure in 9%. Specialist nurses and specialist radiographers were also performing fiducial marker insertion (30%).

The majority of centres used three markers, but one centre reported using two markers per patient. One centre also reported the use of prostate-rectum spacers to reduce dose to rectum.

Radiotherapy planning and delivery

There is widespread use of advanced planning and delivery techniques for prostate radiotherapy. 23 (42%) centres used intensity-modulated radiotherapy (IMRT) for all radical prostate radiotherapy patients, and a further 16 (29%) centres used IMRT for at least 50% of their prostate patients. A variety of advanced delivery systems were used (Table 1), with some centres using different modalities for specific prostate cancer patient groups.

Table 1. Radical prostate cancer radiotherapy – external beam treatment delivery systems

Radiotherapy delivery system	Number of centres (%)
Volumetric modulated arc radiotherapy	34 (64%)
Static beam IMRT	31 (58%)
3-4 field conformal radiotherapy	29 (55%)
Tomotherapy	5 (9%)
Cyberknife	1 (2%)

Dose-fractionation regimens

The most commonly used external beam dose-fractionation regimen was 74 Gy/37# (Table 2). Dose escalation to 78 Gy or by using a HDR brachytherapy boost was carried out in only 6% of centres in this survey. Hypofractionated regimes were used in 24% of centres. Case selection criteria for dose-fractionation regimes were not assessed in this survey.

Table 2. Dose-fractionation regimens for external beam treatment in radical prostate radiotherapy

Dose-fractionation regime	Number of centres (%)
46 Gy to pelvis + HDR prostate boost	1 (2%)
78 Gy/39#	2 (4%)
74 Gy/37#	49 (89%)
60 Gy/20#	8 (16%)
57 Gy/19#	3 (6%)
64 Gy/32#	2 (4%)

Verification imaging

The main verification imaging type used in radical prostate radiotherapy was cone beam CT (CBCT) with soft tissue matching (Fig. 8), used in 35 centres (64%). 16 centres (29%) used fiducial markers in combination with imaging. This was usually in conjunction with KV imaging but seven centres used fiducial markers and CBCT. 5 centres (9%) used planar imaging only (3 portal MV, 2 portal KV). None of the centres reported using ultrasound for routine verification imaging.

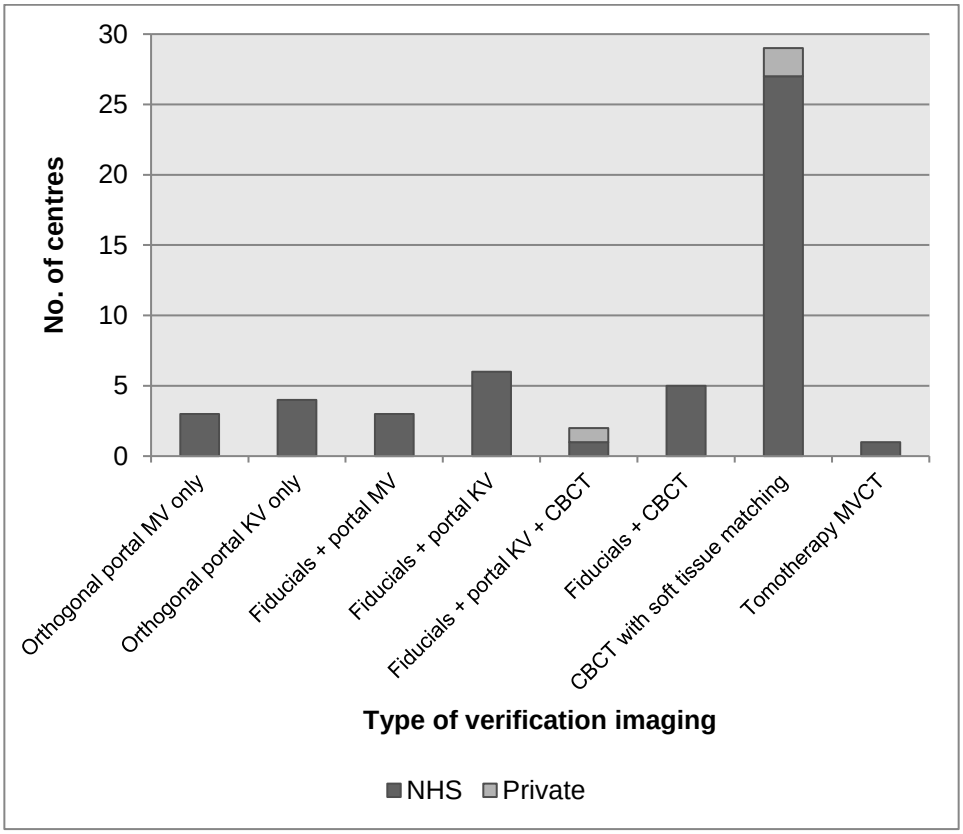

Fig. 8. Type of verification imaging in radical prostate radiotherapy

The most common verification imaging frequency was daily (Fig. 9), used by 32 centres (60%). 24 centres (45%) used a day 1-3 followed by weekly schedule, and four centres (8%) used a day 1-5 followed by weekly schedule. A combination of schedules was used in some centres that changed to daily imaging if there was concern about patient setup. 60% of centres which used CBCT repeated imaging during a fraction and set up the patient again if required.

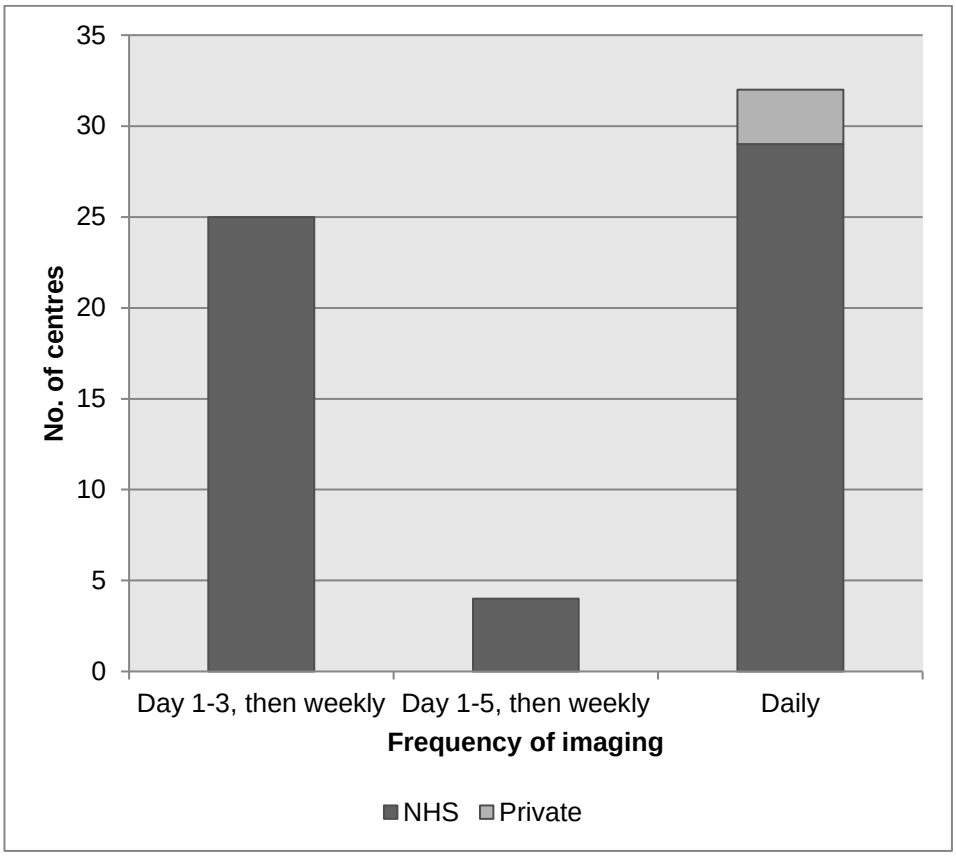

Fig. 9. Frequency of verification imaging in radical prostate radiotherapy

Correction strategy

A variety of correction strategies were described by centres. 41 centres (75%) stated they used an online correction strategy. 21 of these centres used a zero-tolerance protocol. However, 20 centres had an action level for online correction. The action level varied from 1-5 mm. Two centres reported using a combined online-offline protocol. 11 centres used an offline protocol (two with online imaging for part of protocol). 34 centres reported using a systematic correction, with a median threshold of 3 mm (range 1-6 mm). The median threshold for gross error setup correction was 10 mm (range 2-10 mm).

Private sector IGRT practice

In the three private sector providers who responded, all radical prostate radiotherapy was delivered with intensity-modulated radiotherapy. For image-guided radiotherapy, two providers used daily online CBCT soft tissue matching. The other provider used CBCT on day 1-3 and weekly, with daily online matching with fiducials and kV portal imaging on other days. Fiducial marker insertion was consultant-led in all cases.

2.4 Discussion of survey results

This survey captures data on current prostate IGRT practice in the United Kingdom. The high response rate of 85% amongst NHS centres minimized non-response bias. There was a 60% response rate amongst private provider networks, providing an insight into the service offered by non-NHS radiotherapy centres.

There were a few limitations in this survey. I did not evaluate the margins used during generation of the planning target volume. While the CTV-PTV margin should be based on individual institution setup errors, it may be influenced by the type of IGRT available. This study also did not specifically evaluate pelvic lymph node irradiation, which may be associated with specific challenges in relation to image guidance.

The high uptake of volumetric imaging for prostate IGRT shows a trend similar to that identified in surveys in the United States in 2009 (Simpson et al., 2010) and 2014 (Nabavizadeh et al., 2016). In the most recent survey done in the United States, 77% of IGRT for prostate radiotherapy was done using volumetric imaging, with 96% using daily imaging. They did not however find any relationship between frequency of imaging and the CTV-PTV margin employed by participating physicians.

There has been a clear improvement in utilization of advanced radiotherapy techniques in the UK, with a higher use of IMRT and advanced IGRT compared to previous UK surveys. However, there remain some inequities in provision of image guidance technology, with 5 NHS centres using planar imaging only. However, two of these centres specified that they were planning to introduce more advanced image-guided treatment within the next few months.

The majority of centres use a dose-fractionation regimen of 74 Gy/37#. A few centres have started to use dose escalation, in line with clinical trial results which show a benefit in progression-free survival (Kuban et al., 2008, Al-Mamgani et al., 2008) . However, 2 centres reported the use of 64 Gy/32#. This regimen has been shown to have lower toxicity, but lower progression-free survival (Dearnaley et al., 2014). With the widespread availability of advanced IGRT techniques, the use of dose escalation is likely to be better tolerated, and this lower dose regimen would not be considered standard of care in current practice.

In this survey, the use of fiducial markers for radical prostate radiotherapy appears limited. This appears to be related to resource limitations for fiducial insertion and the widespread availability of non-invasive on-board imaging techniques. The ongoing CHHiP IGRT sub-study is evaluating the

clinical outcomes of IGRT using fiducial markers and reduced margins, and long-term results of this study are awaited.

There are two main CBCT imaging frequency protocols currently in use in the UK. Over half the centres were using daily imaging, but many centres used a day 1-3 followed by weekly schedule. Daily online imaging has the best potential to correct for target position variation. However, concomitant pelvic dose of 1-2 Gy during a course of daily kV CBCT imaging (Sykes et al., 2013) should also be taken into consideration. Further research is required to determine the optimal schedule for CBCT verification.

There is continuing progress in image-guided radiotherapy, with the development of prototype hybrid MRI-linear accelerators (Lagendijk et al., 2008). However, this is still a research technology limited to a few centres in the UK. Further research is required on existing IGRT techniques to guide their optimum use. It would also be useful to incorporate details of IGRT technique into clinical trials to consolidate the evidence base for its use in prostate radiotherapy.

Chapter 3. Validation of dose calculation method

3.1 Ethical considerations

My study involved retrospective review of basic demographic and clinical information, radiotherapy plans and dosimetry data in Cancer Partners UK which is a private sector health care network. Institutional approval was granted by the Cancer Partners UK research review body.

All patients were treated in line with standard institutional clinical protocols. Radiation exposures were governed by Ionising Radiation (Medical Exposure) Regulations 2000 (IRMER) (Department of Health, 2000). No additional treatments or radiation exposures were done as a result of my study.

All patient data was anonymized and securely maintained only on a company network, in line with institutional data storage guidelines. The data management guidelines are compliant with the legislative provisions of the Data Protection Act 1998 (Great Britain, 1998).

3.2 Validation study - Material and Methods

37 consecutive CBCT scans from a patient undergoing radical prostate radiotherapy with daily IGRT were included. The total dose delivered was 74 Gy in 37 fractions using 7-field IMRT. The CBCT settings used were 120 kV, 64 mA/frame, 40 ms/frame, a medium field of view (FOV), 15 cm scan length and half fan mode. A full 360-degree acquisition was used at 180 degrees/minute. An amorphous silicon flat panel detector was used for detection. The maximum diameter for reconstruction was 410 mm with the medium FOV. All patients in this study had a medium FOV used. CBCT images were imported into the Pinnacle planning system and registration confirmed.

The prostate, rectum, bladder and pelvic bones were manually contoured on each CBCT slice (Figs. 10, 11). Manual contouring was required as automatic contouring software in development by the manufacturer could not be used on CBCT due to the differences in CT density compared to standard diagnostic CT scans.

At the time of this study, there were no commercial contouring packages which would accurately meet the needs of my investigation. Deformable image registration approaches have been attempted previously in

research settings but have achieved only modest results, with large proportions of unacceptable contours (Thor et al., 2011).

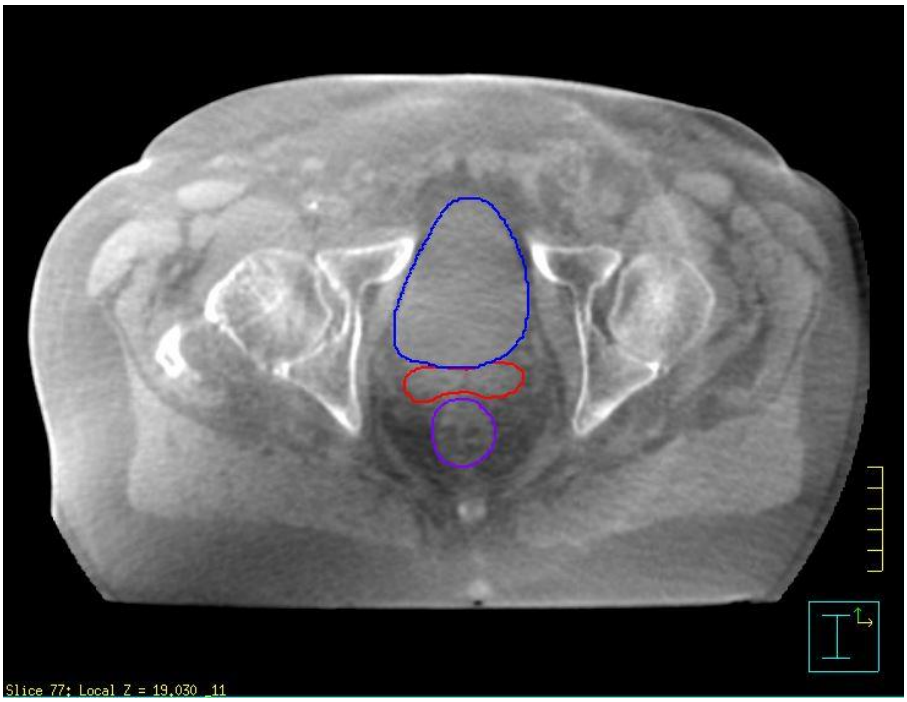

Fig. 10. Axial slice of CBCT showing contoured organs

Bladder (blue), CTV (red), rectum (purple)

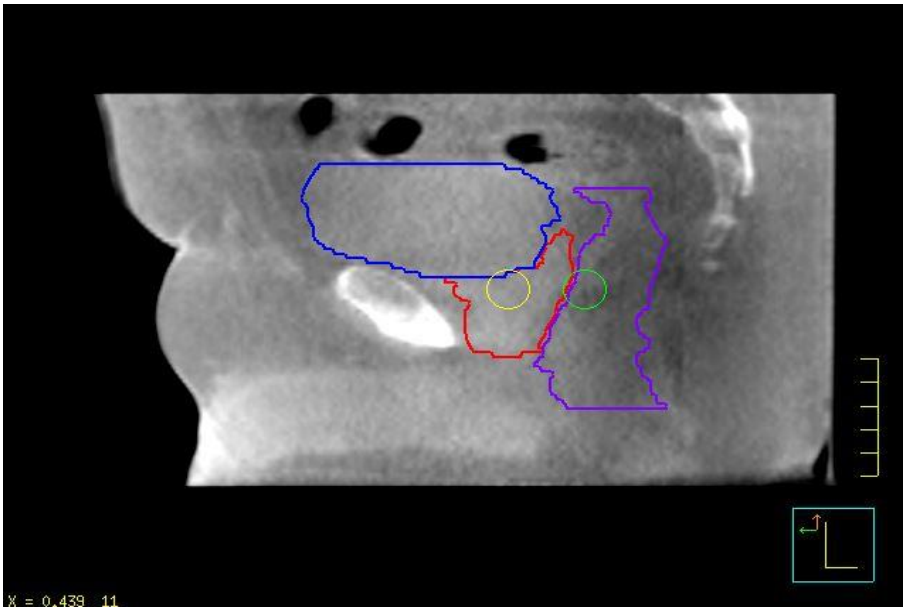

Fig. 11. Sagittal slice of CBCT showing contoured organs

Bladder (blue), CTV (red), rectum (purple)

CBCT contours were assigned to the planning CT and dose calculation performed using the planned treatment fields (Fig. 12). The background for the study technique was from previous prostate dosimetric studies (Orton and Tomé, 2004, Schulze et al., 2009). My hypothesis was that when IMRT with 7 fields is used, the key determinant of dosimetric changes would be organ movement.

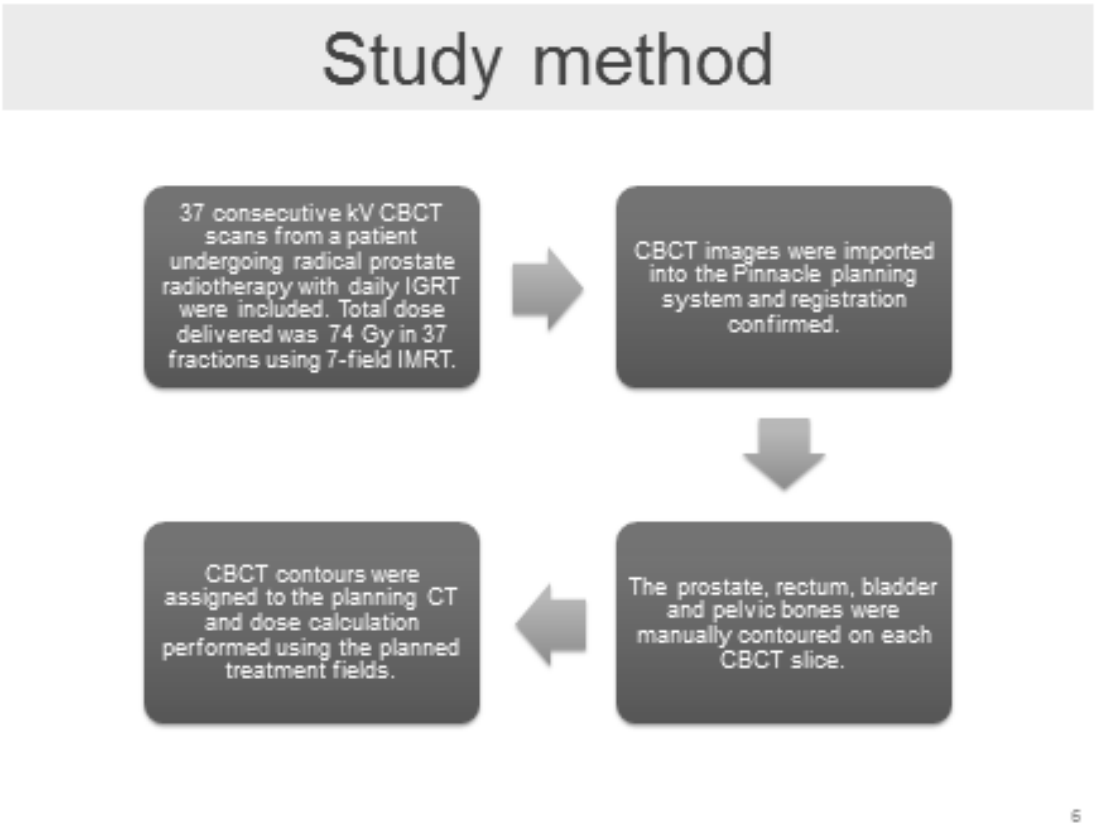

Fig. 12. Schematic of study method

A region of interest mapping approach was used for the comparator density-override method, as described by Fotina et al (Fotina et al., 2012). The same contours were used on CBCT scans, with CT densities for surrounding structures from planning CT (Fig. 13).

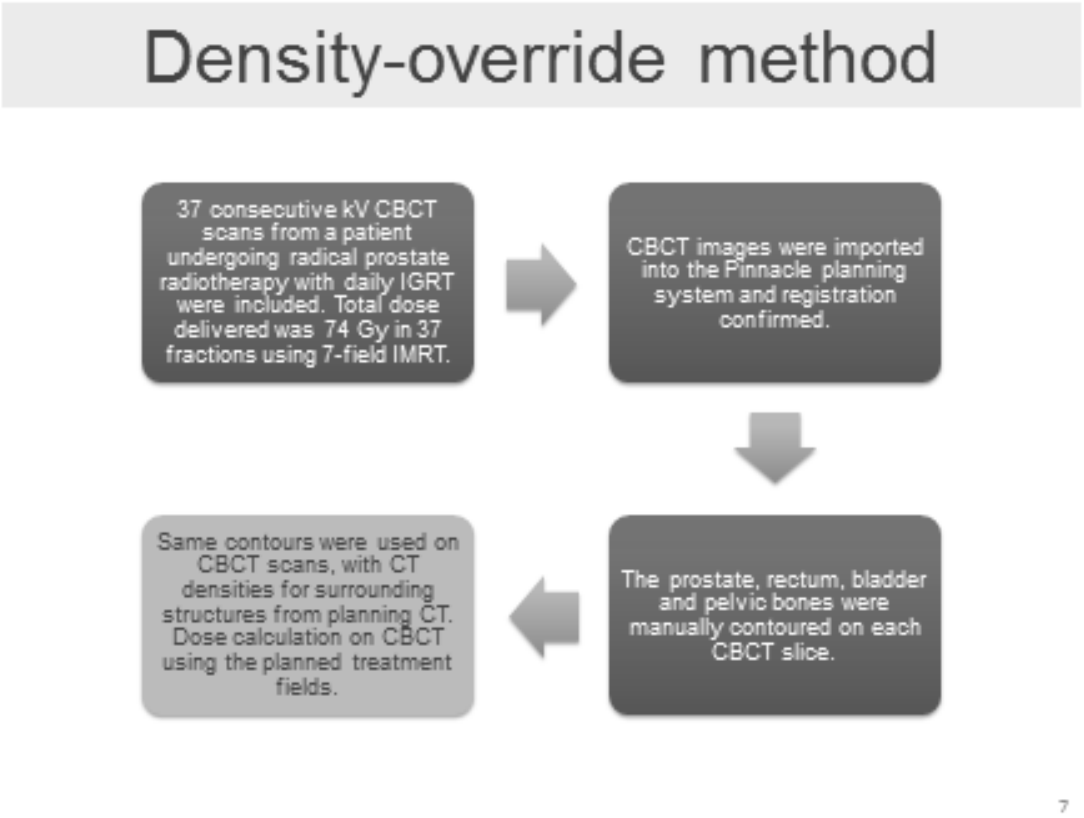

Fig. 13. Schematic of density-override method

Only the first 25 fractions could be used for the density-override method due to planning system capacity constraints. For the density-override technique, the dynamic planning feature of the Pinnacle treatment planning software was used. This added a series of CBCT for each

fraction cumulatively onto the treatment plan. The enormous number of CBCT images stored in each plan led to a progressive slowing of the planning software. At 25 fractions, the validation study had to be stopped for the density-override technique due to the system starting to ‘freeze’.

3.2.1 Statistical tests

Dosimetric parameters were compared using Pearson correlation for the first 25 fractions, using IBM® SPSS® statistical software. To assess agreement between the methods, a Bland-Altman plot was constructed by plotting the difference between results against the mean values. 95% confidence intervals for the difference were calculated to provide limits of agreement for the Bland-Altman plot.

3.3 Validation study - Results

The mean difference between methods was 0.28% for the PTV V95 and 0.64% for the rectal V50. There was excellent correlation between dosimetric results with CBCT contours on the planning CT, in comparison to the use of CBCT with density-override (Figs. 14, 15). The correlation was strongly statistically significant, with $p < 0.001$ in both cases (Table 3).

Table 3. Correlation between methods

Parameter	Pearson correlation coefficient r	p
PTV V95	0.93	$p < 0.001$
Rectal V50	0.98	$p < 0.001$

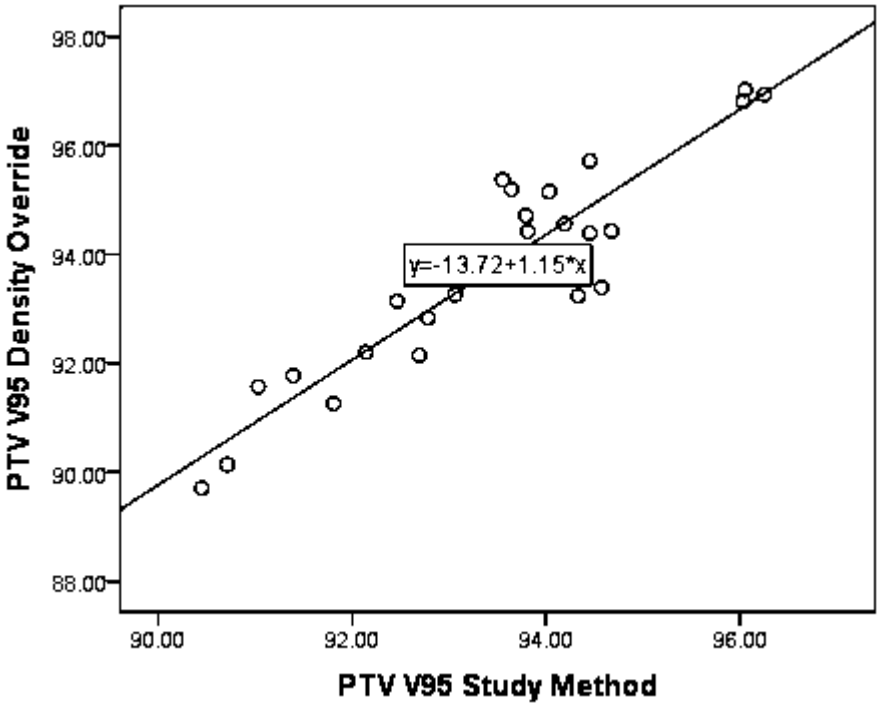

Fig. 14. Correlation between methods for PTV V95

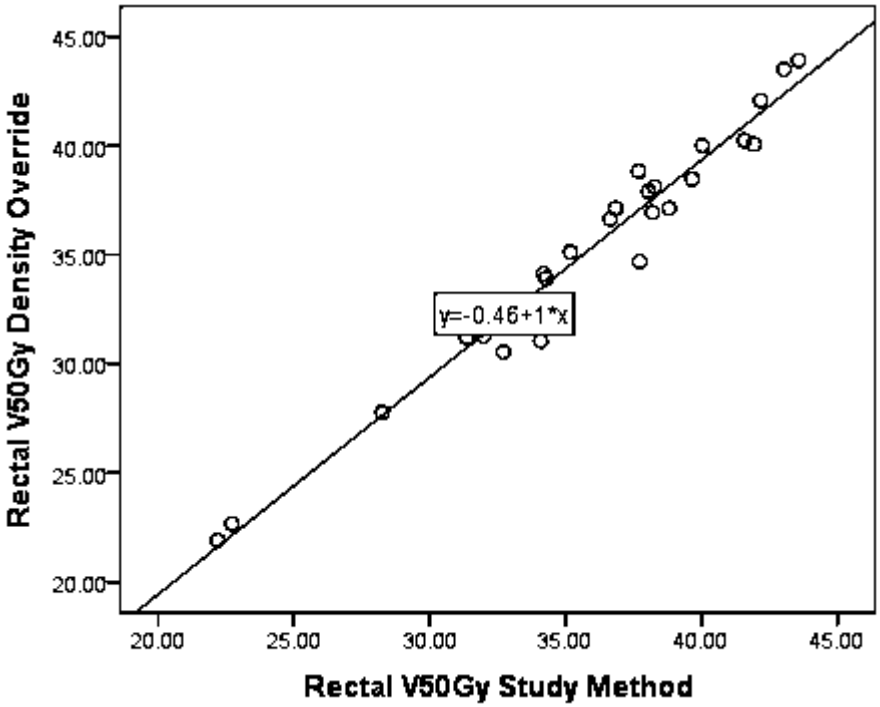

Fig. 15. Correlation between methods for rectal V50Gy

In addition to correlation, there appeared to be good agreement between the methods on plotting the trends of the values over the course of radiotherapy (Figs. 16, 17). Bland-Altman graphs were created to assess agreement statistically. The Bland-Altman analysis demonstrated low levels of bias and good agreement between the methods. All the measured points for PTV V95% fell between the 95% levels of agreement (Fig. 18). For the rectal V50Gy equivalent, 2 data points fell just outside the 95% level of agreement as can be seen in Fig. 19.

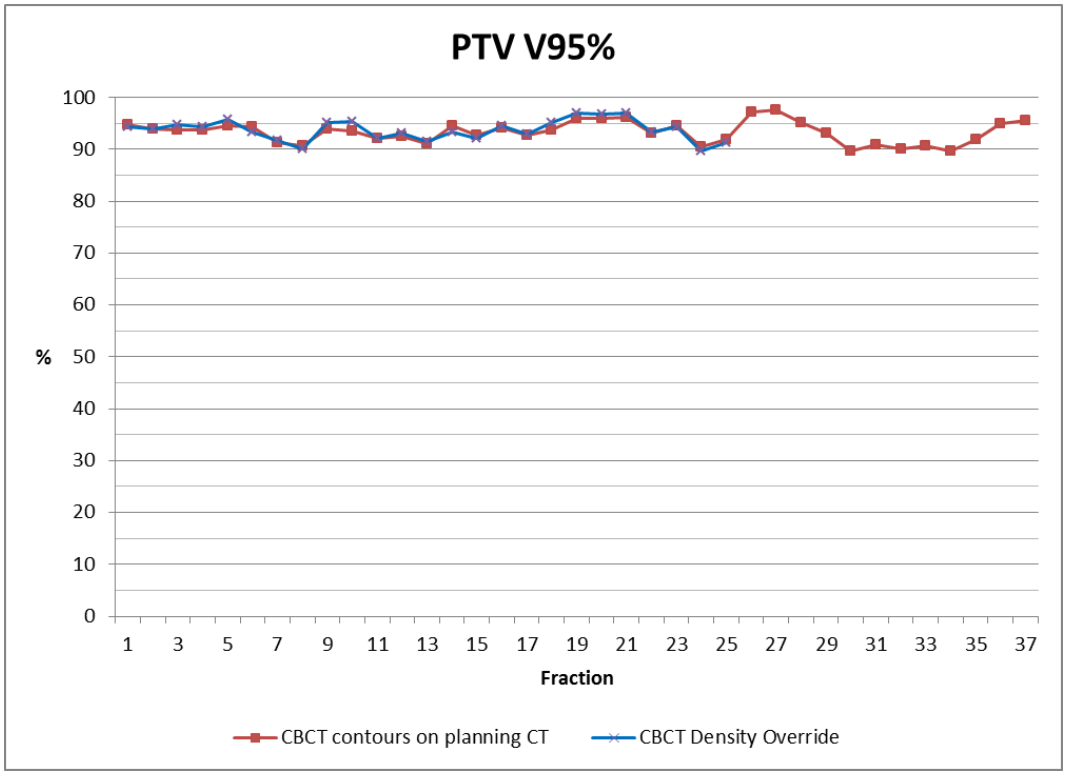

Fig. 16. PTV V95 – Comparison between study method and density-override method

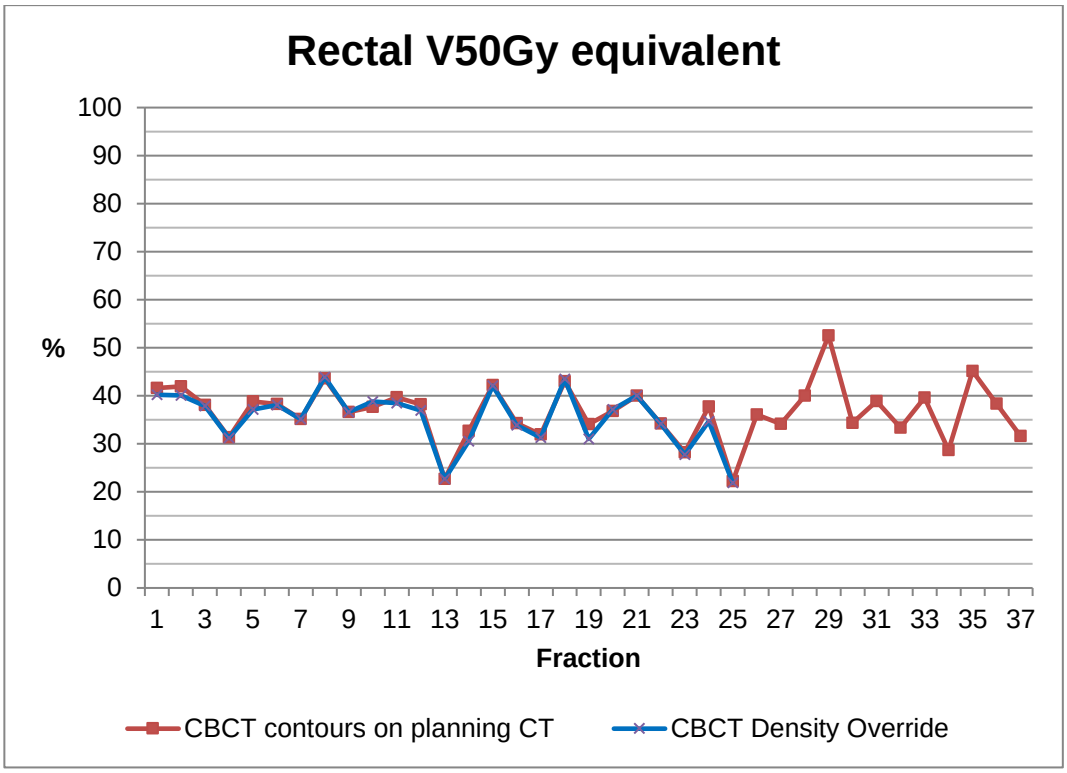

Fig. 17. Rectal dose – Comparison between study method vs density-override method

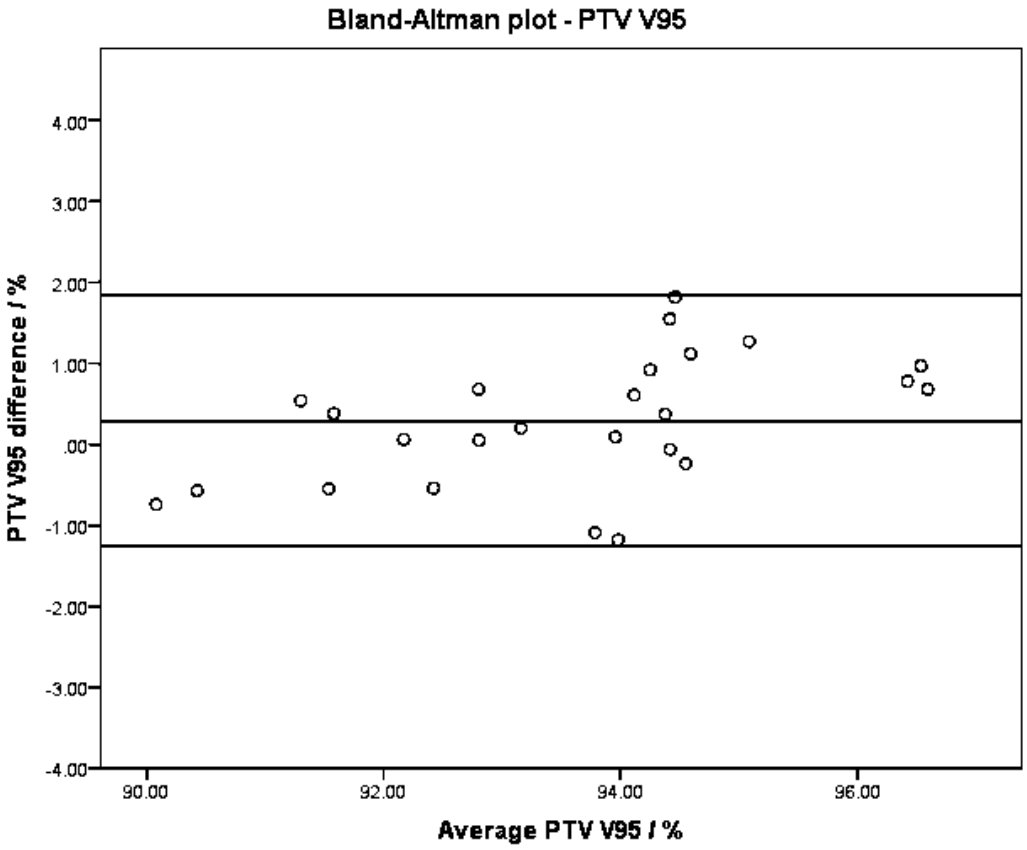

Fig. 18. Bland-Altman plot for PTV dose – study method vs density-override

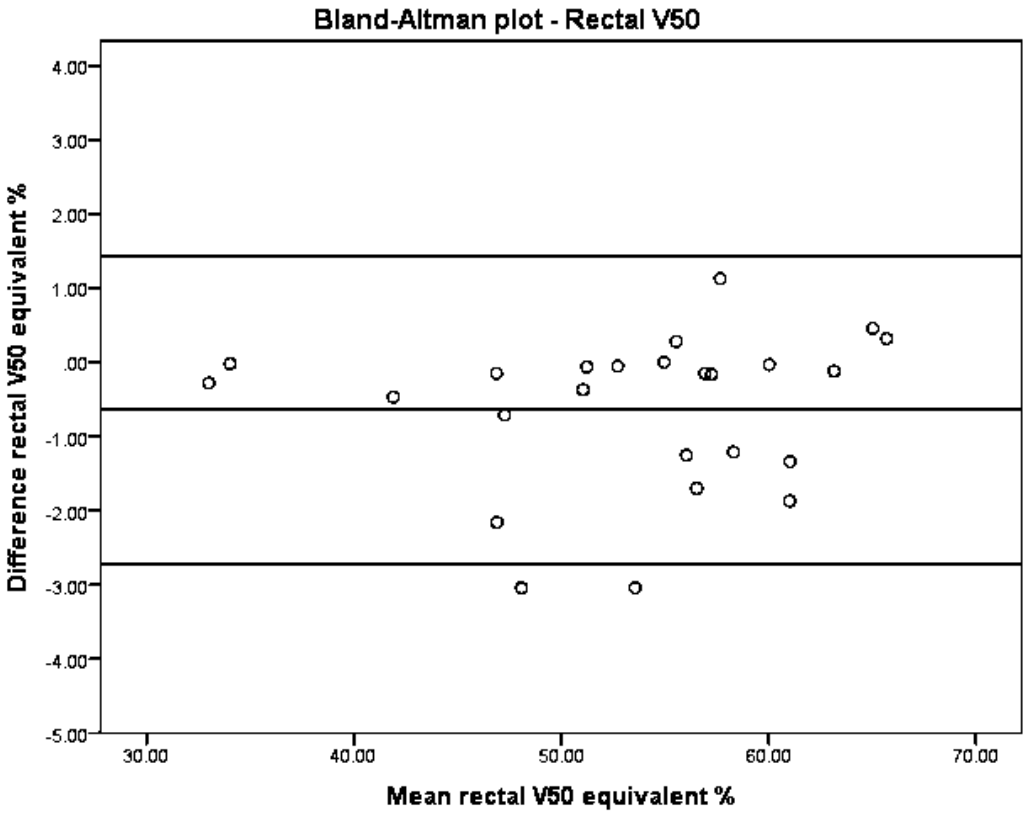

Fig. 19. Bland-Altman plot for rectal dose – study method vs density-override

3.3 Validation study - Discussion

The validation study was an essential exercise at the start of this MD(Res) project. It was useful to develop study workflow and processes, in addition to establishing the validity of dose calculation on CBCT using our method. This was particularly important due to the large-scale data movement between multiple software systems in radiotherapy.

The ROI mapping approach was chosen as a comparator based on my literature survey which showed that it gave the most consistent results for CBCT dose calculation. However, it was very time-intensive due to the need to outline multiple regions of interest for density replacement. As the number of contoured regions increased, there were increasing demands on processing power. This led to the system slowing down to critical levels, and the validation had to be stopped after 25 fractions for the ROI mapping method. Our study method proved to be much more resource-effective, which is an advantage.

A larger validation study would have been preferable. In retrospect, it might also have been preferable to do the validation study using random fractions of multiple subjects to evaluate inter-subject differences.

However, this would have limited our assessment of temporal changes during the course of radiotherapy, between the two methods.

The Bland-Altman technique was chosen to assess agreement. This is because there are limitations to using Pearson correlation to assess agreement between measurements (Martin Bland and Altman, 1986). Correlation provides an indication of the strength of a relationship between two variables. As long as the two variables plotted against each other approximate a straight line, the correlation would be high. However, the values of the variables may be systematically different from each other despite high correlation. Therefore, Bland and Altman suggested the use of a graphical plot of agreement using the difference between measurements against the mean measurement.

There was very good correlation and agreement between methods for key parameters chosen for target coverage and rectal dose. The limits of agreement are in line with the errors observed on other CBCT dose calculation methods. The study also established the feasibility of using the study method with a streamlined and time-effective workflow. This is of relevance if the method is to be used for adaptive radiotherapy. Considering all of the above factors, the study method was selected for use in my dosimetric research.

Chapter 4. CBCT comparison with bone match verification

4.1 CBCT comparison with bone match – materials and methods

592 CBCT verification images from 14 patients who received radical prostate radiotherapy and had a complete CBCT dataset were analysed. All patients received a dose of 74 Gy in 37 fractions of 2 Gy using 7-field step-and-shoot IMRT.

Daily online CBCT soft tissue match verification was done using the Elekta XVI system. The CBCT settings used were 120 kV, 64 mA/frame, 40 ms/frame, a medium field of view (FOV), 15 cm scan length and half fan mode. A full 360-degree acquisition was used at 180 degrees/minute. An amorphous silicon flat panel detector was used for detection. The maximum diameter for reconstruction was 410 mm with the medium FOV. All patients in this study had a medium FOV used.

A bone match verification strategy was used for the study comparison arm, with imaging on day 1-3 followed by weekly. Bone match results were

obtained using automated analysis of bony anatomy on CT. CBCT images were imported into the Pinnacle treatment planning system. CTV, bladder and rectum were contoured manually on each image.

A 7-mm margin in all directions was used on the CTV to obtain the planning target volume. Soft tissue and bone match shifts were applied to each CBCT image. CBCT contours were overlaid on planning CT scan for dose-volume analysis. Dose-volume parameters were assessed for CTV, rectum and bladder.

4.1.1 Statistical tests

Statistical analysis was carried out on IBM® SPSS® version 22. Shapiro-Wilk testing was carried out to assess normality of the difference between paired parameters (SHAPIRO and WILK, 1965). Means and standard errors of means were used to describe normally distributed variables. For variables which violated assumptions of normality, medians and ranges were used to describe the data. Related-sample Wilcoxon signed rank test was used to do non-parametric testing for CTV and PTV variables (Wilcoxon, 1945). Two-sided tests were conducted in all cases, with a level of statistical significance of 5%.

4.2 CBCT comparison with bone match - results

There was improved target coverage with CBCT soft tissue matching in comparison to a bone match protocol. This effect was seen with both CTV V95% and CTV V98% (Fig. 20, 21) on fraction-by-fraction analysis.

Fig. 20. CTV V98 for daily CBCT protocol

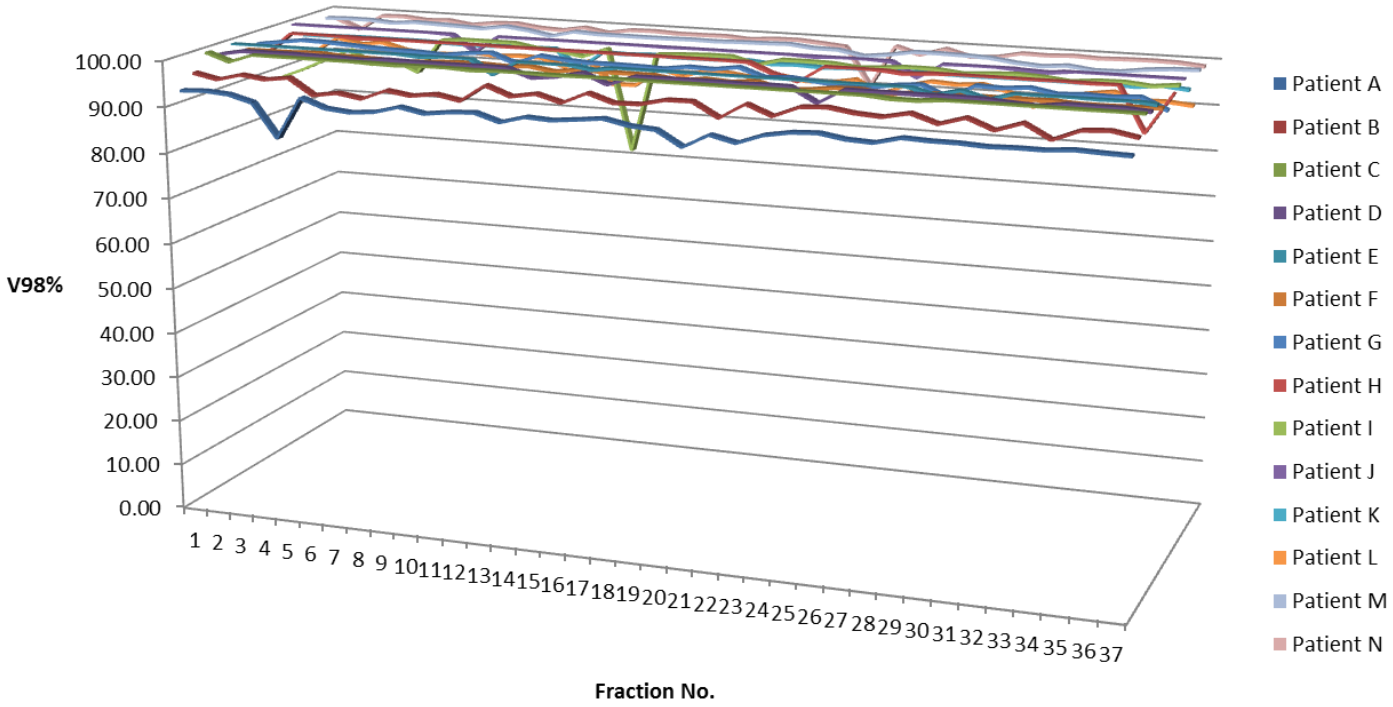

Fig. 21. CTV V98 for bone match

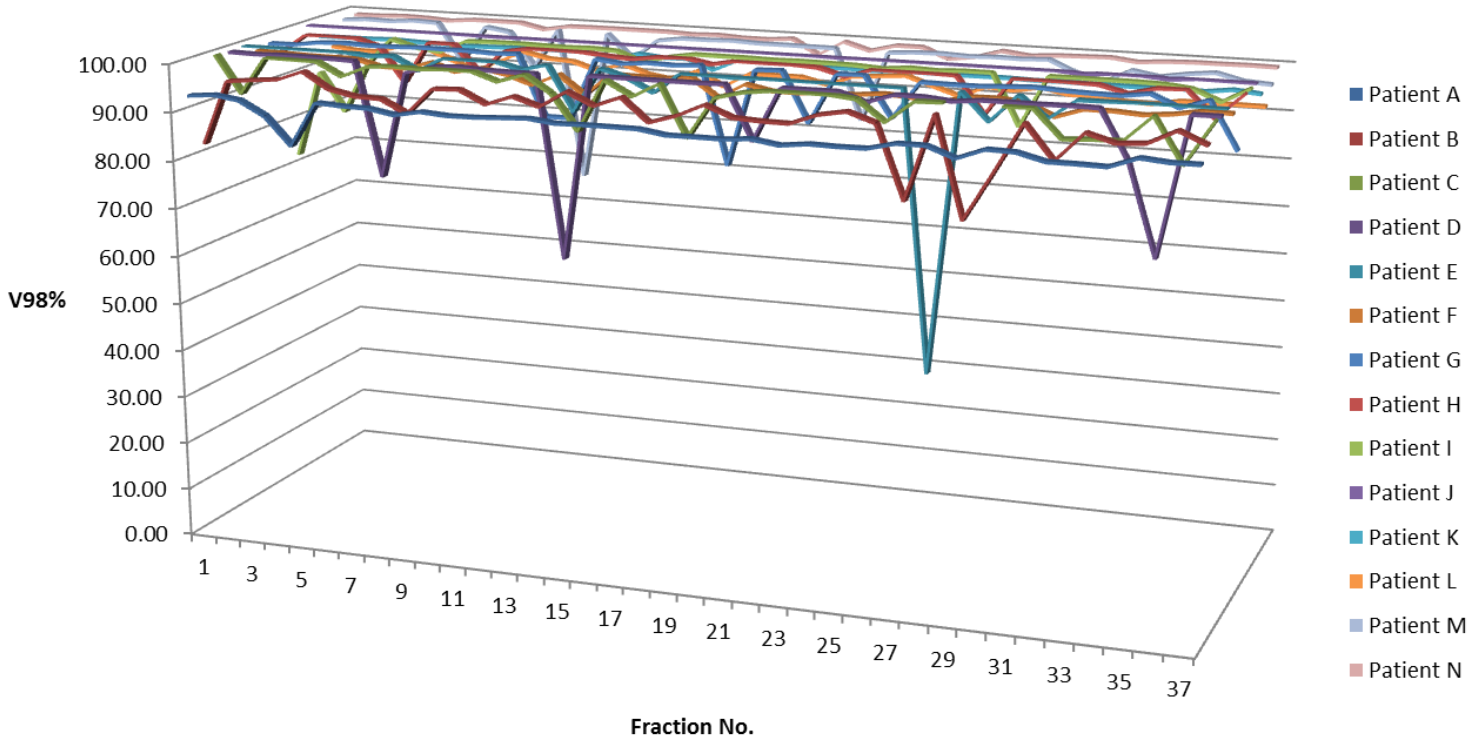

Wilcoxon signed-rank test was used to compare non-parametric dosimetric thresholds for paired samples. There was a significant improvement in CTV coverage and reduction in rectal dose with daily online CBCT (Table 4).

Table 4. Daily CBCT vs bone match

Variable	**Daily CBCT protocol Median% (interquartile range)**	**Bone match protocol Median% (interquartile range)**	**Wilcoxon signed-rank test significance**
CTV V95	99.96 (0.13)	99.50 (1.12)	$p < 0.05$
CTV V98	98.42 (2.96)	97.12 (2.20)	$p < 0.05$
Rectal V50	32.62 (9.53)	35.29 (11.69)	$p < 0.05$

There were reductions in rectal V50Gy in 13/14 patients with a daily online CBCT verification strategy compared with a bone match protocol. The biggest reductions were observed in patients G and H who had relatively high V50Gy (Fig. 22).

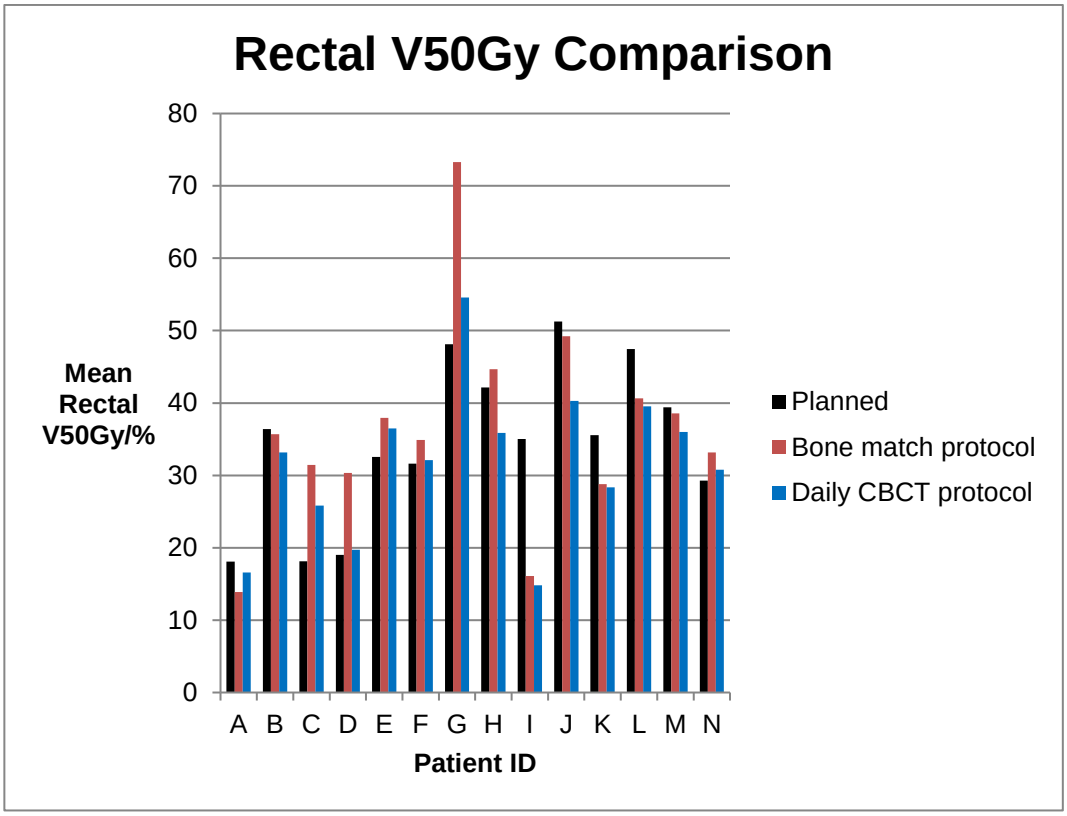

Fig. 22. Rectal V50Gy comparison – planned dose vs bone match protocol vs daily CBCT protocol

4.3. CBCT comparison with bone match – discussion

This cohort demonstrated that use of a day 1-3 followed by weekly bone match protocol led to frequent drops in target coverage during the course of radiotherapy. The improved target coverage with CBCT may be due to both the additional frequency of imaging and the additional soft tissue detail allowing accurate target verification.

This sub-study utilized automated cone beam CT bone matching. This is likely to be more accurate than portal imaging bone matching due to the better image quality. It is therefore likely that use of kV or MV portal imaging for bone match is likely to lead to even worse results in target coverage.

It is reassuring that the rectal dose was also reduced by the use of cone beam CT soft tissue matching. The reductions in rectal dose were of relatively small magnitude for most patients. However, for the patients with the highest V50Gy at planned, CBCT matching appeared to provide most benefit in this cohort.

Chapter 5. CBCT protocol and margin comparison

5.1 CBCT protocol and margin comparison – objectives

1. To assess the effect of frequency of CBCT verification imaging on the dose-volume parameters of the target volume and organs at risk during a course of IGRT for prostate cancer. The study compares two established IGRT protocols:
    a. Daily CBCT imaging with online correction prior to every treatment fraction.
    b. CBCT imaging prior to fractions 1 to 3 and subsequently once weekly. Online corrections are applied prior to treatment for every fraction on which CBCT is carried out. Following the first three fractions the systematic error is calculated and a systematic setup correction applied for any error that is ≥ 0.5 cm.

2. To assess the dosimetric impact of reducing the PTV margin, when daily online imaging is used.

5.2 CBCT protocol and margin comparison - materials and methods

The null hypothesis for this stage of the project was that there is no difference between daily imaging and weekly imaging for prostate target coverage and organ at risk dose.

844 CBCT verification images from 20 patients undergoing radical prostate radiotherapy were analysed retrospectively. Patients were treated between Feb 2012 and Aug 2013 for localized prostate cancer. Organ contouring on the planning computed tomography (CT) scan was carried out by the treating oncologist. The CTV included the prostate and base of seminal vesicles. A uniform margin of 7 mm around the CTV was used to generate the planning target volume (PTV). None of the patients had pelvic lymph node radiation.

Treatment planning was carried out on Philips® Pinnacle^3 software. The planning constraints used are listed in Table 4. ICRU 83 guidelines (Gregoire and Mackie, 2011) recommend the use of median dose D50, near max dose D2, near min dose D98 for the PTV during IMRT planning and reporting. However, these guidelines had not been implemented in the study centres at the time of initial planning of the study patients. The organ

at risk constraints are based on the UK prostate CHHiP clinical trial protocol. These constraints have been shown to lead to better rectal sparing than the MRC RT-01 trial constraints (South et al., 2008).

Table 5. Radiotherapy planning constraints

Organ	Parameter	Constraint
CTV	V95%	100%
PTV	V95%	≥98%
Rectum	V50Gy	< 60%
	V60Gy	< 50%
	V65Gy	< 30%
	V70Gy	< 15%
	V74Gy	< 5%
Bladder	V50Gy	< 50% (optimal)
	V65Gy	< 50% (mandatory)
	V74Gy	< 5%
Small bowel	V50Gy	< 17cc
Femoral heads	V50Gy	< 50%

Patients were treated supine with a comfortably full bladder and were all given dietary advice to minimize rectal distension. Laxatives were used only if required to manage constipation. All patients received a dose of 74 Gy in 37 fractions over 7½ weeks using 7-field intensity-modulated radiotherapy (IMRT) delivered on the Elekta® linear accelerator platform. Early toxicity was assessed using the RTOG acute radiation morbidity scale (Cox et al., 1995).

During treatment, patients had daily online CBCT soft tissue match verification using the Elekta XVI system. Concomitant dose from CBCT was measured using a Perspex phantom using the CT dose index ($CTDI_w$) method (Murphy et al., 2007). 4 imagers were used in the study and the relevant CTDIw measurements are shown in Table 6.

Imager	CTDIw (mGy)
1	25.2
2	27.5
3	27.6
4	30.3

Table 6. CTDIw measurements for CBCT imagers used in study

The CBCT settings used were 120 kV, 64 mA/frame, 40 ms/frame, a medium field of view (FOV), 15 cm scan length and half fan mode. A full 360-degree acquisition was used at 180 degrees/minute. An amorphous silicon flat panel detector was used for detection. The maximum diameter for reconstruction was 410 mm with the medium FOV. All patients in this study had a medium FOV used. The F1 filter setting was used to incorporate an aluminium bowtie filter to reduce skin dose and improve image quality. An amorphous silicon flat panel detector was used for detection.

The time required for CBCT review was assessed in a timing study for 92 CBCT images across 3 centres. The mean acquisition time per CBCT was 130 seconds (range 118 – 175 seconds). The mean time required for review by the treatment radiographer was 100 seconds (range 32 – 326 seconds). The total additional time during treatment fractions was 232 seconds (range 130 – 462 seconds).

If the initial CBCT indicated a significant issue with anatomy (e.g. rectum too full or bladder too empty) the patient was taken off the bed and encouraged to visit the bathroom and walk around, after which they were setup again and CBCT carried out again prior to treatment. Online soft tissue match verification with a 0-cm action level was carried out by one treatment radiographer, and checked by a second treatment radiographer.

Radiographers were accredited for CBCT verification on completion of an in-house training package.

All CBCT images were imported into the Pinnacle^3 treatment planning system. Target volume and organs at risk were contoured manually on each CBCT image by a single investigator, and separately evaluated by the supervising radiation oncologist. Contouring of normal organs was based on the consensus RTOG contouring atlas (Gay et al., 2012). A 7-mm margin in all directions was used around the CTV to obtain the PTV.

Soft tissue match shifts were separately applied to each CBCT image. For the daily imaging protocol, the actual shifts were applied to every CBCT. For the weekly protocol, soft tissue match shifts were applied to imaging days and a systematic correction was applied to non-imaging days, where required. The average was taken from first three days and if any value was greater than 5mm then a systematic correction was applied for that direction.

Systematic and random errors were calculated for the population according to standard calculation formulae (Royal College of Radiologists et al., 2008). First, the overall mean population set-up error (M_{pop}) was calculated using the formula:

$M_{pop} = (m_1+m_2+m_3+\ldots. +m_p) / P$

In this equation, m_1, m_2, m_3…were the means for each individual patient, and P is the number of patients in the analysed group.

The systematic error for the population ($\Sigma_{set\text{-}up}$) was defined as the standard deviations of the mean set-up error about the overall population mean (M_{pop}). The individual random error ($\sigma_{individual}$) was defined as the standard deviation of the setup errors around the mean individual error (m). The population random error ($\sigma_{set\text{-}up}$) was the mean of all the random errors.

The CBCT contours were superimposed on the planning CT scan for dose-volume analysis as described in the validation study methodology (section 3.2). The same contours were used for comparison of a daily online schedule with a protocol of day 1-3 followed by weekly imaging. For the margin comparison, plans were recalculated on Pinnacle with 3 mm and 5 mm margins all around the CTV. Dose calculation was done on Pinnacle^3 version 9.6 using the collapsed cone convolution algorithm (Ahnesjo, 1989).

Dose-volume parameters were assessed for the PTV, CTV, rectum and bladder. As described above, our institution used a V95% threshold during treatment planning. Therefore, the PTV and CTV dose in the study was assessed using the V95%. A target value of 99% was chosen for the CTV V95% coverage, in line with the Stroom threshold for margin calculation (Stroom et al., 1999). The V98% was also assessed for the CTV as a more sensitive indicator of high dose coverage. The V50Gy, V65Gy, mean dose and D2cc were compared for the rectum. The selection of rectal dose parameters to be reported was based on published data which have identified these thresholds as relevant to toxicity (Chennupati et al., 2014). The V65Gy and mean dose were compared for the bladder.

5.1.1 Statistical methods - sample size calculation

Preliminary sample size estimation was carried out prior to data collection. Sample size calculation was done using the open-source software G*Power© version 3.1.9.2. Rectal toxicity reduction was chosen as the primary outcome for sample size estimation purposes. I used an estimated reduction of 1 Gy in mean rectal dose when daily imaging was used. This was based on estimates of potential benefit with online adaptive radiotherapy obtained from a simulation study (Schulze et al., 2009).

I used an alpha value of 0.05 to minimize type 1 error and a beta value of 0.95 to minimize type 2 errors. The estimated total sample size for a paired t-test approach was 16. A sample size of 20 was therefore utilized in my study to provide a further margin of power and accuracy.

5.1.2 Statistical methods - analysis of results

Statistical analysis was carried out on IBM® SPSS® version 22. Shapiro-Wilk testing was carried out to assess normality of the difference between paired parameters. Means and standard errors of means were used to describe normally distributed variables. For variables which violated assumptions of normality, medians and ranges were used to describe the data. The Hodges-Lehman estimate (Hodges and Lehmann, 1963) was used to assess the difference between medians for these variables.

In the protocol comparison, related-sample Wilcoxon signed rank test was used to do non-parametric testing for CTV and PTV variables (Wilcoxon, 1945). Paired t test was used for parametric testing of rectal and bladder variables which were normally distributed.

For the comparison of the three PTV margins, Friedman's test (Friedman, 1937) with Bonferroni correction was carried out for CTV V95% as it was not normally distributed. Repeated measures ANOVA with Bonferroni correction was used for the margin comparison of the parametric rectal and bladder dosimetric results. Two-sided tests were conducted in all cases, with a level of statistical significance of 5%.

5.3 CBCT Protocol comparison - Results

All study patients had localized prostate adenocarcinoma (stage T1-2 N0 M0) with histological confirmation. Patients tolerated the radiotherapy treatment protocol well, with minimal acute toxicity. There was no RTOG Grade 3 or 4 rectal or bladder toxicity during treatment.

844 CBCT scans were included in the study. The population setup errors were calculated using shifts from the daily imaging protocol. The population mean setup error was 0.01 cm (left-right), 0.05 cm (supero-inferior) and -0.13 cm (antero-posterior). The population systematic error (Σ) was 0.27 cm (left-right), 0.15 cm (supero-inferior) and 0.38 cm (antero-posterior). The population random error (σ) was 0.23 cm (left-right), 0.17 cm (supero-inferior) and 0.31 cm (antero-posterior). The setup errors in my investigation are in line with a previously published CBCT verification imaging series (Mayyas et al., 2013).

The median number of CBCT scans per patient was 43 (range 37-48). The most common reason for re-imaging was excessive rectal gas. The quality of the CBCT images was adequate in the clear majority of cases, allowing contouring of the prostate, rectum and bladder. Artefact due to rectal gas affected contouring of the prostate and rectum in only 5 fractions in the

entire cohort (0.6%). In each of these cases, the patients went on to have a 2nd CBCT for the fraction, which was contoured to evaluate the daily treatment schedule. In 6 out of 20 patients, the dome of the bladder was not included in the CBCT scan volume. CTV volume on cone beam CT showed minimal variation from the original CTV. The mean change in CTV volume from the planning CT was 0.2% (range –1.9% to +2.1%) (Fig. 23).

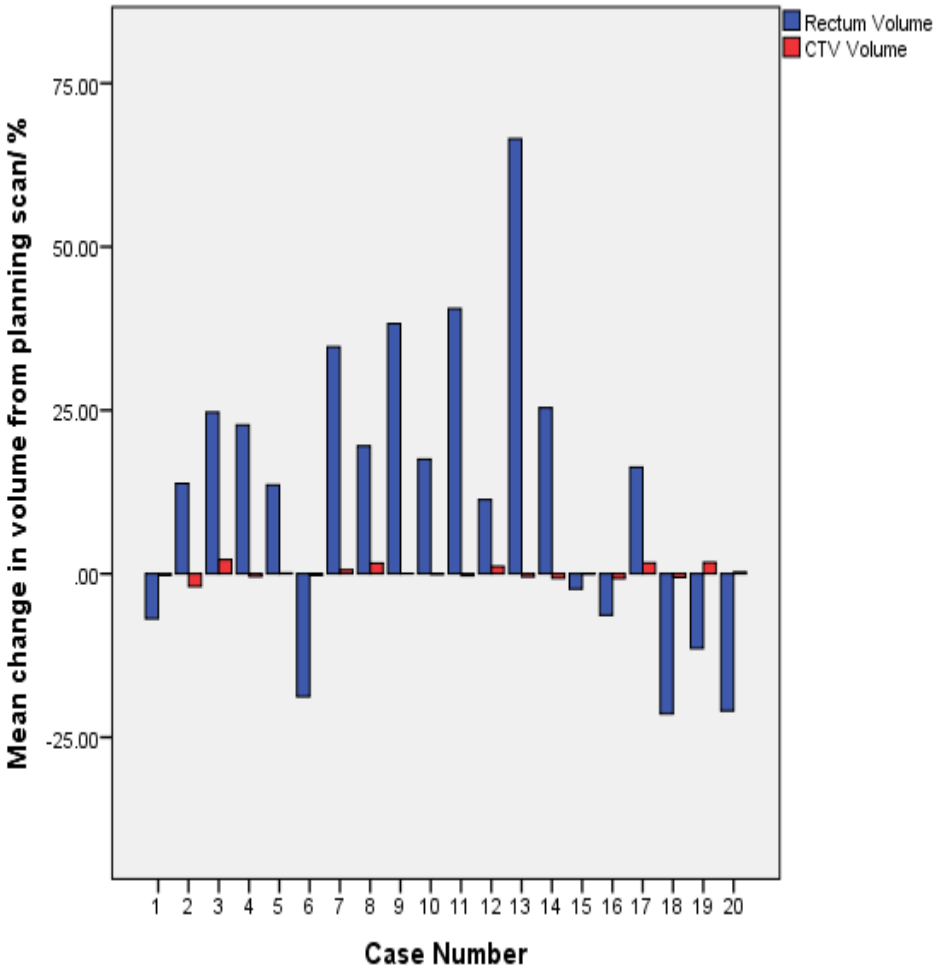

Fig. 23. Mean Rectal and CTV volume change from planning CT

Blue – Rectal volume, Red – CTV volume

Rectal volume showed major fluctuations from the volume on the planning CT scan, throughout the course of treatment. The mean rectal volume during treatment was higher than the planning CT volume in the majority of cases. The mean change in rectal volume from planning volume was 12.8% (range -21.4% to 66.5%). However, there were increases in rectal volume up to 180% of planning volume during treatment (Fig. 24).

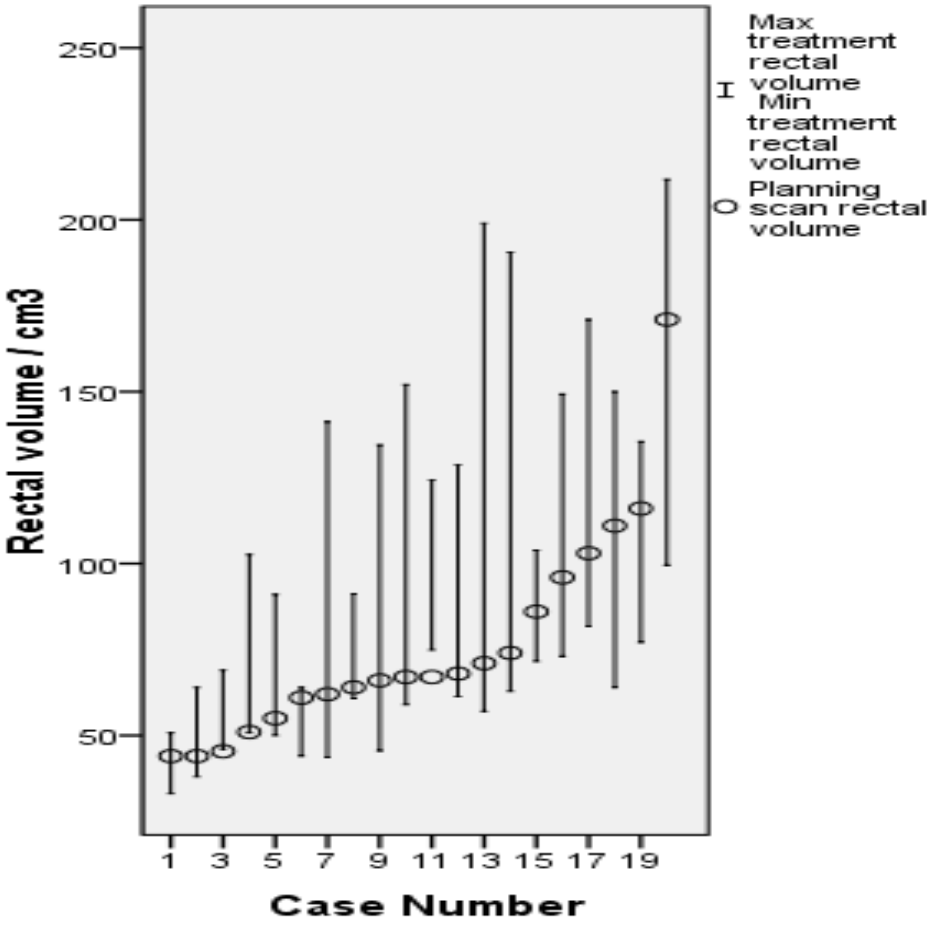

Fig. 24. Change in mean treatment volumes from volume on planning CT scan

There was a moderate correlation between the rectal volume on planning CT scan and the range of rectal volume variation on CBCTs during treatment (Pearson's R = 0.46, $p < 0.05$). However, high rectal volumes on the initial planning CT scan were not associated with a reduction in CTV coverage during treatment, both in the weekly (Spearman's rho 0.1, $p > 0.05$) and daily (Spearman's rho -0.05, $p > 0.05$) CBCT groups (Fig. 25).

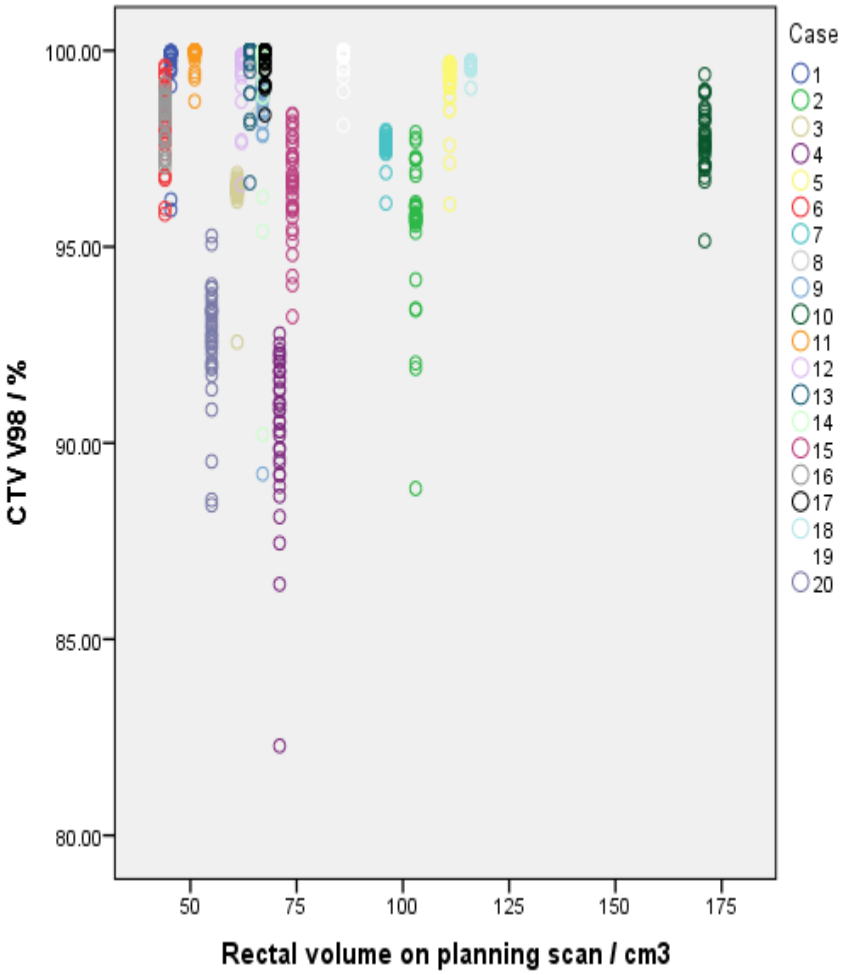

Fig. 25. CTV V98% variation with rectal volume on planning scan

There were improvements in PTV and CTV coverage with daily imaging compared to weekly imaging (Table 7). The There was a 3% improvement in PTV V95% and a 1% improvement in CTV V98% (Hodges-Lehman estimates of difference between medians, $p < 0.001$ on Wilcoxon sign rank testing).

Table 7. Median target volume coverage parameters – daily online vs weekly online verification

Parameter	Daily Online (IQR)	Weekly Online (IQR)	p
PTV V95 / %	94.36 (93.33 – 95.51)	90.97 (88.68 – 92.03)	$p < 0.001$*
CTV V95 / %	99.98 (99.92 – 100.00)	99.74 (98.96 – 99.82)	$p < 0.001$*
CTV V98 / %	98.90 (96.80 – 99.70)	97.65 (95.94 – 98.53)	$p < 0.001$*

n = 20, PTV – Planning target volume, CTV – Clinical target volume, IQR – Interquartile range

*Related-sample Wilcoxon signed-rank test, significant at $p < 0.05$

90% of patients had improvement in prostate target coverage with daily online imaging in comparison to weekly online imaging. Daily online imaging was the best verification protocol, with a median of 37 fractions (out of 37) achieving CTV coverage with daily imaging compared with 34 fractions with the day 1-3 then weekly online protocol (Fig. 26).

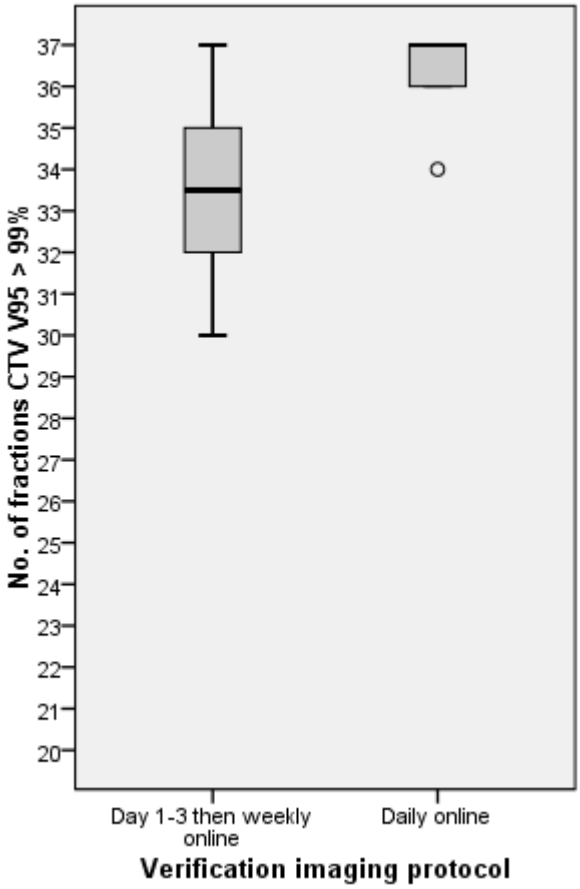

Fig. 26. CTV coverage – Comparison of verification imaging protocols

80% of patients had a reduction in rectal dose with the daily imaging protocol, in comparison to the weekly protocol. On dosimetric analysis, there was a 1.12 Gy reduction in mean rectal dose (Table 8). There was no statistically significant difference in the high-dose region parameter D2cc. There were no significant differences in bladder dose, with the V65Gy and mean bladder dose at low levels with both protocols.

Table 8. Mean pelvic organ at risk parameters – daily online vs weekly online verification

Parameter	Daily Online	Weekly Online	Difference: Daily - Weekly	SEM	p
Rectal V50Gy / %	32.48	34.96	-2.49	0.99	p < 0.05†
Mean rectal dose / Gy	36.56	37.68	-1.12	0.52	p < 0.05†
Rectum D2cc/Gy	73.37	73.35	0.02	0.22	NS†
Bladder V65Gy / %	10.32	9.90	0.42	0.30	NS†
Mean bladder dose / Gy	23.13	22.82	0.31	0.28	NS†

n = 20, SEM – Standard error of mean, NS – Not significant

†Paired t test, significant at p < 0.05

There were 82 radiotherapy fractions where additional CBCT imaging was performed during daily imaging (excluding the first 3 fractions). The daily imaging protocol led to detection of rectal distension and under-filling of the bladder. There was a 17% mean reduction in rectal volume and 52% mean increase in bladder volume in fractions where CBCT imaging was repeated after review. The CTV V98 increased from 92.4% to 97.5% in these fractions.

The magnitude of benefit of daily imaging for a patient could not be predicted by characteristics on the planning CT scan. No significant univariate correlations were identified between the differences in CTV coverage with factors such as rectal volume at planning, mean rectal volume over first 3 fractions, mean treatment rectal volume, CTV volume, initial bladder volume and mean treatment bladder volume.

On unpaired analysis of daily imaging data, there was an association between an increased rectal volume and low bladder volume with a reduction in CTV V98%. (Fig. 27). However, this association was not statistically significant on a mixed model when inter-patient variation was incorporated into the model (Fig. 28).

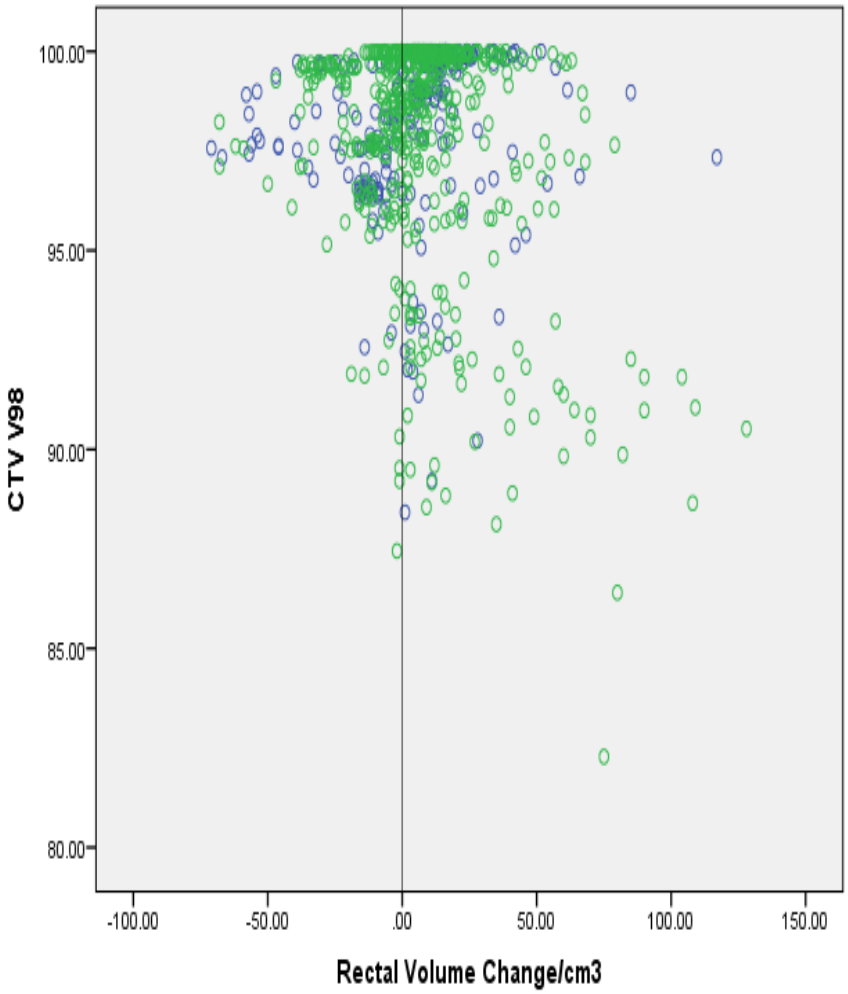

Fig. 27. CTV V98 variation with rectal and bladder volume (unpaired analysis)

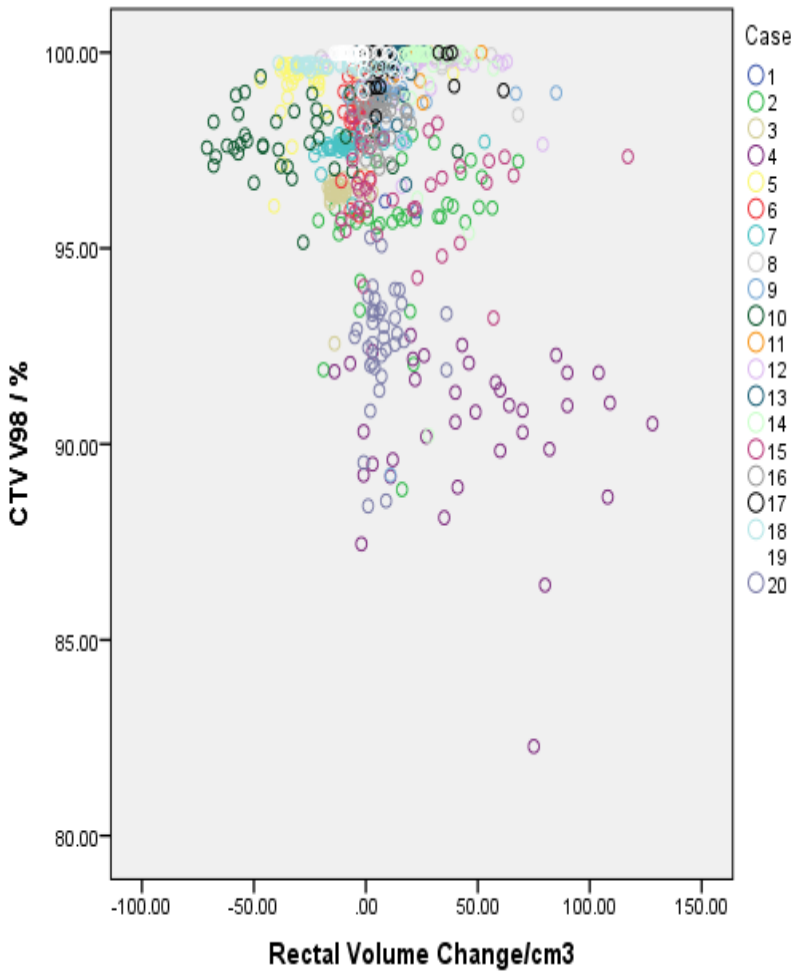

Fig. 28. CTV V98 variation with rectal volume (cases labelled)

I investigated the relationship between rectal volume on each fraction with the rectal dose. For rectal V50Gy, there was a modest negative correlation with rectal volume (Spearman's rho -0.46, $p < 0.001$) (Fig. 29). The correlation was slightly less with mean rectal dose (Spearman's rho -0.40, $p < 0.001$). There was no statistically significant association on linear mixed model testing for rectal V50Gy (F 1.44, $p = 0.42$).

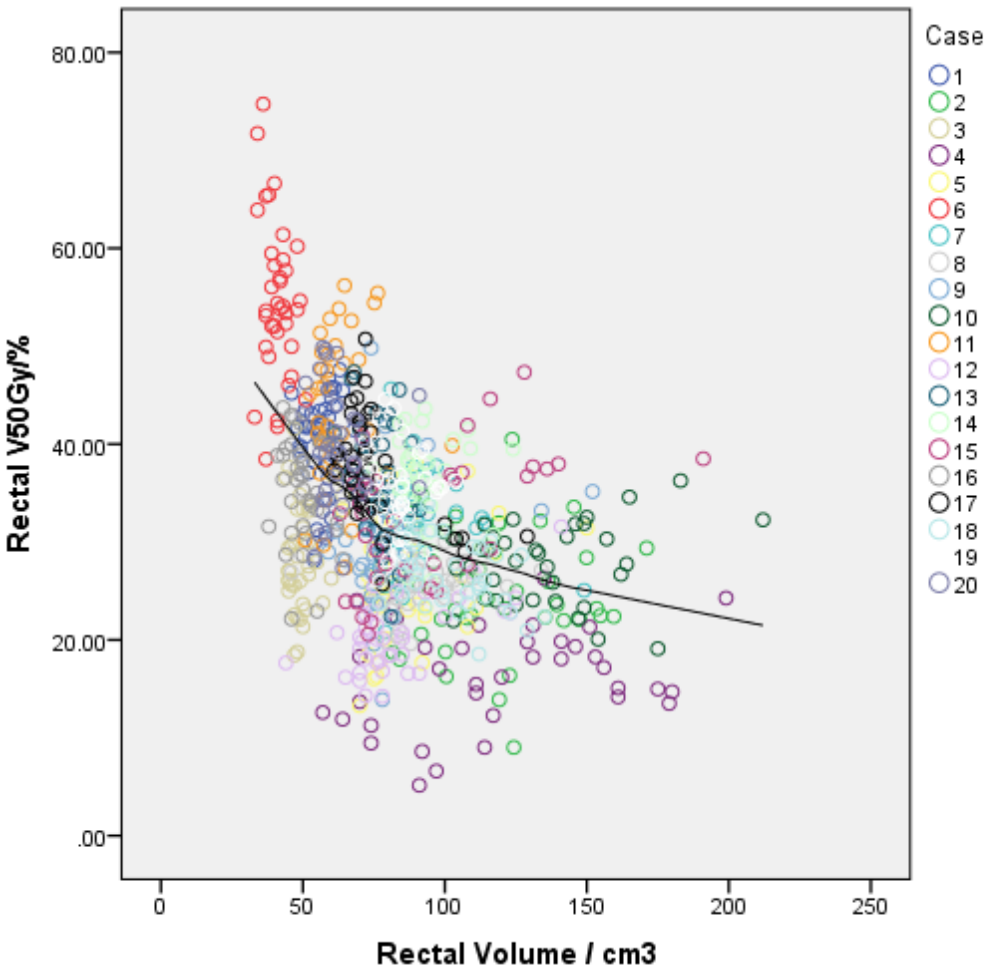

Fig. 29. Rectal V50Gy variation with rectal volume for all fractions with daily imaging

(separate cases colour-labelled; polynomial trend line)

Bladder V65Gy was moderately correlated with bladder volume (Spearman's rho -0.66, $p < 0.001$). For mean bladder dose, there was a strong negative correlation of mean bladder dose with bladder volume (Spearman's rho -0.73, $p < 0.001$) (Fig. 30). This relationship remained

statistically significant on linear mixed model testing for mean bladder dose (F 6.56, p = 0.038) when interpatient variation was incorporated.

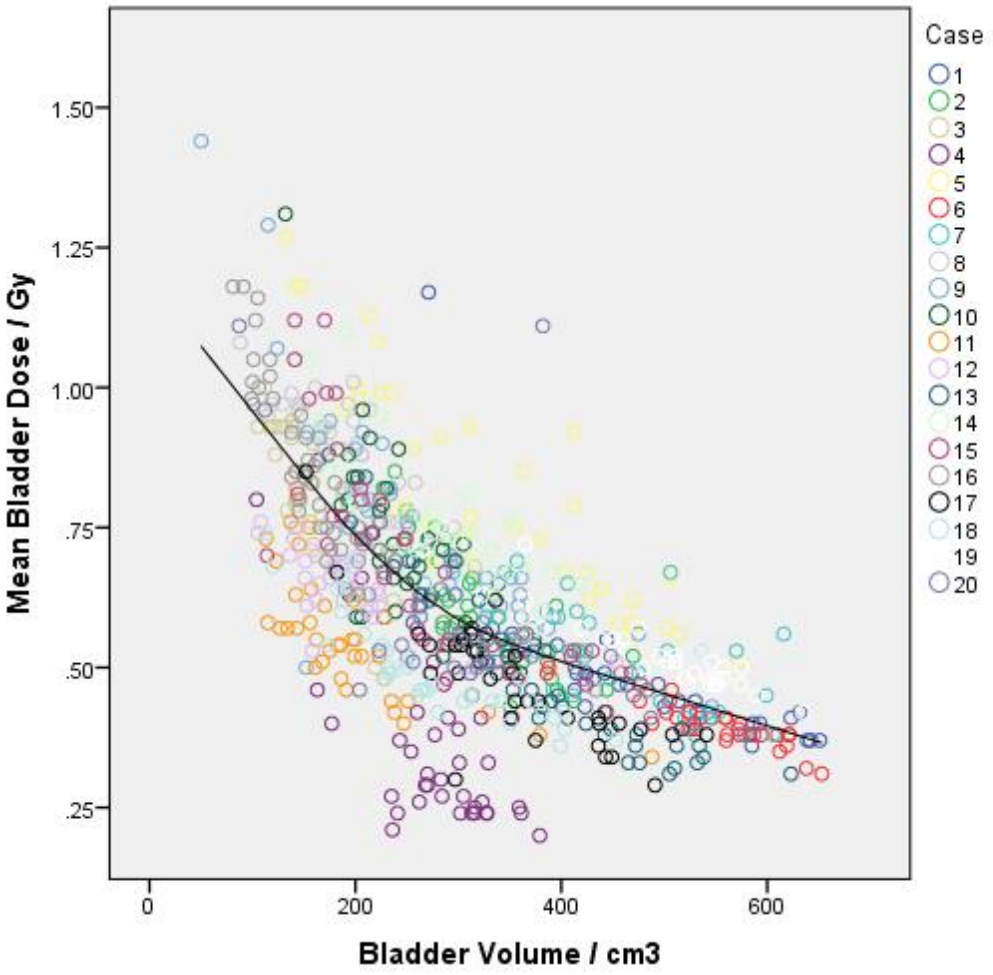

Fig. 30. Mean bladder dose variation with bladder volume for all fractions with daily imaging

(separate cases colour-labelled; polynomial trend line)

5.4 Protocol comparison case studies

I evaluated individual patient rectal and bladder dose-volume relationships for 2 cases to look for trends or predictive factors. These 2 cases were intentionally selected as they showed extremes of systematic or random geographic miss during weekly imaging.

5.3.1 Case 1

Patient 3 had 6 fractions with inadequate coverage using the day 1-3 then weekly online protocol, compared with 1 fraction for the daily online protocol. 3-D dose reconstructions were performed using the 95% isodose as a threshold. The difference in coverage for fraction 23 is illustrated in axial and sagittal images in Fig 31 - 32 (weekly online) compared to Fig. 33 - 34 (daily online). As can be seen, the superior portion of the CTV including the base of the seminal vesicles is outside of the 95% isodose immediately prior to treatment.

In this patient, there was a systematic geographic miss with this area outside the threshold on all 6 fractions on the weekly schedule (Fig. 31-32). This could potentially result in failure of local control if the tumour was

situated at the base of the prostate. Therefore, the clinical impact of daily imaging is clearly high in this situation.

The improvement in target coverage for this patient was associated with a reduction in dose to rectum. The rectum V50Gy was 37.6% with the weekly online simulation compared to 32.7% with the daily online treatment regimen. The mean rectal dose was reduced from 40.5 Gy to 38.1 Gy. There was minimal difference in the rectum D2cc with values of 74.0 Gy with both regimens. There was a slight increase in bladder dose with the daily regimen. However, the higher bladder V65Gy of 12.2% with daily imaging compared to 10.6% with the weekly were both well below the risk thresholds for the organ.

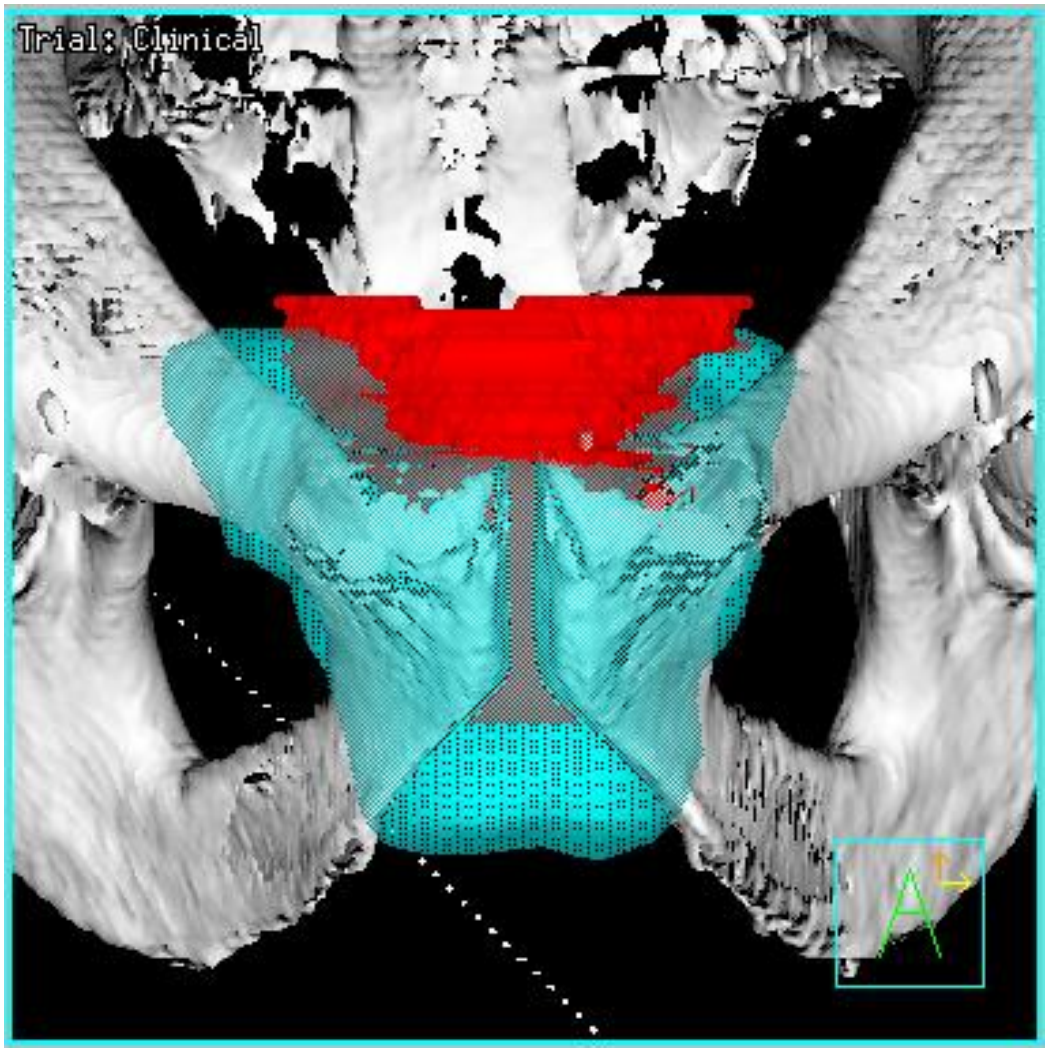

Fig. 31. Case 1: Antero-posterior projection of 95% isodose for CTV with weekly imaging

Fraction 6 – 95% Isodose (blue), CTV (red)

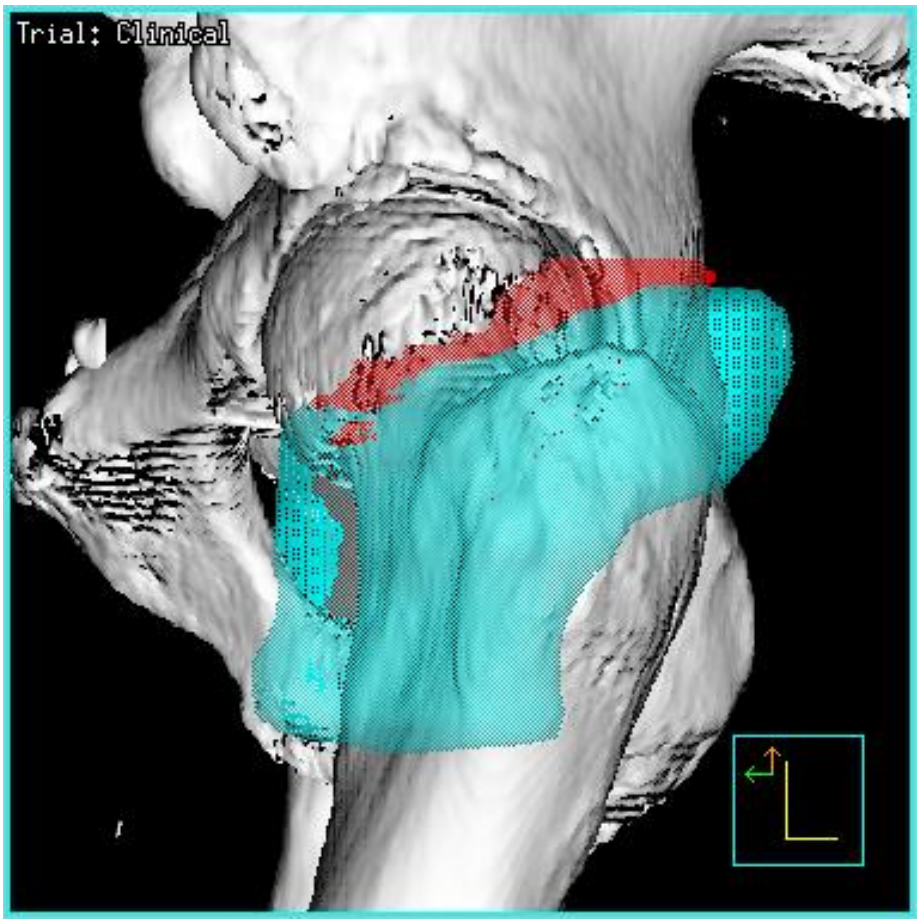

Fig. 32. Case 1: Lateral projection of 95% isodose for CTV with weekly imaging

Fraction 6 – 95% Isodose (blue), CTV (red)

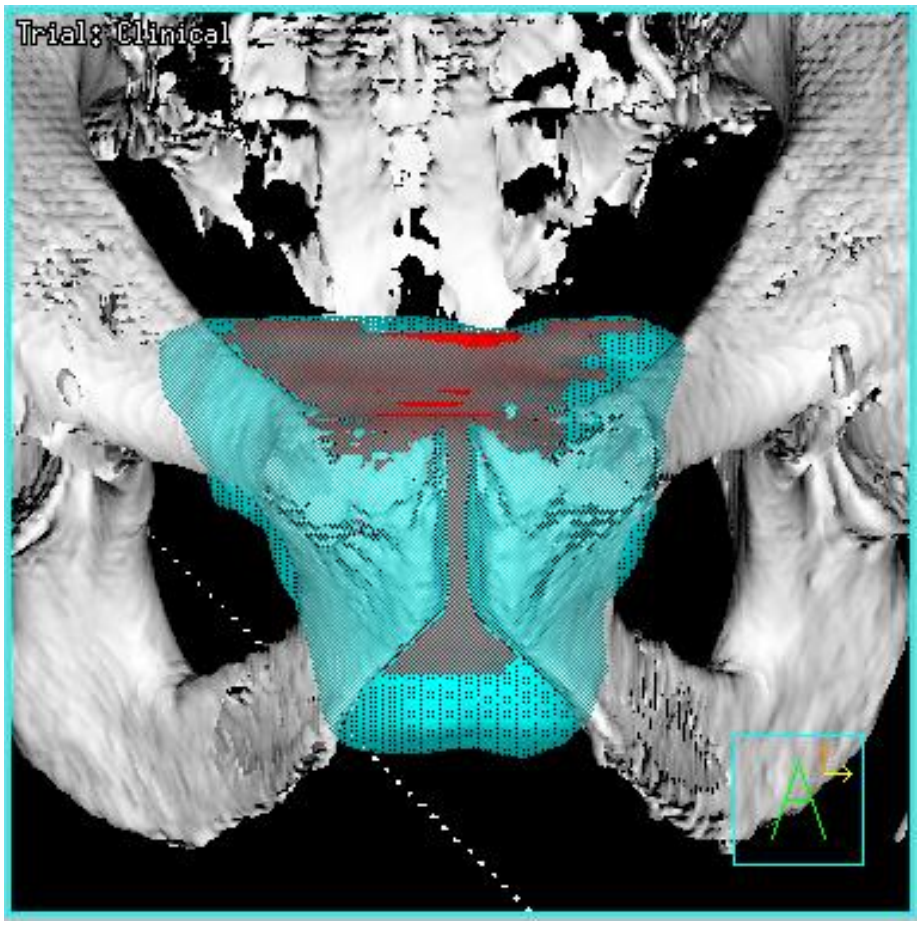

Fig. 33. Case 1: Antero-posterior projection of 95% isodose for CTV with daily imaging

Fraction 6 – 95% Isodose (blue), CTV (red)

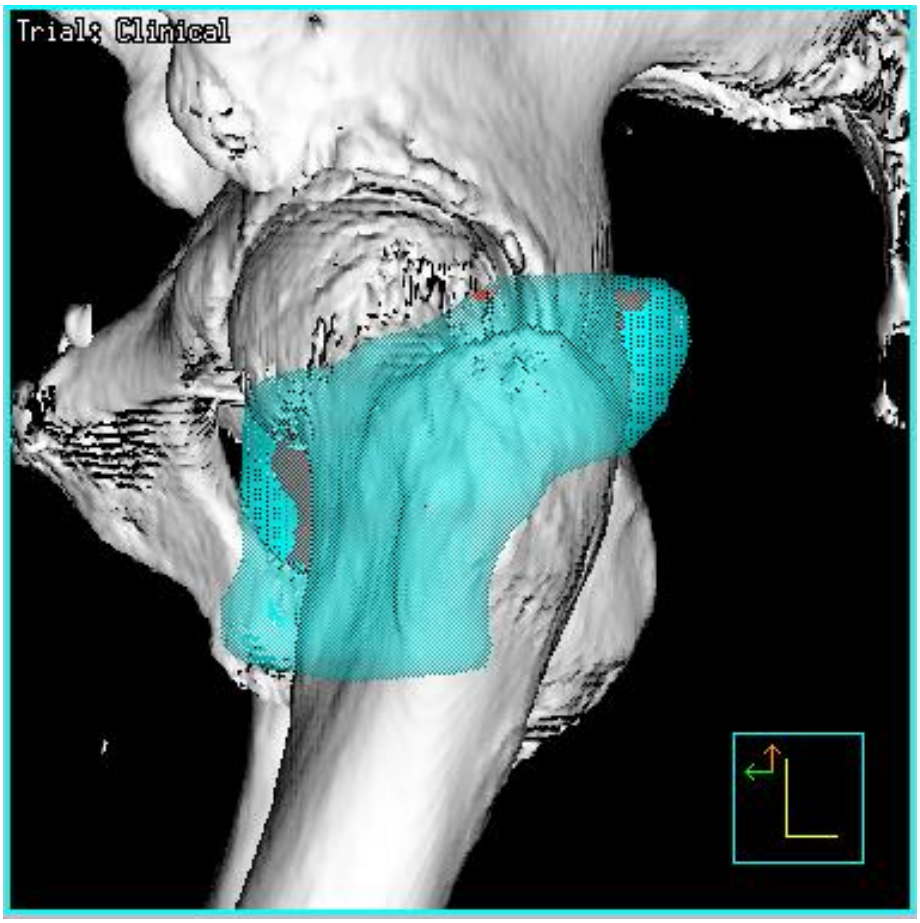

Fig. 34. Case 1: Lateral projection of 95% isodose for CTV with daily imaging

Fraction 6 – 95% Isodose (blue), CTV (red)

Dose-volume histograms (DVH) for the CTV (in red, extreme right of chart), rectum (purple) and bladder (blue) for daily online and day 1-3 then weekly online protocols are shown for the patient in Figs. 35 and 36. The charts show individual DVH lines for each fraction, along with the planned dose distribution for the organs at risk.

Uniformly high CTV coverage is visible on the daily online dose-volume histogram (Fig. 35). In the weekly online figure, there are several fractions where the CTV dose falls off to the left (Fig. 36). The extent of drop of CTV coverage is illustrated in Fig. 37.

For the rectal dose, there is a relatively narrow spread of curves for the daily online protocol (Fig. 35). With weekly imaging, there is a wider spread with rectal dose-volume curves moving to the right of the planned dose, indicating higher dose to the rectum in several fractions (Figs. 36). Fig. 38 shows that there were four fractions where the rectal V50Gy equivalent exceeded 50% in the weekly protocol, compared with none with daily imaging. The rectal V65Gy was 21.3% for the weekly protocol compared with 17.8% for the daily protocol. There was no clear relationship between rectal volume per fraction and rectal dose, with only a modest positive correlation (Fig. 39).

The bladder volume on the planning scan was 276 cm3. The mean treatment bladder volume was 253 cm3 (SD 87 cm3). The wide fluctuation in bladder volume that occurs during treatment, despite the use of daily cone beam imaging is seen in Fig. 40. The bladder dose distribution appears very similar between the two protocols. This is indicated by the bladder V65Gy which is 10.6% in the weekly imaging group and 12.2% in the daily imaging group. This is reflective of the portion of bladder close to the high-dose volume which is unavoidable even with excellent targeting of dose.

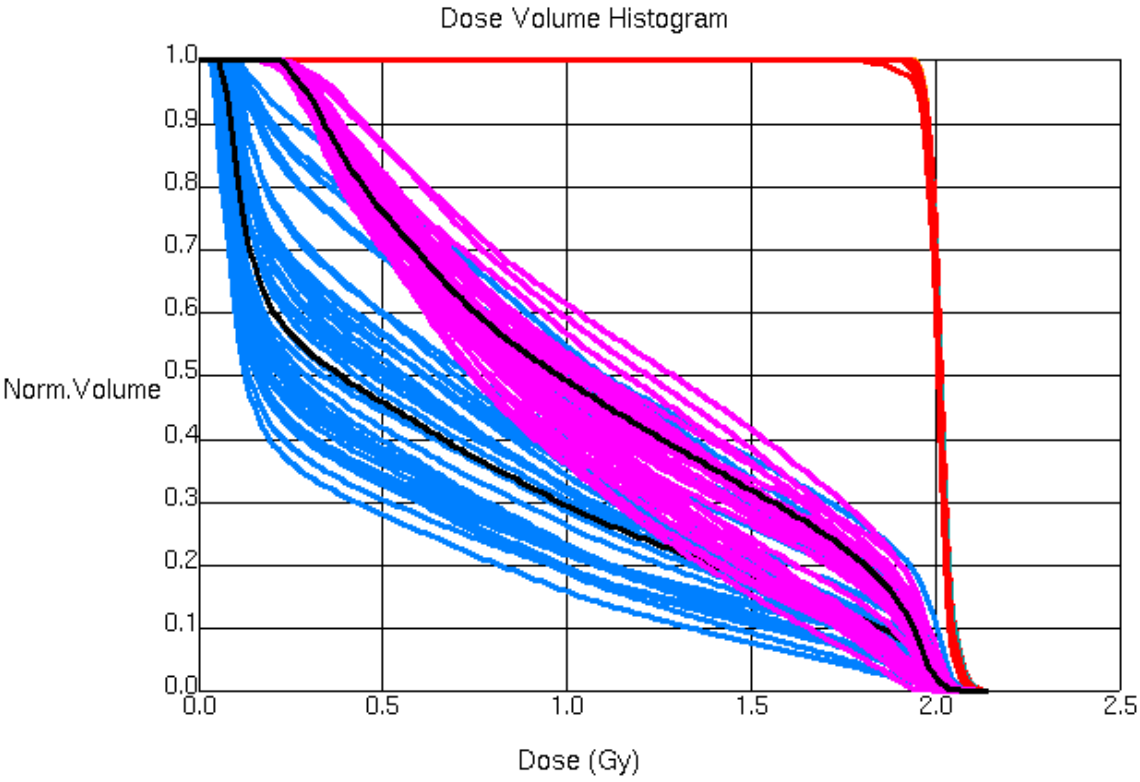

Fig. 35. Case 1: DVH for CTV, bladder and rectum for daily online protocol

CTV – Red, Bladder – Blue, Rectum – Purple, Planned - Black

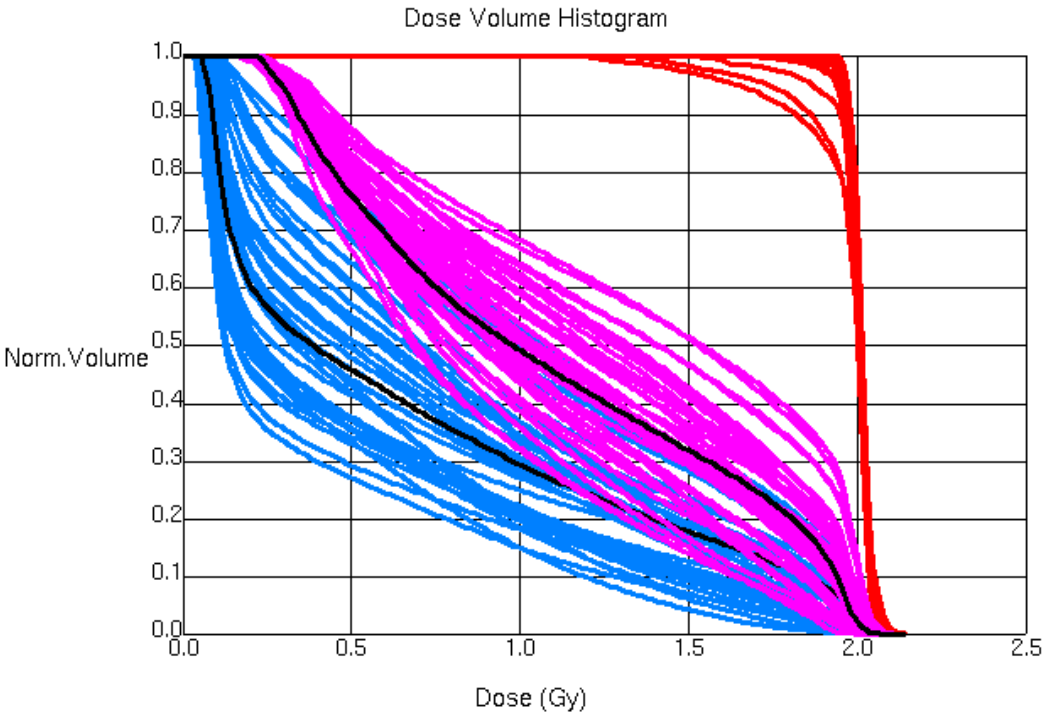

Fig. 36. Case 1: DVH for CTV and rectum for weekly online protocol

CTV – Red, Bladder – Blue, Rectum – Purple, Planned - Black

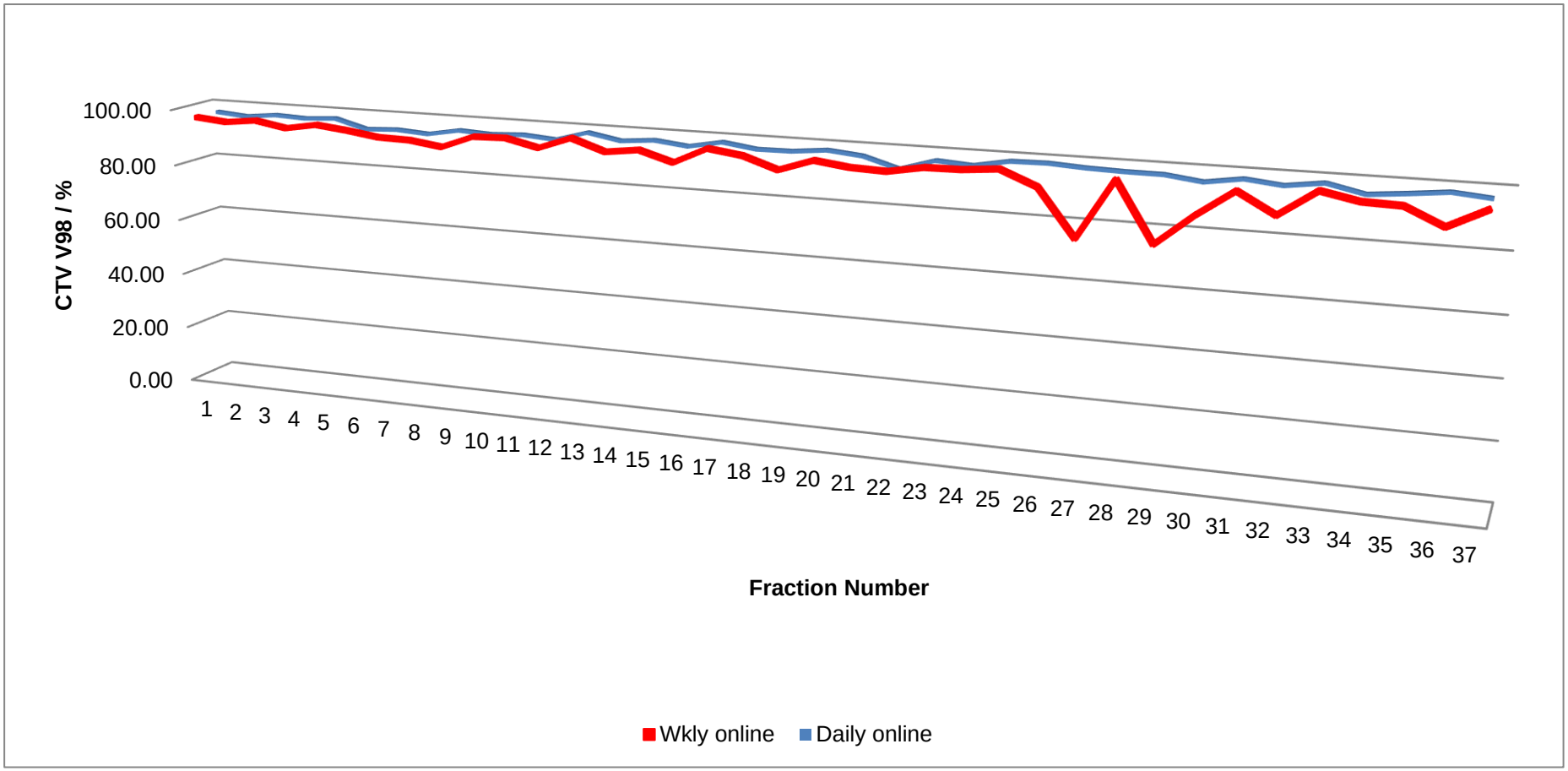

Fig. 37. Case 1: CTV V98 for weekly online compared to daily online protocol

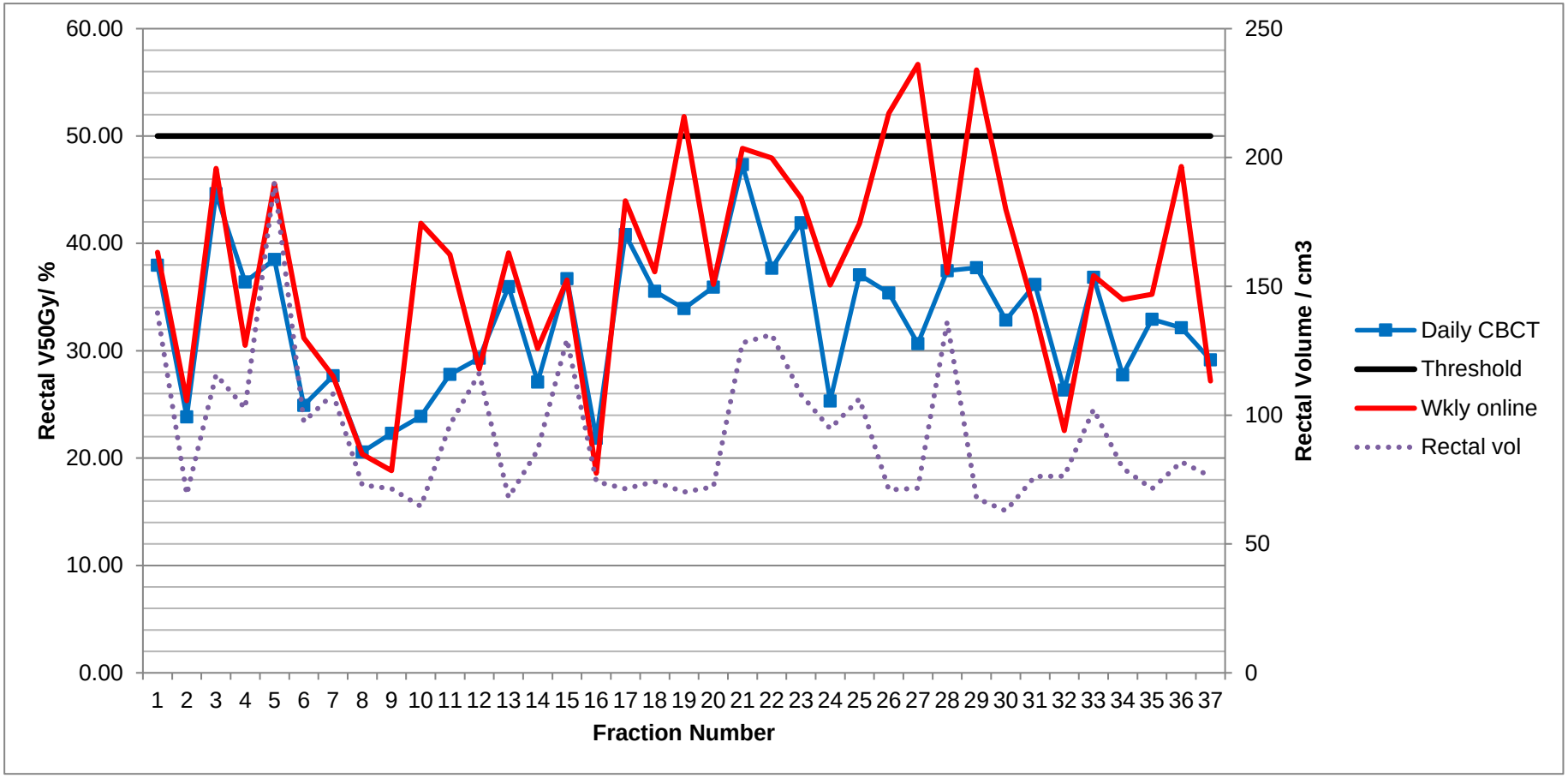

Fig. 38. Case 1: Rectal V50Gy equivalent for weekly online compared to daily online protocol

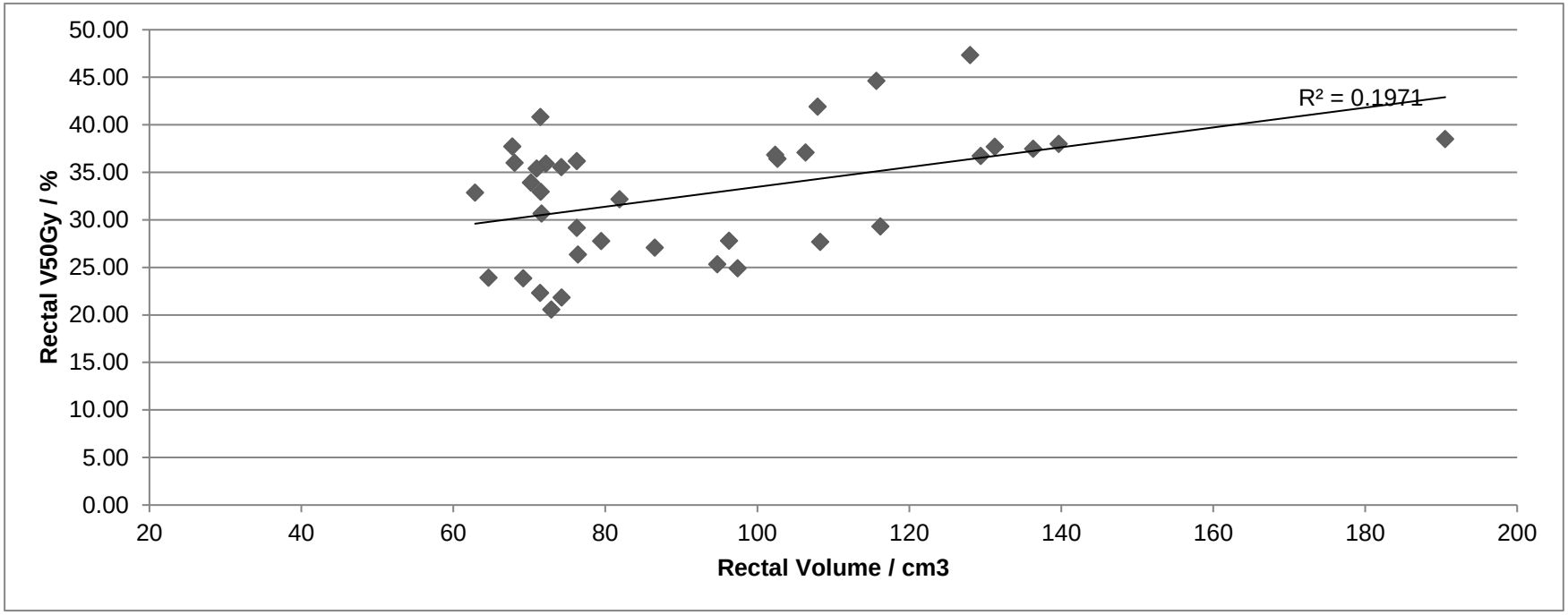

Fig. 39. Case 1: Rectal V50Gy for daily imaging plotted against rectal volume on individual fractions

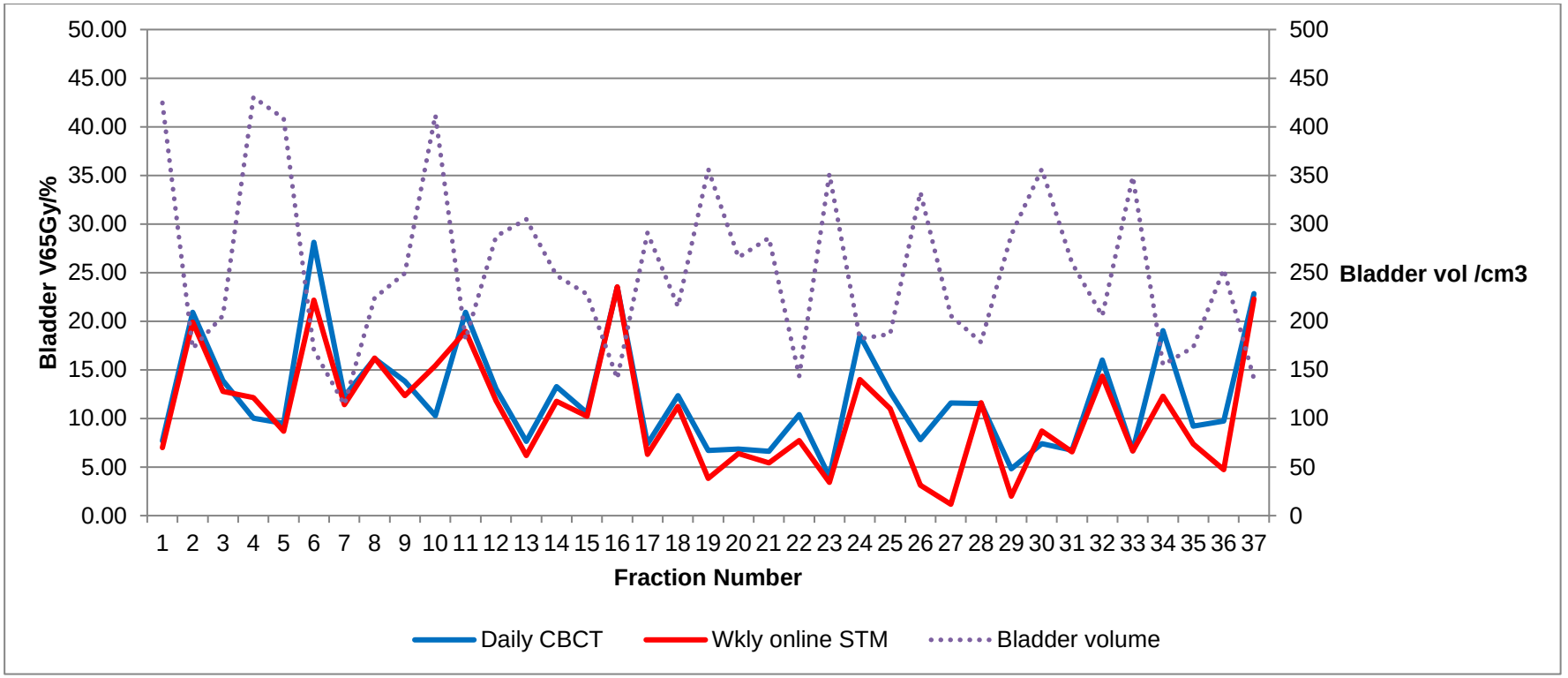

Fig. 40. Case 1: Bladder V65Gy equivalent for weekly online compared to daily online protocol

5.3.2 Case 2

In this case, there was again better CTV coverage dosimetry with daily imaging compared to weekly imaging. This is demonstrated in the dose-volume histograms in Fig. 41 and Fig. 42. There were 6 fractions where the CTV V95 was less than 99% with weekly imaging compared with 3 fractions with daily imaging (Fig. 43). As can be seen in Fig. 44, on each of those 6 fractions, a different area of the prostate was outside the target dose region. Therefore, the clinical impact in terms of disease control is likely to be minimal in this case.

However, the rectal toxicity is likely to be less with daily imaging in this case, as the rectal dose parameters are improved. Rectal V50Gy was 35.9% with daily imaging compared with 41.4% was weekly imaging. There were 9 fractions where the rectal V50Gy equivalent was greater than 50% in the weekly protocol, compared to none with daily imaging (Fig. 45).

The bladder V65Gy was slightly higher in the daily imaging group at 12.7% compared to 11.3% with weekly imaging. There was a visible relationship between bladder volume and V65Gy (Fig. 46), which was confirmed on

correlation analysis (Fig. 47) with a polynomial correlation coefficient of 0.61.

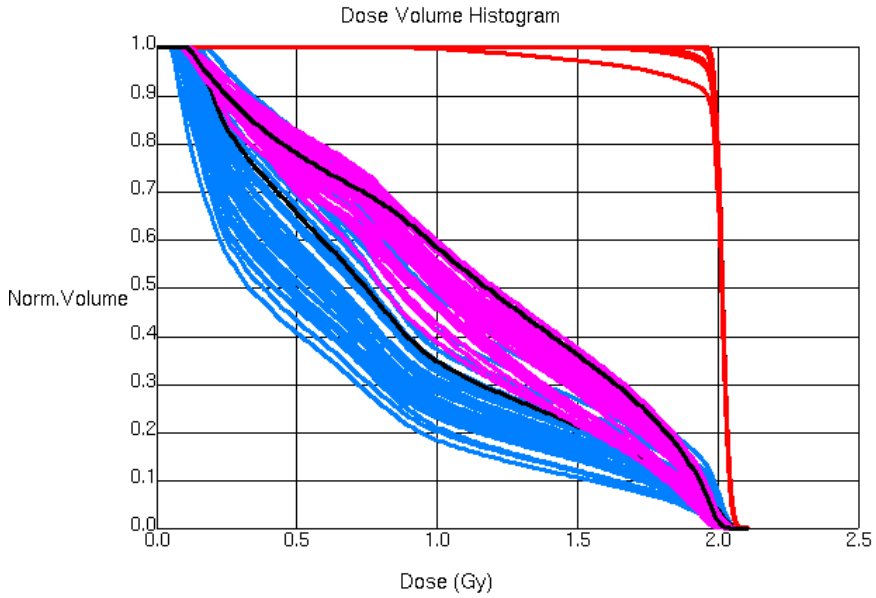

Fig. 41. Case 2: DVH for CTV, bladder and rectum for daily online protocol

CTV – Red, Bladder – Blue, Rectum – Purple, Planned – Black

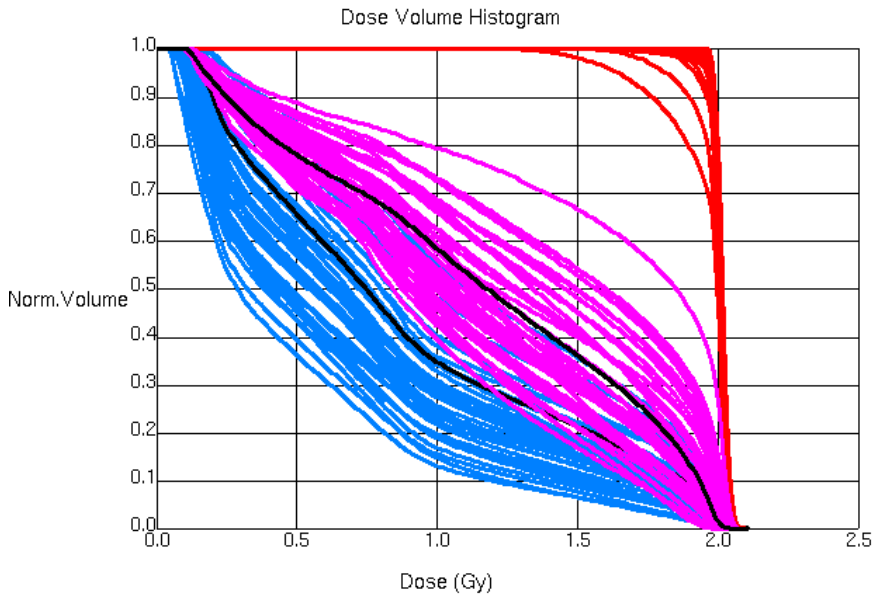

Fig. 42. Case 2: DVH for CTV and rectum for weekly online protocol

CTV – Red, Bladder – Blue, Rectum – Purple, Planned – Black

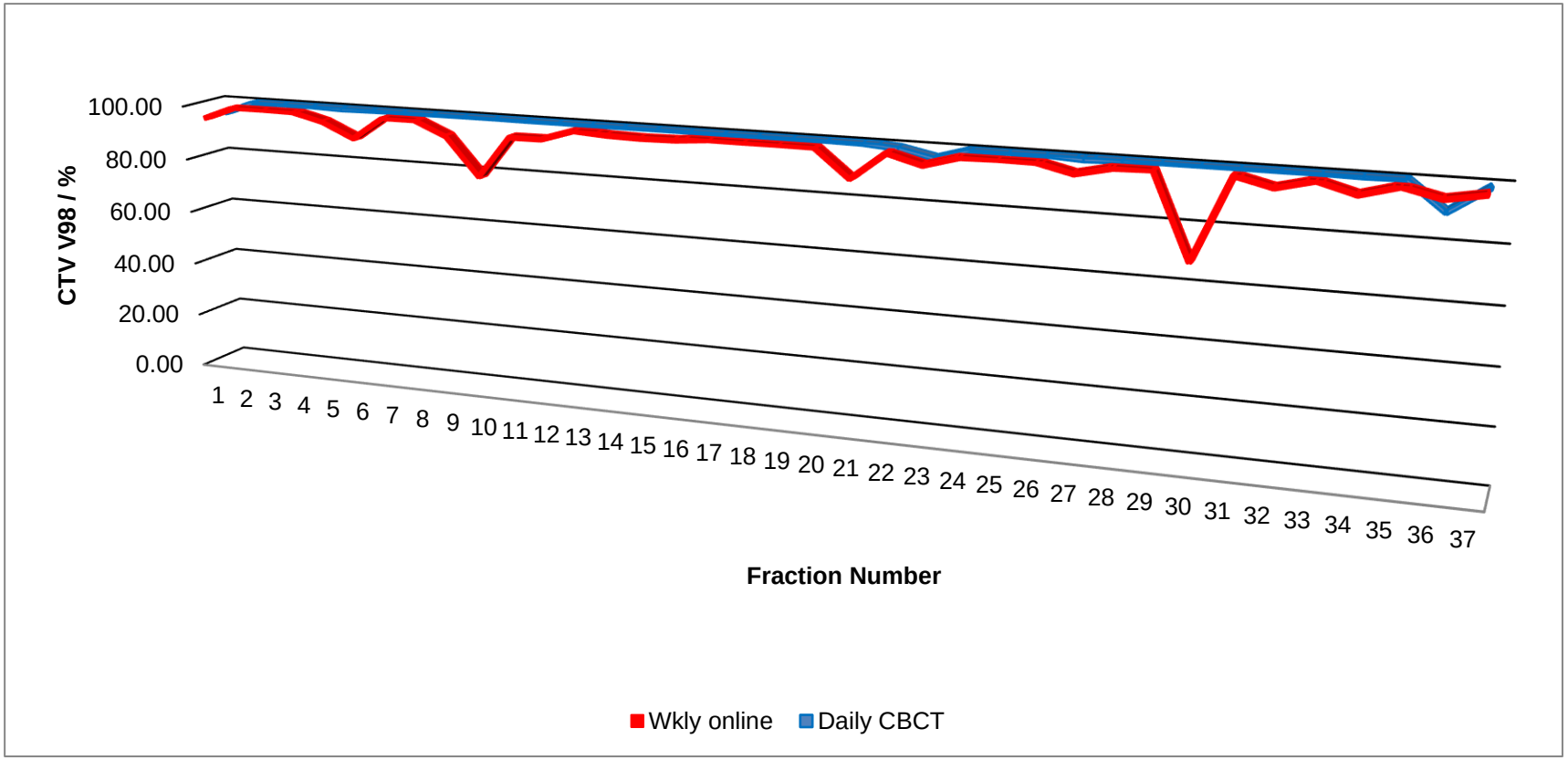

Fig. 43. Case 2: CTV V98 by fraction for daily CBCT versus weekly protocol

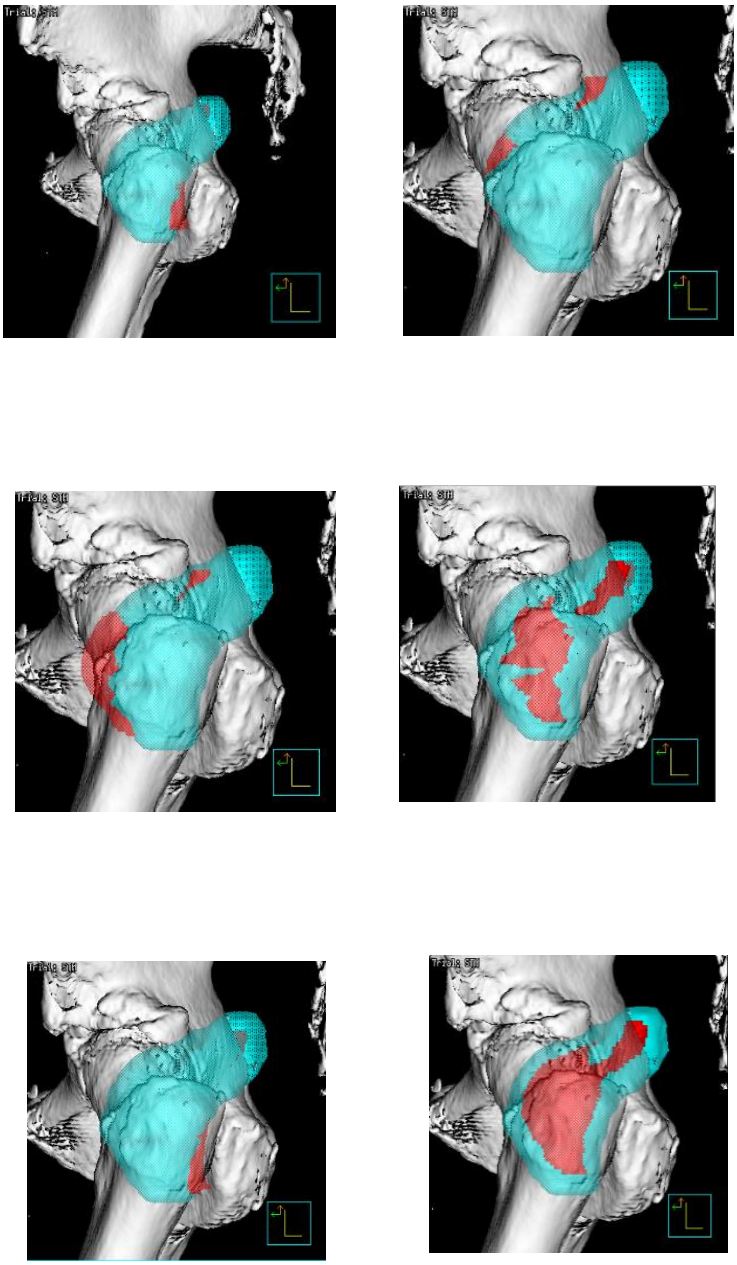

Fig. 44. Case 2: Lateral projections of 95% isodose for 6 fractions where CTV coverage reduced

Red – areas where CTV not covered by 95% isodose

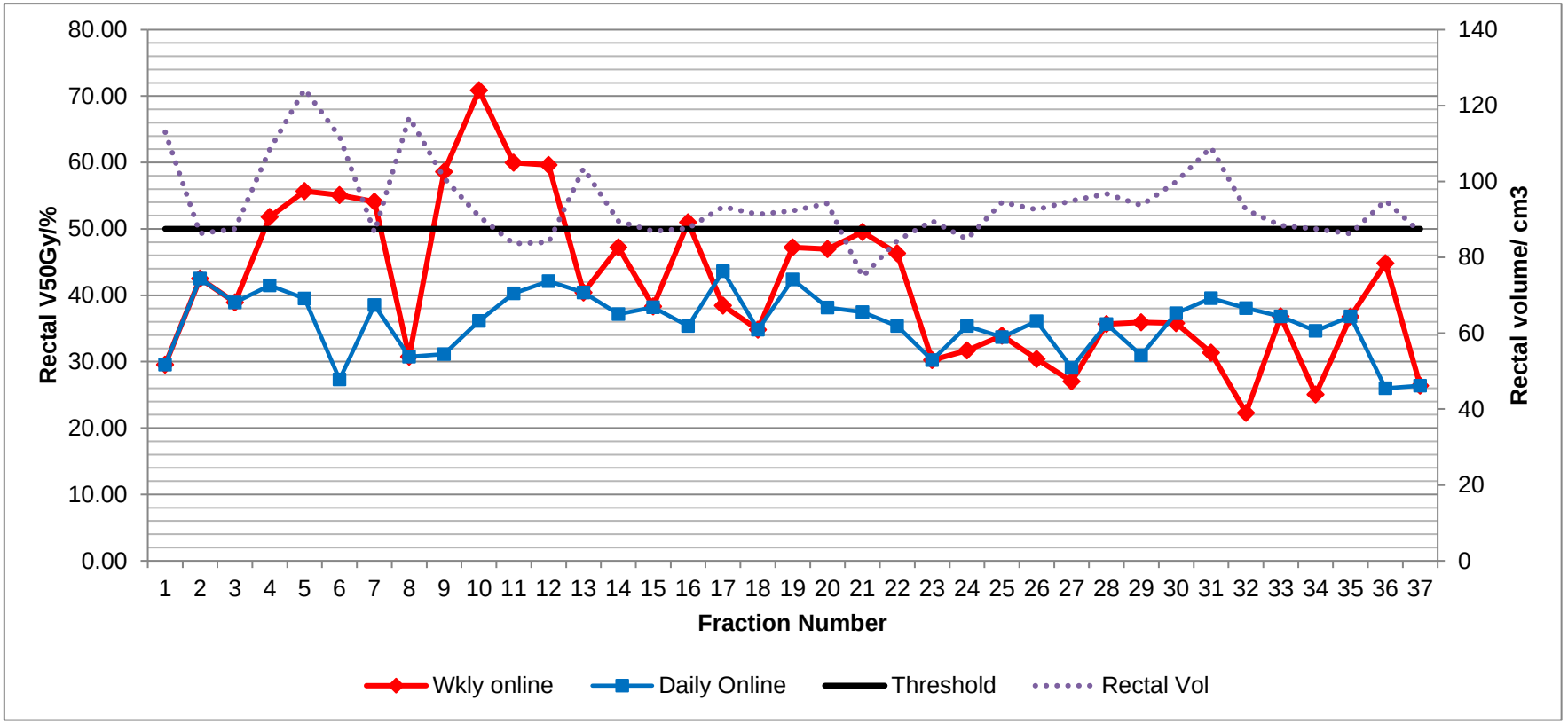

Fig 45. Case 2: Rectal V50Gy equivalent by fraction for daily CBCT versus weekly protocol

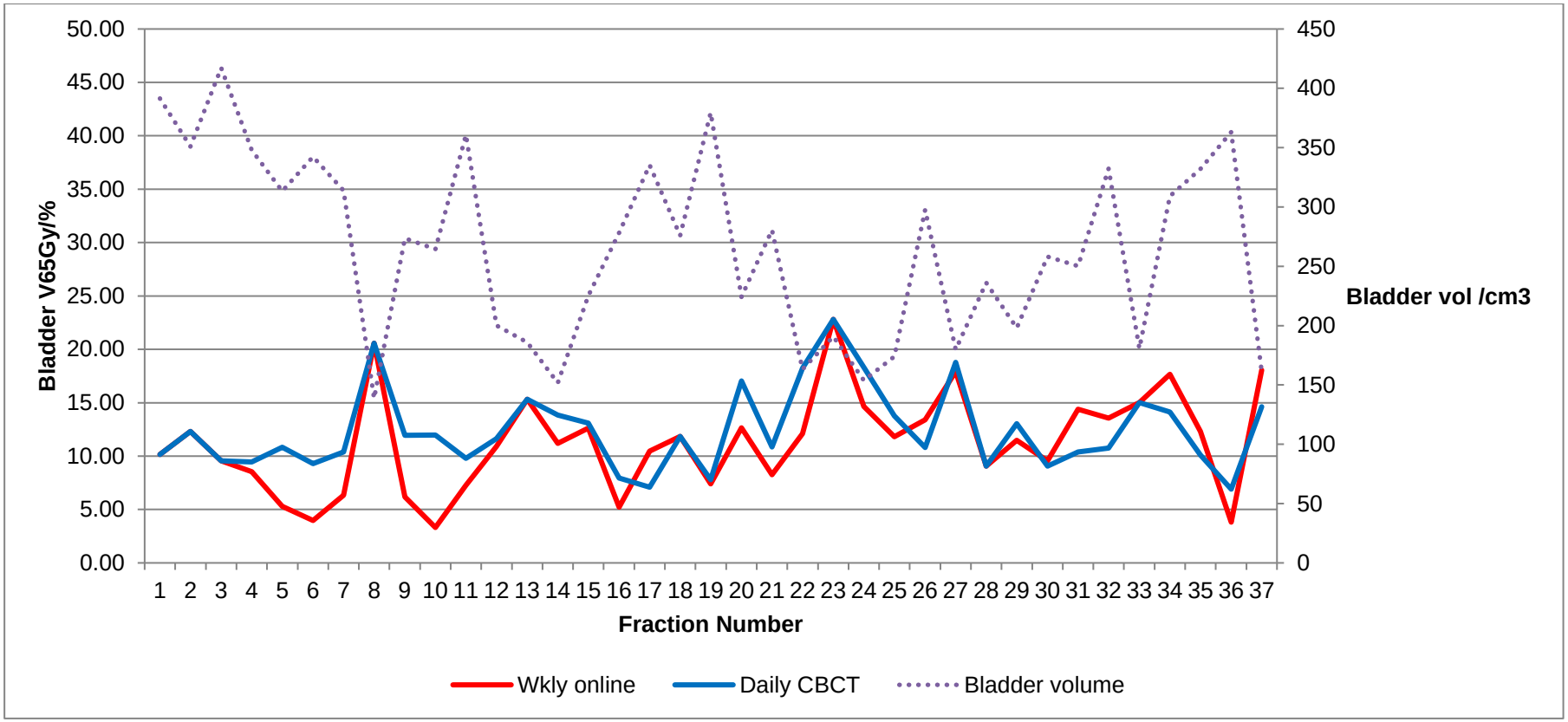

Fig 46. Case 2: Bladder V65Gy equivalent by fraction for daily CBCT versus weekly protocol

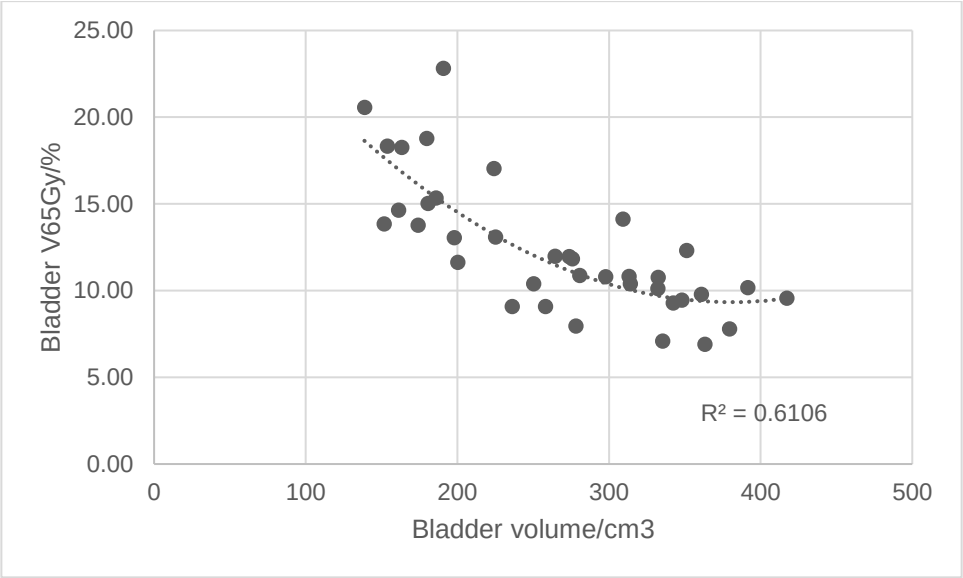

Fig 47. Case 2: Bladder V65Gy equivalent by fraction for daily CBCT versus weekly protocol

5.5 CBCT margin comparison - Results

I evaluated the effect of CTV-PTV margin reduction if daily imaging was used. Margins of 3 and 5 mm were compared to the treatment margin of 7 mm. The median CTV V95% coverage was 99.98% with daily imaging (Table 9). The median coverage was 99.86% and 99.40% with 5 mm and 3 mm margins respectively.

Table 9. Dosimetric parameters – CTV-PTV margin comparison with daily imaging

Parameter	3 mm	5 mm	7 mm	p
CTV V95 / % (median)	99.40	99.86	99.98	<0.001*
Rectal V50Gy / %	21.14	26.34	32.48	<0.001†
Mean rectal dose / Gy	28.99	32.20	36.56	<0.001†
Rectal D2cc / Gy	70.43	72.39	73.37	<0.001†
Bladder V65Gy / %	6.18	8.34	10.32	<0.001†
Mean bladder dose / Gy	18.45	20.75	23.13	<0.001†

n = 20, CTV – Clinical target volume, PTV – Planned target volume

*Friedman's test significant at Bonferroni correction level 0.017 †Repeated measures ANOVA with Bonferroni correction

However, the number of fractions where 99% coverage was not achieved increased progressively with reduced margins. In particular, only 32 fractions of 37 achieved the coverage target with a 3-mm margin (Fig. 48). Rectal and bladder dosimetry showed progressive reduction in dose to these organs at risk with smaller margins, although the doses were within planning constraints even with the 7-mm margin.

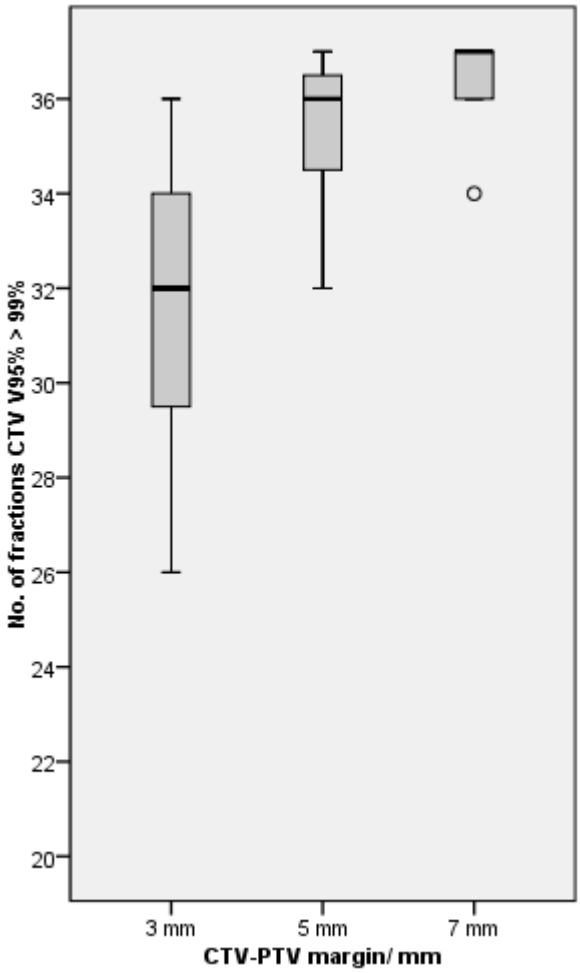

Fig. 48. CTV coverage by CTV-PTV margin with daily imaging

Chapter 6. Discussion

6.1 Strengths of study

6.1.1 Completeness of dataset

A key strength of this study was the analysis of a complete set of daily CBCT images for each patient, allowing full evaluation of the effect of frequency of imaging and PTV margin. In particular, any random variation in organ position during the whole treatment course could be detected. Several previous reported studies have utilized only weekly (Maund et al., 2014, Pawlowski et al., 2010) or twice-weekly (Hatton et al., 2011) CBCT images.

6.1.2 Image quality

The study had the advantage of the use of kV CBCT imaging which has better image quality than MVCT images (Varadhan et al., 2009). Previous dosimetric studies (Battista et al., 2013, Kupelian et al., 2006) used poorer quality MVCT imaging. In my study, there were only a few CBCTs in the whole sample where contouring was affected by image quality. As a result,

there can be more confidence in delineation of difficult areas such as the apex of the prostate and prostate-bladder interface.

6.1.3 Consistency of contouring

All contouring was carried out by the clinical investigator independent of the radiographers who carried out CBCT verification. My contours were further reviewed independently by an experienced clinical oncologist. The use of manual contours was essential for quality assurance. This was because commercial automatic contouring programs were not sufficiently accurate for use with CBCT, at the time of initiation of this project.

The consistency of contouring was apparent from the minimal variation in CTV volume from the planning CT volume (Section 4.3 Fig. 14). The mean change in CTV volume from the planning CT was 0.2%. This is much better than the 9.2% mean variation reported in another CBCT dosimetric study from the United Kingdom (Maund et al., 2014).

6.1.4 Clinical validity

The patients in my study had actual treatment shifts that were based on CBCT soft-tissue matching. This is in comparison to previous studies where CBCT imaging was evaluated but patients had fiducial (Kupelian et al., 2006) or portal imaging (Hammoud et al., 2008) verification for treatment. Therefore, this study provided the opportunity for the dosimetric evaluation of the CBCT verification technique as used in routine clinical practice. In the process, we also managed to evaluate the time implications of the technique in actual clinical practice.

6.1.5 Assessment of benefit of reimaging

In addition to the treatment verification CBCT, the study also assessed the first CBCT in cases where imaging was repeated. This allowed the evaluation of the benefit of repeating CBCT imaging in circumstances such as rectal distension. There are no previous published prostate radiotherapy studies evaluating this practice.

6.2 Weaknesses of study

6.2.1 Study patient numbers

The substantial number of cone beam CT scans limited the number of patients that could be included in this study. Each patient was imaged daily with CBCT during the course of radiotherapy, and had repeat imaging if required during a fraction. On average, each patient had 42 cone beam CT images. Due to the non-availability of commercial auto-contouring software for cone beam CT, manual contouring had to be done for each scan. Due to time constraints, the number of patients had to be therefore limited to 20.

However, this would still be the largest series of prostate radiotherapy patients with a full set of daily cone beam CT reported in the literature. The study numbers also exceeded the number of 16, which was the sample size calculated for detection of rectal toxicity reduction (section 5.1.1). Investigation of predictive factors for IGRT benefit would require a larger sample size.

6.2.2 Validation dataset

The validation study was limited to 25 fractions due to processing power limitations of the planning software. Ideally, we would have carried out validation samples on more patients and included a greater number of fractions. However, the density-override method, using a region of interest mapping technique, is both time-intensive and resource-intensive. As a result, a larger validation study was not possible within the timeframe of this research project.

The main premise of our study method was that density-override may not be required when a multiple field beam arrangement was used, as in modern IMRT. This hypothesis was validated in our sample. The technique is also supported by other published literature (Orton and Tomé, 2004, Schulze et al., 2009, Maund et al., 2014).

However, the method has not been validated with older conformal radiotherapy with three fields, where the effect of the variation in surrounding tissue density and source-surface distance might be higher. It is important to note however that there is no gold standard for dose calculation on CBCT at present.

6.2.3 Spatial information

Dose-volume histograms provide a concise, quantitative representation of dose distributions for radiotherapy plans. Essentially, the three-dimensional dose distribution on each CT slice is converted into a dose-volume distribution by assessing the dose received by each voxel.

Therefore, an inherent limitation is the lack of spatial information on the distribution of dose (Drzymala et al., 1991). There cannot be any assessment of ‘hot spots’ where there is overdosing or ‘cold spots’ due to underdosing.

Attempts have been made to overcome this by the use of spatial DVH such as the zDVH concept (Cheng and Das, 1999). The zDVH is a 2-D analogue of a 3-D DVH. The process involves the generation of DVH data referenced to CT slices. This allows evaluation of high-dose regions within the volume, even if the overall DVH is satisfactory. However, the zDVH concept is not in routine clinical or research use.

The difficulty with assessing three-dimensional distributions for very large numbers of CT sets is that it is cumbersome and difficult to quantify. The

assessment of spatial dose distribution for all patients was outside the scope of this study.

6.2.4 Tumour position

My study did not evaluate the actual tumour position within the prostate, due to obvious limitations of CT imaging for that purpose. Patients within this study group also did not have MRI imaging fused to the planning CT. Therefore, I could not accurately determine if the same area of tumour was missed in these fractions. I did however evaluate the area of CTV missed in each fraction in the case studies during the study (section 5.3). The results of our study indicate the even greater need for regular imaging, if boosting of the primary tumour is being considered.

6.2.5 Seminal vesicle coverage

There is evidence that there is differential motion of seminal vesicles, with a larger magnitude of motion compared to the prostate (Liang et al., 2009). However, the risk of seminal vesicle invasion differs depending on the prostate cancer risk stratification. It is approximately 16% in in patients with PSA in the range of 10-20 ng/ml (Zlotta et al., 2004). In the clear

majority of cases only the base of the seminal vesicles is involved. In a detailed pathologic analysis of 344 patients, only 7% had involvement of more than 1 cm of the seminal vesicle, and only 1% had involvement more than 2 cm (Kestin et al., 2002).

In this study, the seminal vesicles were not contoured separately. This was because only the base of the seminal vesicles was treated, as study patients were in intermediate risk group. During treatment planning, in most patients they were contoured by the treating oncologist as part of a common CTV. To enable comparison with the planned treatment, the same protocol was followed for all patients and a combined CTV was created. Therefore, it is not possible to determine from this study whether seminal vesicle coverage is differentially affected by the IGRT schedule or margin.

6.2.6 Biological dose evaluation

This study has not evaluated radiobiological parameters such as tumour control probability (TCP) and normal tissue complication probability (NTCP). These are obtained using models which use a number of assumptions. This includes the tumour alpha-beta value, for which there are varying estimates in prostate cancer.

Research tools are available to derive TCP and NTCP values from a DVH curve (Sanchez-Nieto and Nahum, 2000, Warkentin et al., 2004, Tsougos et al., 2009). TCP and NTCP estimates are very sensitive to relatively small changes in shape of DVH curves (Drzymala et al., 1991)

There is a potential weakness to creating cumulative dose-volume histograms using simple averages, due to potential differences in differences in volume in each dose bin (Sanchez-Nieto and Nahum, 2000). The treatment planning system used in our centres did not allow a cumulative dose deposition estimate on a voxel-by-voxel basis for the whole course of radiotherapy. As a result, individual dose-volume histograms were obtained for each fraction. A crude summation of dose-volume histograms would have resulted in an inaccurate estimate of TCP and NTCP, and was therefore not attempted.

6.2.7 Bladder volume variation

Due to the limited scan length of the CBCT, there were six patients where the whole of the bladder was not included in the CBCT imaging. In these patients, the dome of the bladder was not available for contouring, leading to a lower contoured bladder volume. This may limit the comparability of

the bladder dosimetric parameters to the planned dose distribution. However, it would not affect the comparison of imaging protocol and PTV margin evaluation.

6.3 Target volume coverage

My work shows that there are statistically significant improvements in target volume coverage during radical prostate radiotherapy when daily CBCT imaging is used. The absolute magnitude of benefit of daily imaging is small over the course of radiotherapy. This is because the effect of the fractions where geographic miss occurs is averaged out over the whole course.

The magnitude of benefit is greater when considering the proportion of fractions where target objectives are met. This is of particular importance if hypofractionated treatment regimens are used. A study using Monte Carlo simulation methods reported a small but consistent reduction in tumour control probability (TCP) of approximately 1% due to geometric uncertainty in hypofractionated regimens (Craig et al., 2003). The national IGRT survey conducted during this project showed that 16% of centres use a 60 Gy in 20 fractions regimen. The effects of geographic miss in a 20-fraction regimen will be proportionately higher than in the 37-fraction regimen used in our study.

The highest benefit was seen on treatment days where intra-fractional re-imaging was performed due to rectal distension on the initial scan. On

these fractions, there was a mean increase in CTV V98 of 5.1%. This should be counterbalanced against the additional radiation dose that is introduced through re-imaging.

There are difficulties in comparing the results of this study to other published data. A major limitation of similar studies (Maund et al., 2014, Pawlowski et al., 2010, Hatton et al., 2011) is that a full data set was not available or analysed in those studies. Therefore, actual daily data was not available for accurate protocol comparisons. One other study using simulated protocol comparisons with more complete data (Battista et al., 2013) used different dose metrics of D95 and TCP to report results.

6.4 Organ at risk dose

DVH parameters have been demonstrated to be useful in assessing the risk of acute and chronic organ toxicity (Huang et al., 2002b, Vargas et al., 2005).

Huang et al. investigated 163 patients treated with 3-D conformal prostate radiotherapy to a dose of 74-78 Gy. They assessed chronic rectal toxicity at 6 years in relation to dosimetric, anatomic and clinical factors. The dosimetric factors were clearly associated with rectal toxicity. In particular, the percentage of rectal volume treated correlated significantly with toxicity, at all dose levels. Clinical factors had limited predictive value.

Vargas et al evaluated 331 patients who had image-guided radiotherapy for localized prostate cancer, in a phase 2 dose escalation trial. Toxicity was evaluated using the NCI CTC version 2.0. They found that rectal wall V50 – V70 was closely predictive of chronic rectal toxicity >= grade 2. Absolute rectal volumes were far less predictive than relative rectal volumes. The dose level used did not predict chronic toxicity. Acute rectal toxicity during treatment also predicted chronic toxicity.

I selected V50Gy as a DVH parameter to evaluate, based on the above studies and the widespread use of this parameter in the UK during radiotherapy planning. My study has confirmed that V50Gy is significantly reduced with the use of daily imaging in comparison to less frequent imaging schedules. This would counterbalance the increased pelvic radiation exposure due to higher overall imaging dose during radiotherapy.

The D2cc high dose value was not reduced by daily IGRT. This is likely to be due to the close approximation of the high-dose region of rectum to the prostate target volume. Improved accuracy of prostate irradiation would result in this region of the rectum continuing to receive a high dose with image guidance.

6.5 Investigation of factors predictive of benefit from IGRT

Rectal distension on planning CT scan has been considered a predictive factor for biochemical failure during prostate radiotherapy (de Crevoisier et al., 2005, Heemsbergen et al., 2007, Engels et al., 2009). However, these studies were done on patients treated without volumetric image guidance. Patients in the de Crevoisier series had verification using skin marks and weekly portal imaging. The Heemsbergen study patients had offline verification using portal imaging. In the Engels series, portal imaging was used again with a minority of patients having fiducial markers.

There have also been dosimetric studies which appear to show a relationship between planning CT rectal volume and reduced CTV coverage. A daily CBCT study showed that rectal volume at planning > 100 cm^3 was associated with lower CTV coverage (Sripadam et al., 2009). However, in this study, the actual verification modality used during treatment was offline portal imaging.

Another study has shown that higher bladder volume, rectal cross-sectional area and body mass index may be predictive of benefit from fiducial-based IGRT (Munck af Rosenschold et al., 2014). They analysed the shift results of 267 patients and estimated interfraction uncertainty to

arrive at this conclusion. However, there was no attempt to review actual dose distributions achieved during treatment.

In my study where patients were treated daily online cone beam CT verification, the rectal volume on the planning CT scan was not predictive of CTV coverage. This is in line with more recent published clinical data which show that outcomes are not affected by the planning CT scan rectal volume if an adaptive IGRT strategy with cone beam CT is used (Park et al., 2012).

In my study, the clear majority of patients benefited from daily CBCT imaging with no pre-treatment predictive factors identified. However, a larger cohort of patients may be required to investigate factors which predict for the actual magnitude of benefit from CBCT image-guidance.

The relationship between bladder and rectal volume during treatment with organ-at-risk dose is in line with results reported from a smaller study (Chen et al., 2016). Their study used a cone beam calibration curve method and obtained comparable results of correlation shown only with mean bladder dose on multivariable analysis. This relationship does highlight the importance of maintaining a full bladder during treatment.

6.6 Concomitant dose

The use of daily verification imaging requires consideration of concomitant dose to organs at risk. Potential long-term effects of radiation include deterministic and stochastic effects. Deterministic effects are dose-related, and of relatively little importance in the context of radiotherapy-related low-dose CBCT use. Stochastic effects occur due to chance, and do not have a specific dose threshold. Stochastic effects include the small risk of carcinogenic effects and even rarer heritable effects.

There is a small additional second cancer risk with additional imaging. This should be borne in mind when patients are informed of risks of treatment. This risk can be estimated using various models. One study has estimated a lifetime attributable risk (LAR) of up to 400 second cancers per 10000 persons with a course of 30 CBCTs (Kim et al., 2013), using the BEIR model. Their estimate is unusually high compared with another published study which estimated risk for CBCT use in breast radiotherapy (Donovan et al., 2012). Moreover, the US National Research Council which developed the BEIR model for risk calculation has admitted that there are many broad assumptions which could limit the accuracy of such LAR estimates (Council, 2006).

Previous simulation studies have shown that CT imaging during radiotherapy has only a small fractional contribution to the total radiation dose received by critical organs (Harrison et al., 2006, Chow et al., 2008, Harrison, 2004). This has also been confirmed by the International Commission for Radiological Protection (ICRP) in their latest guidelines on CBCT use (Rehani et al., 2015).

Chow et al. used Monte Carlo simulation to calculate the additional dose delivered to various pelvic organs from CBCT during prostate radiotherapy. They found that there was minimal effect on the rectum and bladder dose-volume histograms from the CBCT. The highest additional dose was to the femoral heads, but despite this the femoral heads were well below tolerance limits. Their study estimated an increase in rectal NTCP of 0.5% due to the use of CBCT verification during radiotherapy, but this was counterbalanced by an estimated 3% reduction in rectal NTCP if margins could be reduced from 10 mm to 5 mm.

Harrison et al. used an anthropomorphic phantom to calculate concomitant doses. On their highest exposure protocol of 26 CTs, the proportion of dose due to CT was 3% to colon (including rectum) and 1% to bladder. Deng et al. used Monte Carlo simulation and estimated that 3.2% of colon and bladder dose could be attributed to CBCT dose (Deng et al., 2012). Their study found that there was lower concomitant dose to most organs if

a full-fan mode was used for CBCT acquisition. As would be expected, a shorter scan length also reduced dose exposure.

Modern second-generation kV CBCT imagers deliver lower exposure dose than MV portal imaging, although higher dose than kV portal imaging (Ding and Munro, 2013). Reduction in exposure doses have even been achieved by manufacturers improving their imaging settings between version upgrades (Ding et al., 2010).

In our study centres, the average measured concomitant dose to the pelvis was 30 mGy per on-board CBCT exposure. This is in line with concomitant dose reported by other centres for this treatment site (Stock et al., 2012, Amer et al., 2007). The nominal total concomitant dose would be approximately 0.9 Gy per treatment course with daily imaging. The reduction in rectal dose due to increased accuracy with daily CBCT in our study would further reduce concomitant dose.

There are clear limitations to adding concomitant dose from kV imaging directly to MV radiotherapy dose. This is because of intrinsic differences in the type of energy. kV energy has greater photoelectric effects and lead to increased skin and bone dose (Harrison et al., 2006, Downes et al., 2009). The differences in dose distribution would therefore render simple

summation of doses from the two modalities inappropriate. Calculation of stochastic risk using BEIR type models for this dataset was outside the scope of this work.

6.7 Cost-effectiveness of CBCT verification

If daily imaging is used for all patients, the incremental time implications are modest. An economic analysis study in France was conducted in patients undergoing prostate radiotherapy (Perrier et al., 2013). It showed an increase in treatment time by 7.3 minutes per fraction with the use of daily CBCT in comparison to weekly. A further European study has shown that the additional time required for prostate cases using Elekta CBCT equipment was 5.5 minutes (Korreman et al., 2010).

In our study, the mean time for CBCT acquisition and radiographer review was 3.8 minutes (range 2.2 to 7.7 minutes). However, this was across three UK centres where daily CBCT review was well-established as routine practice for prostate radiotherapy staff. A continuing program of radiographer induction and training is vital for radiotherapy centres which incorporate this IGRT strategy. Once training has been established, the interobserver variation in CBCT interpretation can be minimized.

A study comparing CBCT shifts between trained radiographers and oncologists has shown that there is minimal interobserver variation (Jereczek-Fossa et al., 2014). They found substantial agreement (kappa >

0.6) in 10 out of 16 comparisons and moderate agreement in the remainder.

The additional cost implications of CBCT installation and quality assurance also should be considered. This may vary widely between countries. A Canadian study (Ploquin and Dunscombe, 2009) showed a relatively large incremental cost of 2592 euros for a 35-fraction treatment with daily CBCT. This is in comparison to 1772 euros with daily portal imaging. They used a dosimetric parameter ΔEUD to quantify the improvement with IGRT techniques. The incremental cost per ΔEUD of 3379 euros for daily CBCT in comparison to 2310 euros daily portal imaging was reported. However, they have made a key assumption in their calculation that both portal imaging and CBCT are equivalent in imaging characteristics. There is evidence that this assumption is incorrect, as discussed earlier in this thesis.

The European study (Perrier et al., 2013) showed that the incremental cost of daily CBCT per patient was lower at 679 euros. The cost of fiducial-based IGRT was even lower at 187 euros. However, a substantial proportion of this difference was due to the difference in cost of the linear accelerator with on-board imaging. Most UK radiotherapy centres already have appropriately equipped linear accelerators according to our IGRT

survey results. Therefore, the incremental cost of daily CBCT in the UK is likely to be lower than in this European study.

6.8 PTV margin analysis

The PTV margin analysis indicates that a reduction of margin to 5 mm is feasible with daily CBCT imaging. This is comparable to previous studies which have used fiducial-based IGRT (Pawlowski et al., 2010). Their study which utilized prostate fiducials and weekly CBCT imaging demonstrated that reduction of margin to 4 mm (with 3 mm posteriorly) is feasible.

I used the systematic and random errors generated from analysis of shifts to compare our dosimetric margin results with that obtained from a margin formula. The Stroom formula (Stroom et al., 1999) was used, as this is one of the earliest validated margin formulae. It also uses a CTV V95 coverage threshold target of 99%, which is in line with the dosimetric coverage target for each fraction in my study. The other major formula is the van Herk formula (van Herk et al., 2000) which uses a population based coverage threshold of 90% of patients covered by the minimum 95% dose to CTV.

If the Stroom formula was used on our dataset to provide an estimate of required margin, it would be 6.9 mm (left-right), 4.2 mm (sup-inf) and 9.8 mm (ant-post). The magnitude of setup error in the left-right direction was

unexpected but is in line with a previously reported series (Mayyas et al., 2013). In practice, the actual random and systematic errors could be minimized by daily online matching. These results therefore illustrate the conservative nature of margin formulae, and the importance of assessing actual dosimetry during treatment.

Residual errors which could not be assessed in our study have also to be taken in to account when considering the overall margin used between CTV and PTV. These include intrafraction motion (Kron et al., 2010, Thomas et al., 2013, Huang et al., 2002a) during prostate radiotherapy.

Huang et al. evaluated intrafraction shifts during prostate radiotherapy using a B-mode ultrasound system. They demonstrated shifts of 0.01 mm (+/- 0.4 mm), 0.2 mm (+/- 1.3 mm) and 0.1 mm (+/- 1.0 mm) in the left, anterior and superior directions. The intrafraction motion was clearly less than interfraction motion in their study.

Kron et al. assessed intrafraction motion by using orthogonal x-rays done pre- and post-treatment in a series of 184 patients. They found a mean three-dimensional vector shift of 1.7 mm (range 0 – 25 mm), with no trend towards any particular direction. There was no improvement in the intrafraction error through the course of radiotherapy.

Thomas et al. assessed intrafraction motion using MVCT images in helical tomotherapy for prostate cancer. They calculated an additional required margin of 2.2 mm, 2.1 mm and 2.1 mm in the left-right, superior-inferior and antero-posterior directions to account for intrafraction error.

Patients in our study were treated with step-and-shoot IMRT where treatment time would be influenced by the number of fields used. However, intrafraction motion will be of lesser importance with modern IMRT techniques such as arc treatment, where treatment times are shorter. This was confirmed in a study evaluating intrafraction motion during arc radiotherapy (Baker and Behrens, 2016). The investigators found that 3-D vector displacement more than 2 mm occurred in 12% of fractions and only 4% showed displacements larger than 3 mm during a typical 2.5-minute fraction. It also exemplifies the need for individual centres to calculate setup margins based on the particular combination of imaging protocol and equipment used for radiotherapy treatment of prostate patients.

The other type of residual error is registration error during soft-tissue matching. Morrow et al. assessed this error in relation to different modalities of verification CT imaging (Morrow et al., 2012). They found that kV CBCT had lower registration errors than MVCT due to better

image quality. The inter-observer variability ranged from 0.6 to 2.5 mm for the kV imaging in comparison to 1.7 to 3.2 mm for MV CT imaging. The intra-observer variability was much less at approximately 1 mm. The total additional PTV margin required to correct for these residual errors has been estimated to be up to 3 mm in a study where CBCT imaging was repeated post-treatment (Letourneau et al., 2005).

The results of my investigation also caution against further margin reduction to 3 mm. This is because there would then be increasing numbers of radiotherapy fractions where CTV coverage is reduced. A 5-mm margin all around the CTV provides a good balance of target coverage and toxicity reduction. Individual centres should evaluate their PTV margins in relation to the imaging protocol, to optimally use CBCT verification during prostate radiotherapy.

Chapter 7. Conclusion

This MD(Res) project has provided valuable information for optimization of verification imaging during prostate radiotherapy. During preliminary work, I developed and validated a dose calculation strategy on cone beam CT. A national survey of prostate IGRT practice confirmed that the principal difference in verification strategy was the use of daily vs weekly imaging.

Initial work showed the drops in coverage that occur if a bone match strategy is used compared with soft tissue matching. Further analysis of actual dose coverage during each fraction of radiotherapy has allowed an accurate estimation of the quantitative benefit of daily imaging.

The study showed that 90% of patients had improved target coverage with daily online in comparison to weekly online imaging. A median of 37 fractions achieved CTV coverage with daily imaging compared with 34 fractions with a weekly online protocol. 80% of patients had a reduction in rectal dose with the daily protocol. Margin reduction to 5 mm with adequate target coverage was feasible with daily imaging.

In conclusion, daily online CBCT verification improves CTV coverage and reduces rectal dose during IGRT for prostate cancer. Daily CBCT imaging allows reduction of CTV-PTV margin for radiotherapy.

As a result of this MD (Res) project, there have been advances in knowledge in the following areas:

1. Understanding the current state of image-guided radiotherapy practice for prostate cancer in the United Kingdom
2. Validation of a method for dose calculation on cone beam CT for verification and research purposes
3. Quantification of the dosimetric benefits of daily CBCT verification during prostate radiotherapy
4. Providing a dosimetric approach for deciding on the CTV-PTV margin in prostate radiotherapy

The utilization of MRI imaging will revolutionize radiotherapy verification in prostate cancer in the future. Further research will be required to develop MRI-guided prostate radiotherapy. The dose calculation techniques and results of this study will be useful in design of verification strategies on different platforms.

References

AHNESJO, A. 1989. Collapsed cone convolution of radiant energy for photon dose calculation in heterogeneous media. *Med Phys,* 16**,** 577-92.

AL-MAMGANI, A., VAN PUTTEN, W. L., HEEMSBERGEN, W. D., VAN LEENDERS, G. J., SLOT, A., DIELWART, M. F., INCROCCI, L. & LEBESQUE, J. V. 2008. Update of Dutch multicenter dose-escalation trial of radiotherapy for localized prostate cancer. *Int J Radiat Oncol Biol Phys,* 72**,** 980-8.

AMER, A., MARCHANT, T., SYKES, J., CZAJKA, J. & MOORE, C. 2007. Imaging doses from the Elekta Synergy X-ray cone beam CT system. *Br J Radiol,* 80**,** 476-82.

BAKER, M. & BEHRENS, C. F. 2016. Determining intrafractional prostate motion using four dimensional ultrasound system. *BMC Cancer,* 16**,** 1-7.

BARNEY, B. M., LEE, R. J., HANDRAHAN, D., WELSH, K. T., COOK, J. T. & SAUSE, W. T. 2011. Image-guided radiotherapy (IGRT) for prostate cancer comparing kV imaging of fiducial markers with cone beam computed tomography (CBCT). *Int J Radiat Oncol Biol Phys,* 80**,** 301-5.

BATTISTA, J. J., JOHNSON, C., TURNBULL, D., KEMPE, J., BZDUSEK, K., VAN DYK, J. & BAUMAN, G. 2013. Dosimetric and

radiobiological consequences of computed tomography-guided adaptive strategies for intensity modulated radiation therapy of the prostate. *Int J Radiat Oncol Biol Phys,* 87**,** 874-80.

BIGGS, P. J., GOITEIN, M. & RUSSELL, M. D. 1985. A diagnostic X ray field verification device for a 10 MV linear accelerator. *Int J Radiat Oncol Biol Phys,* 11**,** 635-43.

CHAN, M. F., YANG, J., SONG, Y., BURMAN, C., CHAN, P. & LI, S. 2011. Evaluation of imaging performance of major image guidance systems. *Biomedical Imaging and Intervention Journal,* 7**,** e11.

CHEN, Z., YANG, Z., WANG, J. & HU, W. 2016. Dosimetric impact of different bladder and rectum filling during prostate cancer radiotherapy. *Radiation Oncology,* 11**,** 1-8.

CHENG, C.-W. & DAS, I. J. 1999. Treatment plan evaluation using dose–volume histogram (DVH) and spatial dose–volume histogram (zDVH). *International Journal of Radiation Oncology*Biology*Physics,* 43**,** 1143-1150.

CHENNUPATI, S. K., PELIZZARI, C. A., KUNNAVAKKAM, R. & LIAUW, S. L. 2014. Late toxicity and quality of life after definitive treatment of prostate cancer: redefining optimal rectal sparing constraints for intensity-modulated radiation therapy. *Cancer Medicine,* 3**,** 954-961.

CHOW, J. C., LEUNG, M. K., ISLAM, M. K., NORRLINGER, B. D. & JAFFRAY, D. A. 2008. Evaluation of the effect of patient dose from

cone beam computed tomography on prostate IMRT using Monte Carlo simulation. *Med Phys,* 35**,** 52-60.

COUNCIL, N. R. 2006. *Health Risks from Exposure to Low Levels of Ionizing Radiation: BEIR VII Phase 2,* Washington, DC, The National Academies Press.

COX, J. D., STETZ, J. & PAJAK, T. F. 1995. Toxicity criteria of the Radiation Therapy Oncology Group (RTOG) and the European Organization for Research and Treatment of Cancer (EORTC). *Int J Radiat Oncol Biol Phys,* 31**,** 1341-6.

CRAIG, T., MOISEENKO, V., BATTISTA, J. & VAN DYK, J. 2003. The impact of geometric uncertainty on hypofractionated external beam radiation therapy of prostate cancer. *International Journal of Radiation Oncology*Biology*Physics,* 57**,** 833-842.

D'AMICO, A. V., WHITTINGTON, R., MALKOWICZ, S. B., SCHULTZ, D., BLANK, K., BRODERICK, G. A., TOMASZEWSKI, J. E., RENSHAW, A. A., KAPLAN, I. & BEARD, C. J. 1998. Biochemical outcome after radical prostatectomy, external beam radiation therapy, or interstitial radiation therapy for clinically localized prostate cancer. *Jama,* 280**,** 969-974.

DE CREVOISIER, R., TUCKER, S. L., DONG, L., MOHAN, R., CHEUNG, R., COX, J. D. & KUBAN, D. A. 2005. Increased risk of biochemical and local failure in patients with distended rectum on the planning CT for prostate cancer radiotherapy. *Int J Radiat Oncol Biol Phys,* 62**,** 965-73.

DEARNALEY, D. P., JOVIC, G., SYNDIKUS, I., KHOO, V., COWAN, R. A., GRAHAM, J. D., AIRD, E. G., BOTTOMLEY, D., HUDDART, R. A., JOSE, C. C., MATTHEWS, J. H. L., MILLAR, J. L., MURPHY, C., RUSSELL, J. M., SCRASE, C. D., PARMAR, M. K. B. & SYDES, M. R. 2014. Escalated-dose versus control-dose conformal radiotherapy for prostate cancer: long-term results from the MRC RT01 randomised controlled trial. *The Lancet Oncology,* 15**,** 464-473.

DEARNALEY, D. P., SYDES, M. R., GRAHAM, J. D., AIRD, E. G., BOTTOMLEY, D., COWAN, R. A., HUDDART, R. A., JOSE, C. C., MATTHEWS, J. H. L., MILLAR, J., MOORE, A. R., MORGAN, R. C., RUSSELL, J. M., SCRASE, C. D., STEPHENS, R. J., SYNDIKUS, I. & PARMAR, M. K. B. 2007. Escalated-dose versus standard-dose conformal radiotherapy in prostate cancer: first results from the MRC RT01 randomised controlled trial. *The Lancet Oncology,* 8**,** 475-487.

DENG, J., CHEN, Z., YU, J. B., ROBERTS, K. B., PESCHEL, R. E. & NATH, R. 2012. Testicular doses in image-guided radiotherapy of prostate cancer. *Int J Radiat Oncol Biol Phys,* 82**,** e39-47.

DEPARTMENT OF HEALTH 2000. Ionising Radiation (Medical Exposure) Regulations 2000 (IRMER). *In:* HEALTH, D. O. (ed.). London: Department of Health.

DEPARTMENT OF HEALTH 2007. Radiotherapy: developing a world class service for England. Report to Ministers from National Radiotherapy Advisory Group. London.

DING, G. X. & MUNRO, P. 2013. Radiation exposure to patients from image guidance procedures and techniques to reduce the imaging dose. *Radiotherapy and Oncology,* 108**,** 91-98.

DING, G. X., MUNRO, P., PAWLOWSKI, J., MALCOLM, A. & COFFEY, C. W. 2010. Reducing radiation exposure to patients from kV-CBCT imaging. *Radiotherapy and Oncology,* 97**,** 585-592.

DONOVAN, E. M., JAMES, H., BONORA, M., YARNOLD, J. R. & EVANS, P. M. 2012. Second cancer incidence risk estimates using BEIR VII models for standard and complex external beam radiotherapy for early breast cancer. *Medical Physics,* 39**,** 5814-5824.

DOWNES, P., JARVIS, R., RADU, E., KAWRAKOW, I. & SPEZI, E. 2009. Monte Carlo simulation and patient dosimetry for a kilovoltage cone-beam CT unit. *Medical physics,* 36**,** 4156-4167.

DRZYMALA, R. E., MOHAN, R., BREWSTER, L., CHU, J., GOITEIN, M., HARMS, W. & URIE, M. 1991. Dose-volume histograms. *International Journal of Radiation Oncology*Biology*Physics,* 21**,** 71-78.

ENGELS, B., SOETE, G., VERELLEN, D. & STORME, G. 2009. Conformal arc radiotherapy for prostate cancer: increased biochemical failure in patients with distended rectum on the

planning computed tomogram despite image guidance by implanted markers. *Int J Radiat Oncol Biol Phys,* 74**,** 388-91.

FARGIER-VOIRON, M., GUILLET, L., POMMIER, P., SARRUT, D. & BISTON, M. 2015. MO-DE-210-04: Repositioning and Monitoring of Prostate Cancer Radiotherapy with a New 4D Ultrasound Intra-Modality IGRT Device. *Medical Physics,* 42**,** 3560-3560.

FOSTER, R. D., SOLBERG, T. D., LI, H. S., KERKHOFF, A., ENKE, C. A., WILLOUGHBY, T. R. & KUPELIAN, P. A. 2010. Comparison of transabdominal ultrasound and electromagnetic transponders for prostate localization. *J Appl Clin Med Phys,* 11**,** 2924.

FOTINA, I., HOPFGARTNER, J., STOCK, M., STEININGER, T., LUTGENDORF-CAUCIG, C. & GEORG, D. 2012. Feasibility of CBCT-based dose calculation: comparative analysis of HU adjustment techniques. *Radiother Oncol,* 104**,** 249-56.

FRIEDMAN, M. 1937. The Use of Ranks to Avoid the Assumption of Normality Implicit in the Analysis of Variance. *Journal of the American Statistical Association,* 32**,** 675-701.

GAY, H. A., BARTHOLD, H. J., O'MEARA, E., BOSCH, W. R., EL NAQA, I., AL-LOZI, R., ROSENTHAL, S. A., LAWTON, C., LEE, W. R., SANDLER, H., ZIETMAN, A., MYERSON, R., DAWSON, L. A., WILLETT, C., KACHNIC, L. A., JHINGRAN, A., PORTELANCE, L., RYU, J., SMALL, W., JR., GAFFNEY, D., VISWANATHAN, A. N. & MICHALSKI, J. M. 2012. Pelvic normal tissue contouring guidelines

for radiation therapy: a Radiation Therapy Oncology Group consensus panel atlas. *Int J Radiat Oncol Biol Phys,* 83**,** e353-62.

GHILEZAN, M. J., JAFFRAY, D. A., SIEWERDSEN, J. H., VAN HERK, M., SHETTY, A., SHARPE, M. B., ZAFAR JAFRI, S., VICINI, F. A., MATTER, R. C., BRABBINS, D. S. & MARTINEZ, A. A. 2005. Prostate gland motion assessed with cine-magnetic resonance imaging (cine-MRI). *Int J Radiat Oncol Biol Phys,* 62**,** 406-17.

GILL, S., LI, J., THOMAS, J., BRESSEL, M., THURSKY, K., STYLES, C., TAI, K. H., DUCHESNE, G. M. & FOROUDI, F. 2012. Patient-reported complications from fiducial marker implantation for prostate image-guided radiotherapy. *The British Journal of Radiology,* 85**,** 1011-1017.

GILL, S., THOMAS, J., FOX, C., KRON, T., ROLFO, A., LEAHY, M., CHANDER, S., WILLIAMS, S., TAI, K. H., DUCHESNE, G. M. & FOROUDI, F. 2011. Acute toxicity in prostate cancer patients treated with and without image-guided radiotherapy. *Radiat Oncol,* 6**,** 145.

GILL, S. K., REDDY, K., CAMPBELL, N., CHEN, C. & PEARSON, D. 2015. Determination of optimal PTV margin for patients receiving CBCT-guided prostate IMRT: comparative analysis based on CBCT dose calculation with four different margins. *JACMP,* 16.

GRAF, R., BOEHMER, D., BUDACH, V. & WUST, P. 2012. Interfraction rotation of the prostate as evaluated by kilovoltage X-ray fiducial

marker imaging in intensity-modulated radiotherapy of localized prostate cancer. *Med Dosim,* 37**,** 396-400.

GREAT BRITAIN 1998. Data Protection Act 1998. London: The Stationery Office (TSO).

GREGOIRE, V. & MACKIE, T. R. 2011. State of the art on dose prescription, reporting and recording in Intensity-Modulated Radiation Therapy (ICRU report No. 83). *Cancer Radiother,* 15**,** 555-9.

HAMMOUD, R., PATEL, S. H., PRADHAN, D., KIM, J., GUAN, H., LI, S. & MOVSAS, B. 2008. Examining margin reduction and its impact on dose distribution for prostate cancer patients undergoing daily cone-beam computed tomography. *Int J Radiat Oncol Biol Phys,* 71**,** 265-73.

HARRISON, R. M. 2004. Second cancers following radiotherapy: a suggested common dosimetry framework for therapeutic and concomitant exposures. *Br J Radiol,* 77**,** 986-90.

HARRISON, R. M., WILKINSON, M., SHEMILT, A., RAWLINGS, D. J., MOORE, M. & LECOMBER, A. R. 2006. Organ doses from prostate radiotherapy and associated concomitant exposures. *Br J Radiol,* 79**,** 487-96.

HATTON, J. A., GREER, P. B., TANG, C., WRIGHT, P., CAPP, A., GUPTA, S., PARKER, J., WRATTEN, C. & DENHAM, J. W. 2011. Does the planning dose–volume histogram represent treatment doses in image-guided prostate radiation therapy? Assessment with

cone-beam computerised tomography scans. *Radiotherapy and Oncology,* 98**,** 162-168.

HEEMSBERGEN, W. D., HOOGEMAN, M. S., WITTE, M. G., PEETERS, S. T., INCROCCI, L. & LEBESQUE, J. V. 2007. Increased risk of biochemical and clinical failure for prostate patients with a large rectum at radiotherapy planning: results from the Dutch trial of 68 GY versus 78 Gy. *Int J Radiat Oncol Biol Phys,* 67**,** 1418-24.

HILMAN, S., SMITH, R., MASSON, S., COOMBER, H., BAHL, A., CHALLAPALLI, A. & JACOBS, P. Implementation of a Daily Transperineal Ultrasound System as Image-guided Radiotherapy for Prostate Cancer. *Clinical Oncology,* 29**,** e49.

HODGES, J. L. & LEHMANN, E. L. 1963. Estimates of Location Based on Rank Tests. 598-611.

HOLLOWAY, A. F. 1958. A Localising Device for a Rotating Cobalt Therapy Unit. *The British Journal of Radiology,* 31**,** 227-227.

HU, W., YE, J., WANG, J., MA, X. & ZHANG, Z. 2010. Use of kilovoltage X-ray volume imaging in patient dose calculation for head-and-neck and partial brain radiation therapy. *Radiat Oncol,* 5**,** 29.

HUANG, E., DONG, L., CHANDRA, A., KUBAN, D. A., ROSEN, I. I., EVANS, A. & POLLACK, A. 2002a. Intrafraction prostate motion during IMRT for prostate cancer. *International Journal of Radiation Oncology*Biology*Physics,* 53**,** 261-268.

HUANG, E. H., POLLACK, A., LEVY, L., STARKSCHALL, G., DONG, L., ROSEN, I. & KUBAN, D. A. 2002b. Late rectal toxicity: dose-volume

effects of conformal radiotherapy for prostate cancer. *International Journal of Radiation Oncology*Biology*Physics,* 54**,** 1314-1321.

JAFFRAY, D. A. & SIEWERDSEN, J. H. 2000. Cone-beam computed tomography with a flat-panel imager: Initial performance characterization. *Medical Physics,* 27**,** 1311-1323.

JAFFRAY, D. A., SIEWERDSEN, J. H., WONG, J. W. & MARTINEZ, A. A. 2002. Flat-panel cone-beam computed tomography for image-guided radiation therapy. *International Journal of Radiation Oncology*Biology*Physics,* 53**,** 1337-1349.

JERECZEK-FOSSA, B. A., POBBIATI, C., SANTORO, L., FODOR, C., FANTI, P., VIGORITO, S., BARONI, G., ZERINI, D., DE COBELLI, O. & ORECCHIA, R. 2014. Prostate positioning using cone-beam computer tomography based on manual soft-tissue registration. *Strahlentherapie und Onkologie,* 190**,** 81-87.

JOHNS, H. E. & CUNNINGHAM, J. R. 1959. A precision cobalt 60 unit for fixed field and rotation therapy. *Am J Roentgenol Radium Ther Nucl Med,* 81**,** 4-12.

KAMATH, S., SONG, W., CHVETSOV, A., OZAWA, S., LU, H., SAMANT, S., LIU, C., LI, J. G. & PALTA, J. R. 2011. An image quality comparison study between XVI and OBI CBCT systems. *Journal of Applied Clinical Medical Physics,* 12**,** 376-390.

KEALL, P. J., BARTON, M. & CROZIER, S. 2014. The Australian Magnetic Resonance Imaging–Linac Program. *Seminars in Radiation Oncology,* 24**,** 203-206.

KESTIN, L., GOLDSTEIN, N., VICINI, F., YAN, D., KORMAN, H. & MARTINEZ, A. 2002. Treatment of prostate cancer with radiotherapy: should the entire seminal vesicles be included in the clinical target volume? *Int J Radiat Oncol Biol Phys,* 54**,** 686-97.

KIM, D. W., CHUNG, W. K. & YOON, M. 2013. Imaging doses and secondary cancer risk from kilovoltage cone-beam CT in radiation therapy. *Health Phys,* 104**,** 499-503.

KORREMAN, S., RASCH, C., MCNAIR, H., VERELLEN, D., OELFKE, U., MAINGON, P., MIJNHEER, B. & KHOO, V. 2010. The European Society of Therapeutic Radiology and Oncology–European Institute of Radiotherapy (ESTRO–EIR) report on 3D CT-based in-room image guidance systems: A practical and technical review and guide. *Radiotherapy and Oncology,* 94**,** 129-144.

KRON, T., THOMAS, J., FOX, C., THOMPSON, A., OWEN, R., HERSCHTAL, A., HAWORTH, A., TAI, K. H. & FOROUDI, F. 2010. Intra-fraction prostate displacement in radiotherapy estimated from pre- and post-treatment imaging of patients with implanted fiducial markers. *Radiother Oncol,* 95**,** 191-7.

KUBAN, D. A., TUCKER, S. L., DONG, L., STARKSCHALL, G., HUANG, E. H., CHEUNG, M. R., LEE, A. K. & POLLACK, A. 2008. Long-term results of the M. D. Anderson randomized dose-escalation trial for prostate cancer. *Int J Radiat Oncol Biol Phys,* 70**,** 67-74.

KUPELIAN, P., WILLOUGHBY, T., MAHADEVAN, A., DJEMIL, T., WEINSTEIN, G., JANI, S., ENKE, C., SOLBERG, T., FLORES, N.,

LIU, D., BEYER, D. & LEVINE, L. 2007. Multi-institutional clinical experience with the Calypso System in localization and continuous, real-time monitoring of the prostate gland during external radiotherapy. *International Journal of Radiation Oncology*Biology*Physics,* 67**,** 1088-1098.

KUPELIAN, P. A., LANGEN, K. M., ZEIDAN, O. A., MEEKS, S. L., WILLOUGHBY, T. R., WAGNER, T. H., JESWANI, S., RUCHALA, K. J., HAIMERL, J. & OLIVERA, G. H. 2006. Daily variations in delivered doses in patients treated with radiotherapy for localized prostate cancer. *Int J Radiat Oncol Biol Phys,* 66**,** 876-82.

LAGENDIJK, J. J., RAAYMAKERS, B. W., RAAIJMAKERS, A. J., OVERWEG, J., BROWN, K. J., KERKHOF, E. M., VAN DER PUT, R. W., HARDEMARK, B., VAN VULPEN, M. & VAN DER HEIDE, U. A. 2008. MRI/linac integration. *Radiother Oncol,* 86**,** 25-9.

LEHMANN, J., PERKS, J., SEMON, S., HARSE, R. & PURDY, J. A. 2007. Commissioning experience with cone-beam computed tomography for image-guided radiation therapy. *J Appl Clin Med Phys,* 8**,** 2354.

LEONG, J. 1986. Use of digital fluoroscopy as an on-line verification device in radiation therapy. *Phys Med Biol,* 31**,** 985-92.

LETOURNEAU, D., MARTINEZ, A. A., LOCKMAN, D., YAN, D., VARGAS, C., IVALDI, G. & WONG, J. 2005. Assessment of residual error for online cone-beam CT-guided treatment of prostate cancer patients. *Int J Radiat Oncol Biol Phys,* 62**,** 1239-46.

LIANG, J., WU, Q. & YAN, D. 2009. THE ROLE OF SEMINAL VESICLE MOTION IN TARGET MARGIN ASSESSMENT FOR ONLINE IMAGE GUIDED RADIOTHERAPY (IGRT) FOR PROSTATE CANCER. *International journal of radiation oncology, biology, physics,* 73**,** 935-943.

LOH, J., BAKER, K., SRIDHARAN, S., GREER, P., WRATTEN, C., CAPP, A., GALLAGHER, S. & MARTIN, J. 2015. Infections after fiducial marker implantation for prostate radiotherapy: are we underestimating the risks? *Radiation Oncology,* 10**,** 38.

LOU, Y., NIU, T., JIA, X., VELA, P. A., ZHU, L. & TANNENBAUM, A. R. 2013. Joint CT/CBCT deformable registration and CBCT enhancement for cancer radiotherapy. *Medical Image Analysis,* 17**,** 387-400.

MAIL, N., MOSELEY, D., SIEWERDSEN, J. & JAFFRAY, D. 2009. The influence of bowtie filtration on cone-beam CT image quality. *Medical Physics,* 36**,** 22-32.

MARCHANT, T. E., MOORE, C. J., ROWBOTTOM, C. G., MACKAY, R. I. & WILLIAMS, P. C. 2008. Shading correction algorithm for improvement of cone-beam CT images in radiotherapy. *Phys Med Biol,* 53**,** 5719-33.

MARTIN BLAND, J. & ALTMAN, D. 1986. STATISTICAL METHODS FOR ASSESSING AGREEMENT BETWEEN TWO METHODS OF CLINICAL MEASUREMENT. *The Lancet,* 327**,** 307-310.

MAUND, I. F., BENSON, R. J., FAIRFOUL, J., COOK, J., HUDDART, R. & POYNTER, A. 2014. Image-guided radiotherapy of the prostate using daily CBCT: the feasibility and likely benefit of implementing a margin reduction. *Br J Radiol,* 87**,** 20140459.

MAYLES, W. P. & RADIOTHERAPY DEVELOPMENT, B. 2010. Survey of the availability and use of advanced radiotherapy technology in the UK. *Clin Oncol (R Coll Radiol),* 22**,** 636-42.

MAYYAS, E., CHETTY, I. J., CHETVERTKOV, M., WEN, N., NEICU, T., NURUSHEV, T., REN, L., LU, M., STRICKER, H., PRADHAN, D., MOVSAS, B. & ELSHAIKH, M. A. 2013. Evaluation of multiple image-based modalities for image-guided radiation therapy (IGRT) of prostate carcinoma: a prospective study. *Med Phys,* 40**,** 041707.

MILLER, C. W. 1954. An 8-MeV linear accelerator for X-ray therapy. *Proceedings of the IEE-Part I: General,* 101**,** 207-221.

MORROW, N. V., LAWTON, C. A., QI, X. S. & LI, X. A. 2012. Impact of computed tomography image quality on image-guided radiation therapy based on soft tissue registration. *Int J Radiat Oncol Biol Phys,* 82**,** e733-8.

MOSELEY, D. J., WHITE, E. A., WILTSHIRE, K. L., ROSEWALL, T., SHARPE, M. B., SIEWERDSEN, J. H., BISSONNETTE, J. P., GOSPODAROWICZ, M., WARDE, P., CATTON, C. N. & JAFFRAY, D. A. 2007. Comparison of localization performance with implanted fiducial markers and cone-beam computed tomography for on-line

image-guided radiotherapy of the prostate. *Int J Radiat Oncol Biol Phys,* 67**,** 942-53.

MUNCK AF ROSENSCHOLD, P., DESAI, N. B., OH, J. H., APTE, A., HUNT, M., KALIKSTEIN, A., MECHALAKOS, J., HAPPERSETT, L., DEASY, J. O. & ZELEFSKY, M. J. 2014. Modeling positioning uncertainties of prostate cancer external beam radiation therapy using pre-treatment data. *Radiother Oncol,* 110**,** 251-5.

MURPHY, M. J., BALTER, J., BALTER, S., BENCOMO, J. A., DAS, I. J., JIANG, S. B., MA, C.-M., OLIVERA, G. H., RODEBAUGH, R. F., RUCHALA, K. J., SHIRATO, H. & YIN, F.-F. 2007. The management of imaging dose during image-guided radiotherapy: Report of the AAPM Task Group 75. *Medical Physics,* 34**,** 4041-4063.

NABAVIZADEH, N., ELLIOTT, D. A., CHEN, Y., KUSANO, A. S., MITIN, T., THOMAS JR, C. R. & HOLLAND, J. M. 2016. Image Guided Radiation Therapy (IGRT) Practice Patterns and IGRT's Impact on Workflow and Treatment Planning: Results From a National Survey of American Society for Radiation Oncology Members. *International Journal of Radiation Oncology*Biology*Physics,* 94**,** 850-857.

NATIONAL CLINICAL ANALYSIS AND SPECIALIZED APPLICATIONS TEAM 2011. The UK Survey of Radiotherapy Equipment 2010.

NATIONAL RADIOTHERAPY IMPLEMENTATION GROUP 2012. Image Guided Radiotherapy (IGRT): Guidance for implementation and use.

NICHOL, A. M., BROCK, K. K., LOCKWOOD, G. A., MOSELEY, D. J., ROSEWALL, T., WARDE, P. R., CATTON, C. N. & JAFFRAY, D. A. 2007. A magnetic resonance imaging study of prostate deformation relative to implanted gold fiducial markers. *International Journal of Radiation Oncology*Biology*Physics,* 67**,** 48-56.

ORTON, N. P. & TOMÉ, W. A. 2004. The impact of daily shifts on prostate IMRT dose distributions. *Medical Physics,* 31**,** 2845.

PADHANI, A. R., KHOO, V. S., SUCKLING, J., HUSBAND, J. E., LEACH, M. O. & DEARNALEY, D. P. 1999. Evaluating the effect of rectal distension and rectal movement on prostate gland position using cine MRI. *International Journal of Radiation Oncology*Biology*Physics,* 44**,** 525-533.

PARK, S. S., YAN, D., MCGRATH, S., DILWORTH, J. T., LIANG, J., YE, H., KRAUSS, D. J., MARTINEZ, A. A. & KESTIN, L. L. 2012. Adaptive image-guided radiotherapy (IGRT) eliminates the risk of biochemical failure caused by the bias of rectal distension in prostate cancer treatment planning: clinical evidence. *Int J Radiat Oncol Biol Phys,* 83**,** 947-52.

PAWLOWSKI, J. M., YANG, E. S., MALCOLM, A. W., COFFEY, C. W. & DING, G. X. 2010. Reduction of Dose Delivered to Organs at Risk in Prostate Cancer Patients via Image-Guided Radiation Therapy. *International Journal of Radiation Oncology*Biology*Physics,* 76**,** 924-934.

PERRIER, L., MORELLE, M., POMMIER, P., LAGRANGE, J.-L., LAPLANCHE, A., DUDOUET, P., SUPIOT, S., CHAUVET, B., NGUYEN, T.-D., CREHANGE, G., BECKENDORF, V., PENE, F., MURACCIOLE, X., BACHAUD, J.-M., LE PRISÉ, E. & DE CREVOISIER, R. 2013. Cost of prostate image-guided radiation therapy: Results of a randomized trial. *Radiotherapy and Oncology,* 106**,** 50-58.

PLOQUIN, N. & DUNSCOMBE, P. 2009. A cost-outcome analysis of Image-Guided Patient Repositioning in the radiation treatment of cancer of the prostate. *Radiotherapy and Oncology,* 93**,** 25-31.

POULIOT, J., BANI-HASHEMI, A., JOSEPHINE, C., SVATOS, M., GHELMANSARAI, F., MITSCHKE, M., AUBIN, M., XIA, P., MORIN, O., BUCCI, K., ROACH, M., HERNANDEZ, P., ZHENG, Z., HRISTOV, D. & VERHEY, L. 2005. Low-dose megavoltage cone-beam CT for radiation therapy. *International Journal of Radiation Oncology*Biology*Physics,* 61**,** 552-560.

REHANI, M. M., GUPTA, R., BARTLING, S., SHARP, G. C., PAUWELS, R., BERRIS, T. & BOONE, J. M. 2015. ICRP Publication 129: Radiological Protection in Cone Beam Computed Tomography (CBCT). *Annals of the ICRP,* 44**,** 7-127.

RICHTER, A., HU, Q., STEGLICH, D., BAIER, K., WILBERT, J., GUCKENBERGER, M. & FLENTJE, M. 2008. Investigation of the usability of conebeam CT data sets for dose calculation. *Radiat Oncol,* 3**,** 42.

ROYAL COLLEGE OF RADIOLOGISTS, SOCIETY AND COLLEGE OF RADIOGRAPHERS & INSTITUTE OF PHYSICS AND ENGINEERING IN MEDICINE 2008. On target : ensuring geometric accuracy in radiotherapy. London: Royal College of Radiologists.

RUCHALA, K., OLIVERA, G., SCHLOESSER, E. & MACKIE, T. 1999. Megavoltage CT on a tomotherapy system. *Physics in Medicine and Biology,* 44**,** 2597.

SANCHEZ-NIETO, B. & NAHUM, A. E. 2000. BIOPLAN: software for the biological evaluation of. Radiotherapy treatment plans. *Med Dosim,* 25**,** 71-6.

SCHULZE, D., LIANG, J., YAN, D. & ZHANG, T. 2009. Comparison of various online IGRT strategies: The benefits of online treatment plan re-optimization. *Radiother Oncol,* 90**,** 367-76.

SCHULZE, R., HEIL, U., GROSS, D., BRUELLMANN, D. D., DRANISCHNIKOW, E., SCHWANECKE, U. & SCHOEMER, E. 2011. Artefacts in CBCT: a review. *Dentomaxillofac Radiol,* 40**,** 265-73.

SHANG, Q., SHEPLAN OLSEN, L. J., STEPHANS, K., TENDULKAR, R. & XIA, P. 2013. Prostate rotation detected from implanted markers can affect dose coverage and cannot be simply dismissed. *J Appl Clin Med Phys,* 14**,** 4262.

SHAPIRO, S. S. & WILK, M. B. 1965. An analysis of variance test for normality (complete samples). *Biometrika,* 52**,** 591-611.

SHI, W., LI, J. G., ZLOTECKI, R. A., YEUNG, A., NEWLIN, H., PALTA, J., LIU, C., CHVETSOV, A. V. & OLIVIER, K. 2011. Evaluation of kV Cone-Beam CT Performance for Prostate IGRT: A Comparison of Automatic Grey-Value Alignment to Implanted Fiducial-Marker Alignment. *American Journal of Clinical Oncology,* 34**,** 16-21.

SHIRATO, H., HARADA, T., HARABAYASHI, T., HIDA, K., ENDO, H., KITAMURA, K., ONIMARU, R., YAMAZAKI, K., KURAUCHI, N., SHIMIZU, T., SHINOHARA, N., MATSUSHITA, M., DOSAKA-AKITA, H. & MIYASAKA, K. 2003. Feasibility of insertion/implantation of 2.0-mm-diameter gold internal fiducial markers for precise setup and real-time tumor tracking in radiotherapy. *International Journal of Radiation Oncology*Biology*Physics,* 56**,** 240-247.

SIMPSON, D. R., LAWSON, J. D., NATH, S. K., ROSE, B. S., MUNDT, A. J. & MELL, L. K. 2010. A survey of image-guided radiation therapy use in the United States. *Cancer,* 116**,** 3953-60.

SOCIETY OF RADIOGRAPHERS 2013. Image-guided radiotherapy (IGRT) Clinical Support Program in England 2012-2013.

SOUTH, C. P., KHOO, V. S., NAISMITH, O., NORMAN, A. & DEARNALEY, D. P. 2008. A comparison of treatment planning techniques used in two randomised UK external beam radiotherapy trials for localised prostate cancer. *Clin Oncol (R Coll Radiol),* 20**,** 15-21.

SRIPADAM, R., STRATFORD, J., HENRY, A. M., JACKSON, A., MOORE, C. J. & PRICE, P. 2009. Rectal motion can reduce CTV coverage and increase rectal dose during prostate radiotherapy: A daily cone-beam CT study. *Radiother Oncol,* 90**,** 312-7.

STANESCU, T., TADIC, T., MARLE, J., WINTER, J., PETROPOULOS, L., SWEITZER, M. & JAFFRAY, D. 2013. WE-G-WAB-02: BEST IN PHYSICS (JOINT IMAGING-THERAPY)-MR and Linac Magnetic Field Mutual Decoupling for An MRI-Guided Radiation Therapy System. *Medical Physics,* 40**,** 505-505.

STOCK, M., PALM, A., ALTENDORFER, A., STEINER, E. & GEORG, D. 2012. IGRT induced dose burden for a variety of imaging protocols at two different anatomical sites. *Radiother Oncol,* 102**,** 355-63.

STOCK, M., PASLER, M., BIRKFELLNER, W., HOMOLKA, P., POETTER, R. & GEORG, D. 2009. Image quality and stability of image-guided radiotherapy (IGRT) devices: A comparative study. *Radiother Oncol,* 93**,** 1-7.

STROOM, J. C., DE BOER, H. C. J., HUIZENGA, H. & VISSER, A. G. 1999. Inclusion of geometrical uncertainties in radiotherapy treatment planning by means of coverage probability. *International Journal of Radiation Oncology*Biology*Physics,* 43**,** 905-919.

SVEISTRUP, J., AF ROSENSCHÖLD, P. M., DEASY, J. O., OH, J. H., POMMER, T., PETERSEN, P. M. & ENGELHOLM, S. A. 2014. Improvement in toxicity in high risk prostate cancer patients treated with image-guided intensity-modulated radiotherapy compared to

3D conformal radiotherapy without daily image guidance. *Radiat Oncol,* 9**,** 44.

SYKES, J. R., LINDSAY, R., IBALL, G. & THWAITES, D. I. 2013. Dosimetry of CBCT: methods, doses and clinical consequences. *Journal of Physics: Conference Series,* 444**,** 012017.

THE ROYAL COLLEGE OF RADIOLOGISTS 2013. Clinical Oncology UK Workforce Report 2012. London: Royal College of Radiologists.

THOMAS, S. J., ASHBURNER, M., TUDOR, G. S., TREEBY, J., DEAN, J., ROUTSIS, D., RIMMER, Y. L., RUSSELL, S. G. & BURNET, N. G. 2013. Intra-fraction motion of the prostate during treatment with helical tomotherapy. *Radiother Oncol,* 109**,** 482-6.

THOR, M., PETERSEN, J. B., BENTZEN, L., HOYER, M. & MUREN, L. P. 2011. Deformable image registration for contour propagation from CT to cone-beam CT scans in radiotherapy of prostate cancer. *Acta Oncol,* 50**,** 918-25.

TSOUGOS, I., GROUT, I., THEODOROU, K. & KAPPAS, C. 2009. A free software for the evaluation and comparison of dose response models in clinical radiotherapy (DORES). *Int J Radiat Biol,* 85**,** 227-37.

VAN HERK, M. & MEERTENS, H. A matrix ionisation chamber imaging device for on-line patient setup verification during radiotherapy. *Radiotherapy and Oncology,* 11**,** 369-378.

VAN HERK, M., REMEIJER, P., RASCH, C. & LEBESQUE, J. V. 2000. The probability of correct target dosage: dose-population

histograms for deriving treatment margins in radiotherapy. *International Journal of Radiation Oncology*Biology*Physics,* 47**,** 1121-1135.

VANASEK, J., ODRAZKA, K., DOLEZEL, M., KOLAROVA, I., JARKOVSKY, J., PAVLIK, T., HLAVKA, A. & DUSEK, L. 2013. Statistical Analysis of Dose–Volume Profiles and its Implication for Radiation Therapy Planning in Prostate Carcinoma. *International Journal of Radiation Oncology*Biology*Physics,* 86**,** 769-776.

VARADHAN, R., HUI, S. K., WAY, S. & NISI, K. 2009. Assessing prostate, bladder and rectal doses during image guided radiation therapy--need for plan adaptation? *J Appl Clin Med Phys,* 10**,** 2883.

VARGAS, C., MARTINEZ, A., KESTIN, L. L., YAN, D., GRILLS, I., BRABBINS, D. S., LOCKMAN, D. M., LIANG, J., GUSTAFSON, G. S., CHEN, P. Y., VICINI, F. A. & WONG, J. W. 2005. Dose-volume analysis of predictors for chronic rectal toxicity after treatment of prostate cancer with adaptive image-guided radiotherapy. *International Journal of Radiation Oncology*Biology*Physics,* 62**,** 1297-1308.

WANG, X. & NING, R. 1999. A cone-beam reconstruction algorithm for circle-plus-arc data-acquisition geometry. *IEEE Trans Med Imaging,* 18**,** 815-24.

WARKENTIN, B., STAVREV, P., STAVREVA, N., FIELD, C. & FALLONE, B. G. 2004. A TCP-NTCP estimation module using DVHs and

known radiobiological models and parameter sets. *J Appl Clin Med Phys,* 5**,** 50-63.

WILCOXON, F. 1945. Individual Comparisons by Ranking Methods. *Biometrics Bulletin,* 1**,** 80-83.

WILLOUGHBY, T. R., KUPELIAN, P. A., POULIOT, J., SHINOHARA, K., AUBIN, M., ROACH III, M., SKRUMEDA, L. L., BALTER, J. M., LITZENBERG, D. W., HADLEY, S. W., WEI, J. T. & SANDLER, H. M. 2006. Target localization and real-time tracking using the Calypso 4D localization system in patients with localized prostate cancer. *International Journal of Radiation Oncology*Biology*Physics,* 65**,** 528-534.

XIE, Y., DJAJAPUTRA, D., KING, C. R., HOSSAIN, S., MA, L. & XING, L. 2008. Intrafractional Motion of the Prostate During Hypofractionated Radiotherapy. *International Journal of Radiation Oncology*Biology*Physics,* 72**,** 236-246.

YANG, Y., SCHREIBMANN, E., LI, T., WANG, C. & XING, L. 2007. Evaluation of on-board kV cone beam CT (CBCT)-based dose calculation. *Phys Med Biol,* 52**,** 685-705.

ZELEFSKY, M., LEIBEL, S., GAUDIN, P., KUTCHER, G., FLESHNER, N., VENKATRAMEN, E. S., REUTER, V., FAIR, W., LING, C. C. & FUKS, Z. 1998. Dose escalation with three-dimensional conformal radiation therapy affects the outcome in prostate cancer. *International Journal of Radiation Oncology*Biology*Physics,* 41**,** 491-500.

ZELEFSKY, M. J., FUKS, Z., HUNT, M., YAMADA, Y., MARION, C., LING, C. C., AMOLS, H., VENKATRAMAN, E. S. & LEIBEL, S. A. 2002. High-dose intensity modulated radiation therapy for prostate cancer: early toxicity and biochemical outcome in 772 patients. *International Journal of Radiation Oncology*Biology*Physics,* 53**,** 1111-1116.

ZELEFSKY, M. J., KOLLMEIER, M., COX, B., FIDALEO, A., SPERLING, D., PEI, X., CARVER, B., COLEMAN, J., LOVELOCK, M. & HUNT, M. 2012. Improved clinical outcomes with high-dose image guided radiotherapy compared with non-IGRT for the treatment of clinically localized prostate cancer. *Int J Radiat Oncol Biol Phys,* 84**,** 125-9.

ZLOTTA, A. R., ROUMEGUERE, T., RAVERY, V., HOFFMANN, P., MONTORSI, F., TURKERI, L., DOBROVRITS, M., SCATTONI, V., EKANE, S., BOLLENS, R., VANDEN BOSSCHE, M., DJAVAN, B., BOCCON-GIBOD, L. & SCHULMAN, C. C. 2004. Is seminal vesicle ablation mandatory for all patients undergoing radical prostatectomy? A multivariate analysis on 1283 patients. *Eur Urol,* 46**,** 42-9.

Appendix 1 – National IGRT Survey Tool

1. Name of radiotherapy centre

2. Please enter your job designation

3. How many new patients with prostate cancer were treated with radical radiotherapy in February 2014 in your centre?

4. What type of planning is used for radical prostate radiotherapy patients? Please select all applicable
    a. 3-4 field conformal
    b. Intensity-modulated (static beam)
    c. Volumetric modulated arc therapy (eg. RapidArc)
    d. Tomotherapy
    e. Cyberknife
    f. Linac-based stereotactic RT
    g. Other….

5. If intensity-modulated planning is used for radical prostate radiotherapy, what percentage of patients is planned in this way?
        i. %

6. What dose-fractionation regimens are used for radical prostate radiotherapy in your centre? Please select all applicable
    a. 78 Gy/39#
    b. 74 Gy/37#
    c. 50 Gy/16#
    d. 60 Gy/20#
    e. 57 Gy/19#
    f. Other – please specify

7. Are fiducial markers used for radical prostate radiotherapy in your centre?
    a. For all patients
    b. Some patients
    c. Not at all
    d. If fiducial markers are used for some patients, please specify indication/s

8. Who inserts the fiducial markers for prostate radiotherapy?
    a. Consultant Oncologist
    b. Consultant Urologist
    c. Consultant Radiologist
    d. Other – please specify

9. How many fiducial markers are inserted in each prostate radiotherapy patient in your centre?

10. Are prostate rectum spacers used in your centre for radiotherapy?
    a. Yes
    b. No

11. What bowel preparation protocol is used in your centre for prostate radiotherapy?
    a. No specific preparation
    b. High-fibre diet information
    c. Daily micro-enema
    d. Other – please specify

12. Please outline your bladder filling protocol for prostate radiotherapy.

13. What is the main verification imaging technique that is used for radical prostate radiotherapy in your centre?
    a. Orthogonal portal MV imaging
    b. Orthogonal portal KV imaging
    c. 3-D cone beam CT imaging with soft tissue matching
    d. Fiducial markers + KV imaging
    e. Fiducial markers + cone beam CT
    f. Fiducial markers + KV imaging + cone beam CT
    g. Other – please specify

14. What is the frequency of verification imaging for prostate IGRT in your centre?
    a. Day 1-3, followed by weekly
    b. Day 1-5, followed by weekly
    c. Daily
    d. Other – please specify if you have different protocols for different imaging

15. If cone beam CT is used, what is the frequency of use during prostate radiotherapy?
    a. Daily
    b. Weekly
    c. Other, please specify

16. Please specify if cone beam CTs are repeated during a fraction if needed

17. What method of correction do you use for prostate IGRT?
    a. Offline
    b. Online (zero tolerance action level protocol)
    c. Online (No Action level protocol)
    d. Other – please specify

18. If online correction with a No Action level protocol is used, please specify your action level in mm

19. If systematic correction is used, what threshold (mm) do you use for systematic correction?

20. If applicable, what threshold in mm do you use for gross errors to recheck immobilization and setup?

21. Comments (optional)

Thank you for your participation in this survey

Appendix 2 – List of publications arising from this research study

1. Ariyaratne H, Chesham H, Alonzi R. Image-guided radiotherapy for prostate cancer in the United Kingdom: a national survey. British Journal of Radiology 2017; 90(1070).

2. Ariyaratne H, Chesham H, Pettingell J, Alonzi R. Image-guided radiotherapy for prostate cancer with cone beam CT – dosimetric effects of imaging frequency and PTV margin. Radiotherapy and Oncology 2016; 121(1): 103-108.

Appendix 3 – List of conference presentations arising from this research study

1. Ariyaratne H, Alonzi R. Rectal and bladder dose-volume relationships during image-guided radiotherapy for prostate cancer. Oral and poster presentation at NCRI Conference, Liverpool, Nov 2017

2. Ariyaratne H, Alonzi R. Image-guided radiotherapy for prostate cancer – quantification of benefit of daily online CBCT imaging. Poster presentation at NCRI Conference, Liverpool, Nov 2017

3. Ariyaratne H, Chesham H, Alonzi R. Image-guided radiotherapy strategies for prostate cancer in the United Kingdom. Poster presentation at UKRO 2016, Jun 2016

4. Ariyaratne H, Chesham H, Alonzi R. Target coverage during image-guided radiotherapy for prostate cancer - how relevant is the initial rectal volume? Poster presentation at NCRI Conference, Liverpool, Nov 2015. Awarded National Cancer Research Institute Prize

5. Ariyaratne H, Chesham H, Pettingell J, Sikora K, Alonzi R. Comparison of cone beam CT imaging protocols in image-guided

radiotherapy for prostate cancer. Poster presentation at 3rd ESTRO Forum, Barcelona, Apr 2015

6. Ariyaratne H, Chesham H, Pettingell J, Alonzi R. Image-guided radiotherapy in prostate cancer: validation of a dose calculation method based on cone beam CT contours. Oral presentation and National Cancer Research Institute Prize Award at NCRI Conference, Liverpool, Nov 2014. Shortlisted for RCR Ross Prize.

7. Chesham H, Ariyaratne H, Pettingell J, Alonzi R, Walsh K. Reduced PTV margins for prostate IMRT with daily on-line IGRT: a retrospective analysis. Poster presentation at ESTRO 33, Vienna, Apr 2014. Awarded Best Poster Award.

8. Ariyaratne H, Chesham H, Pettingell J, Sikora K, Alonzi R. Dosimetric effects of image-guided radiotherapy using daily online cone beam CT for prostate radiotherapy. Poster presentation at ESTRO 33, Vienna, Apr 2014